Supporting Information

Direct C(sp^3)–H Cross Coupling Enabled by Catalytic Generation of Chlorine Radicals

Benjamin J. Shields[1] and Abigail G. Doyle[1]

[1]Department of Chemistry, Princeton University, Princeton, NJ 08544, USA.

correspondence to: agdoyle@princeton.edu

Table of Contents

I. Materials and Methods

Materials

Commercial reagents were purchased from Sigma Aldrich, Oakwood, Acros, Alfa Aesar, Strem, or TCI, and stored in a N_2-filled glovebox. All ethers were purchased from Sigma Aldrich in Sure Seal bottles and stored over activated molecular sieves in a N_2-filled glovebox. THF was purchased inhibitor free, dried by passing through activated alumina columns and stored over activated molecular sieves in a N_2-filled glovebox. Toluene and dioxane were dried by passing through activated alumina columns and stored over activated molecular sieves in a N_2-filled glovebox.

Methods

Unless otherwise noted, reactions were performed with rigorous exclusion of air and moisture. Solvent was freshly distilled/degassed prior to use unless otherwise noted. Reactions were monitored by thin-layer chromatography (TLC) on EMD Silica Gel 60 F254 plates, visualizing with UV-light (254 nm) fluorescence quenching. Organic solutions were concentrated under reduced pressure using a rotary evaporator (23 °C, <50 torr). Automated column chromatography was performed using silica gel cartridges on a Biotage SP4 (40-53 μm, 60 Å).

Instrumentation

Proton nuclear magnetic resonance (^{1}H NMR) spectra were recorded on a Bruker 500 AVANCE spectrometer (500 MHz) or a Bruker NB 300 spectrometer (300 MHz). Deuterium nuclear magnetic resonance (^{2}H NMR) spectra were recorded on a Bruker 500 AVANCE spectrometer (77 MHz). Carbon nuclear magnetic resonance (^{13}C NMR) spectra were recorded on a Bruker 500 AVANCE spectrometer (126 MHz). Fluorine nuclear magnetic resonance (^{19}F NMR) spectra were recorded on a Bruker NB 300 spectrometer (282 MHz). Chemical shifts for protons are reported in parts per million downfield from tetramethylsilane and are referenced to residual protium in the NMR solvent ($CHCl_3$ = δ 7.26 ppm, , DCM = δ 5.32 ppm, THF = δ 1.73 and 3.58 ppm). Chemical shifts for deuterons are reported in parts per million downfield from tetramethylsilane and are referenced to residual deuterium in solvent (THF = δ 1.73 and 3.58 ppm). Chemical shifts for carbon are reported in parts per million downfield from tetramethylsilane and are referenced to the carbon resonances of the solvent residual peak ($CDCl_3$ = δ 77.16 ppm, DCM-d_2 = δ 54.0 ppm, THF = δ 25.4 and 67.6 ppm). Chemical shifts for fluorine are reported in parts per million referenced to $CFCl_3$ (δ 0 ppm). NMR data are represented as follows: chemical shift (δ ppm), multiplicity (s = singlet, d = doublet, t = triplet, q = quartet, p = pentet, m = multiplet), coupling constant in Hertz (Hz), integration. Reversed-phase liquid chromatography/mass spectrometry (LC/MS) was performed on an Agilent 1260 Infinity analytical LC and Agilent 6120 Quadrupole LC/MS system, using electrospray ionization/atmospheric-pressure chemical ionization (ESI/APCI), and UV detection at 254 and 280 nm. High-resolution mass spectra were obtained on an Agilent 6220 LC/MS using electrospray ionization time-of-flight (ESI-TOF) or Agilent 7200 gas chromatography/mass spectrometry using electron impact time-of-flight (EI-TOF). Gas chromatography was performed on an Agilent 7890A series instrument equipped with a split-mode capillary injection

system and flame ionization detectors. Fourier transform infrared (FT-IR) spectra were recorded on a Perkin-Elmer Spectrum 100 and are reported in terms of frequency of absorption (cm^{-1}). Linear ultraviolet-visible absorption spectra were collected on an Aligent 8453 diode array Spectrophotometer using 10 mm quartz cuvettes. Emission spectra were collected on an Agilent Cary Eclipse Fluorescence Spectrophotometer in 10 mm quartz cuvettes. Elemental analysis was carried out by Robertson Microlit Laboratories.

Light Sources

Reactions were carried out using 25W blue LED arrays (12-inch Sapphire Flex LED Strips 5050, High Density, 12V DC Power Leads, Waterproof, Black backing) purchased from Creative Lightings or 34W blue LED lamps (Kessil H150 LED Grow Lights) purchased from Kessil. Blue LED arrays were assembled by wrapping three strips inside of a Pyrex crystallizing dish. Emission spectra for each lamp can be seen in Fig. S34.
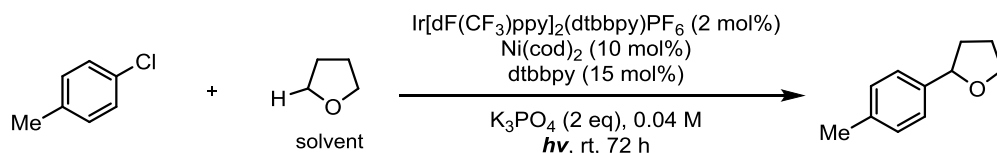
II. Reaction Optimization and Control Experiments

Procedure for Reaction Optimization. A one-dram vial (VWR part number: 66011-041) equipped with a PTFE-coated stir bar was brought into a N_2-filled glove box and charged with K_3PO_4 (21 mg, 0.1 mmol, 2 equiv.). To the reaction vial the following were added successively: a clear solution of 4-chloroacetophenone (7.7 mg, 0.05 mmol, 1 equiv) in THF (0.25 mL), a yellow solution of $Ir[dF(CF_3)ppy]_2(dtbbpy)PF_6$ (1.1 mg, 1 μmol, 0.02 equiv.) in THF (0.5 mL) and a dark purple solution of $Ni(cod)_2$ (1.4 mg, 5 μmol, 0.1 equiv.) and 4,4′-di-*tert*-butyl-2,2′-bipyridine (2.0 mg, 7.5 μmol, 0.15 equiv.) in THF (0.5 mL). The vial was capped with a Teflon septum cap and sealed with electrical tape. The reaction vial was removed from the glove box, set to stir (800 rpm) and irradiated with a blue LED array (2 cm away, with cooling fan to keep the reaction at room temperature) for 72 hours. The crude product was analyzed by ^{1}H NMR (10 s delay) relative to 1-fluoronaphthalene as an external standard. Experiments with 34 W blue LED lamps were carried out according to the same procedure in threaded 16×125 mm borosilicate reaction tubes (Kimble part number: 73750-16125) equipped with PTFE-coated stir bars and Teflon septum caps.
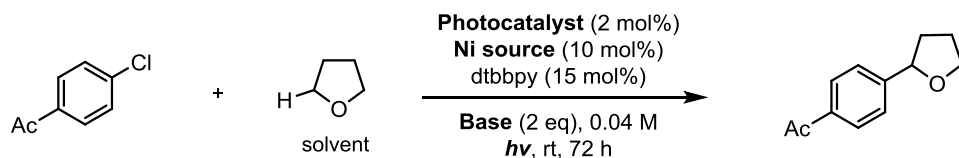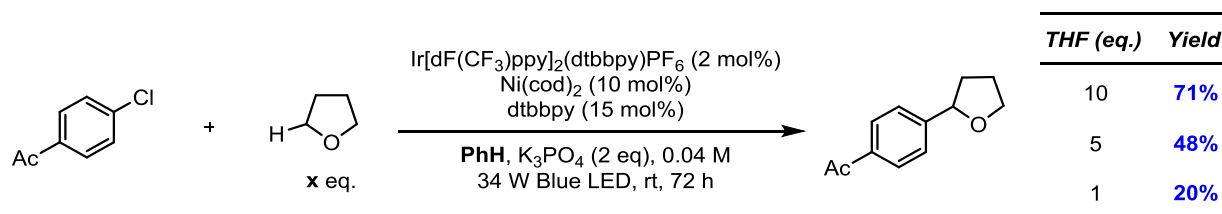

Entry	Photocatalyst	hv	Ni source	Base	Yield
1	$Ir[dF(CF_3)ppy]_2(dtbbpy)PF_6$	Blue LED Array	$Ni(cod)_2$	K_3PO_4	**92%**
2	none	Blue LED Array	$Ni(cod)_2$	K_3PO_4	**0%**
3	$Ru(bpy)_3Cl_2$	Blue LED Array	$Ni(cod)_2$	K_3PO_4	**0%**
4	$Ir[dF(CF_3)ppy]_2(dtbbpy)PF_6$	dark	$Ni(cod)_2$	K_3PO_4	**0%**
5	$Ir[dF(CF_3)ppy]_2(dtbbpy)PF_6$	Blue LED Array	$NiCl_2 \cdot$ glyme	K_3PO_4	**61%**
6	$Ir[dF(CF_3)ppy]_2(dtbbpy)PF_6$	Blue LED Array	none	K_3PO_4	**0%**
7	$Ir[dF(CF_3)ppy]_2(dtbbpy)PF_6$	Blue LED Array	$Ni(cod)_2$	none	**13%**

Table S1. Controls and optimization for THF α-arylation reaction. Yield determined by ^{1}H NMR spectroscopy using 1-fluoronaphthalene as an internal standard. Reactions were carried out at 0.05 mmol scale.

Table S2 Scheme

Ir[dF(CF$_3$)ppy]$_2$(dtbbpy)PF$_6$ (2 mol%)
Ni(cod)$_2$ (10 mol%)
dtbbpy (15 mol%)
—————
K$_3$PO$_4$ (2 eq), 0.04 M
hv, rt, 72 h

(4-chlorotoluene) + (THF, H) in solvent → (2-(4-methylphenyl)tetrahydrofuran)

Entry	*hv*	Conversion	Yield
1	34 W Blue LED Lamp	87%	**65%**
2	25 W Blue LED Array	41%	**33%**

Table S2. Lighting conditions. Yield and conversion determined by GC-FID using 1-fluoronaphthalene as an external standard. Reactions were carried out at 0.05 mmol scale. See Fig. S34 for reaction lamp emission spectra.
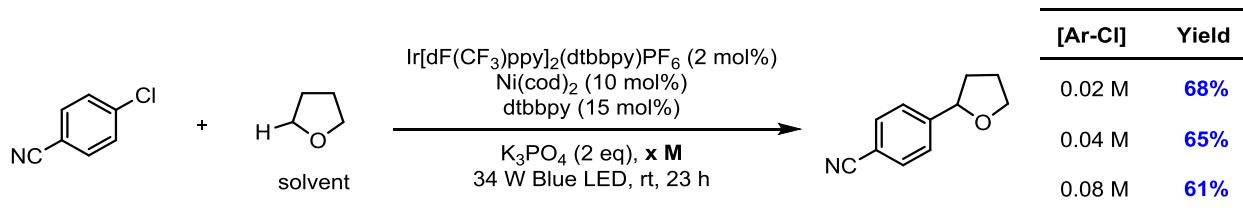
Table S3 Scheme

Ir[dF(CF$_3$)ppy]$_2$(dtbbpy)PF$_6$ (2 mol%)
Ni(cod)$_2$ (10 mol%)
dtbbpy (15 mol%)
—————
PhH, K$_3$PO$_4$ (2 eq), 0.04 M
34 W Blue LED, rt, 72 h

(Ac-phenyl-Cl) + (THF, H) **x** eq. → (Ac-phenyl-tetrahydrofuran)

THF (eq.)	Yield
10	**71%**
5	**48%**
1	**20%**

Table S3. Evaluation of benzene as a solvent for THF α-arylation reaction. Yield determined by ^{1}H NMR using 1-fluoronaphthalene as an external standard. Reactions were carried out at 0.1 mmol scale.

Table S4 Scheme

Ir[dF(CF$_3$)ppy]$_2$(dtbbpy)PF$_6$ (2 mol%)
Ni(cod)$_2$ (10 mol%)
dtbbpy (15 mol%)
—————
PhH, K$_3$PO$_4$ (2 eq), 0.04 M
25 W Blue LEDs, rt, 72 h

(Ac-phenyl-Cl) + (cyclohexane, H) **x** eq. → (Ac-phenyl-cyclohexane)

CyH (eq.)	Yield
1	**8%**
2	**11%**
5	**16%**
10	**41%**

Table S4. Arylation of cyclohexane. Yield determined by GC-FID using 1-fluoronaphthalene as an external standard. Reactions were carried out at 0.05 mmol scale.

Table S5 Scheme

Ir[dF(CF$_3$)ppy]$_2$(dtbbpy)PF$_6$ (2 mol%)
Ni(cod)$_2$ (10 mol%)
dtbbpy (15 mol%)
—————
K$_3$PO$_4$ (2 eq), **x M**
34 W Blue LED, rt, 23 h

(NC-phenyl-Cl) + (THF, H) solvent → (NC-phenyl-tetrahydrofuran)

[Ar-Cl]	Yield
0.02 M	**68%**
0.04 M	**65%**
0.08 M	**61%**

Table S5. Concentration screen. Yields determined by ^{1}H NMR using 1-fluoronaphthalene as an external standard. Reactions were carried out at 0.1 mmol scale.

III. Isolated Yields and Characterization of Products

General Procedure for Csp³–H Functionalization. A threaded 16 × 125 mm borosilicate reaction tube (Kimble part number: 73750-16125) equipped with a PTFE-coated stir bar and two-dram vial equipped with a PTFE-coated stir bar were brought into a N₂-filled glove box. To the two-dram vial was added Ni(cod)₂ (6.1 mg, 22 μmol) followed by 4,4′-di-*tert*-butyl-2,2′-bipyridine (8.9 mg, 33 μmol) and Csp³–H coupling partner (3.3 mL). The mixture was stirred for 10 min to give a dark purple solution (solution 1). The reaction tube was charged with aryl chloride (0.2 mmol, 1 equiv.), Ir[dF(CF₃)ppy]₂(dtbbpy)PF₆ (4.5 mg, 4 μmol, 0.02 equiv.), K₃PO₄ (85 mg, 0.4 mmol, 2 equiv.) and Csp³–H coupling partner (2 mL) and stirred. Solution 1 (3 mL, 0.1 equiv Ni(cod)₂, 0.15 equiv. 4,4′-di-*tert*-butyl-2,2′-bipyridyl) was added and the reaction tube was capped with a Teflon septum cap and sealed with electrical tape. The reaction tube was removed from the glove box, set to stir (800 rpm) and irradiated with a 34 W blue LED lamp (2 cm away, with cooling fan to keep the reaction at room temperature). After 36-75 hours, the reaction was filtered through cotton and concentrated *in vacuo*. The crude reaction mixture was then purified by automated silica gel column chromatography using the indicated solvent system to give the desired product.
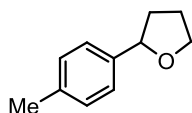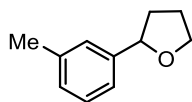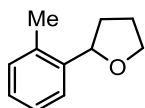

2-(*p*-tolyl)tetrahydrofuran (10). Prepared according to the general procedure (72 hours) from 4-chlorotoluene and THF. The title compound was isolated via flash chromatography (gradient 100/0 – 80/20 hexanes/ethyl acetate) as a clear oil (22.8 mg, 0.141 mmol, 70% yield).
¹H NMR (501 MHz, CDCl₃): δ 7.23 (d, J = 7.9 Hz, 2H), 7.15 (d, J = 7.7 Hz, 2H), 4.86 (t, J = 7.2 Hz, 1H), 4.11 – 4.07 (m, 1H), 3.95 – 3.90 (m, 1H), 2.34 (s, 3H), 2.29 (dt, J = 12.5, 6.5 Hz, 1H), 2.08 – 1.94 (m, 2H), 1.85 – 1.75 (m, 1H).
¹³C NMR (126 MHz, CDCl₃): δ 140.50, 136.85, 129.09, 125.74, 80.72, 68.71, 34.72, 26.18, 21.25.
HRMS: (ESI-TOF) calculated for ([C₁₁H₁₄O + Na]⁺): 185.0937, found: 185.0934.
**FTIR (ATR, cm⁻¹):** 2947, 2868, 1683, 1513, 1452, 1361, 1306, 1179, 1058, 1020, 920, 810, 750, 719.

2-(*m*-tolyl)tetrahydrofuran (11). Prepared according to the general procedure (72 hours) from 3-chlorotoluene and THF. The title compound was isolated via flash chromatography (gradient 100/0 – 90/10 hexanes/ethyl acetate) as a clear oil (24.3 mg, 0.150 mmol, 75% yield).
¹H NMR (501 MHz, CDCl₃): δ 7.22 (t, J = 7.5 Hz, 1H), 7.16 (s, 1H), 7.13 (d, J = 7.6 Hz, 1H), 7.07 (d, J = 7.4 Hz, 1H), 4.86 (t, J = 7.2 Hz, 1H), 4.10 (q, J = 7.3 Hz, 1H), 3.93 (q, J = 7.3 Hz, 1H), 2.35 (s, 3H), 2.31 (dt, J = 12.5, 7.0 Hz, 1H), 2.08 – 1.94 (m, 2H), 1.81 (dq, J = 12.2, 7.9 Hz, 1H).
¹³C NMR (126 MHz, CDCl₃): δ 143.48, 138.04, 128.32, 128.00, 126.42, 122.86, 80.84, 68.79, 34.70, 26.19, 21.62.
HRMS: (ESI-TOF) calculated for ([C₁₁H₁₄O + H]⁺): 163.1117, found: 163.1116.
FTIR (ATR, cm⁻¹): 2971, 2865, 1609, 1488, 1458, 1355, 1179, 1060, 923, 881, 783, 700.

2-(*o*-tolyl)tetrahydrofuran (12). Prepared according to the general procedure (72 hours) from 2-chlorotoluene and THF. The title compound was isolated via flash chromatography (gradient 100/0 – 90/10 hexanes/ethyl acetate) as a light yellow oil (16.5 mg, 0.102 mmol, 51% yield). Spectroscopic data matched those previously reported *(12)*.

^{1}H NMR (501 MHz, CDCl$_3$): δ 7.45 (d, *J* = 7.6 Hz, 1H), 7.23 – 7.18 (m, 1H), 7.18 – 7.10 (m, 2H), 5.07 (t, *J* = 7.2 Hz, 1H), 4.19 – 4.12 (m, 1H), 3.94 (q, *J* = 7.2 Hz, 1H), 2.36 (dq, *J* = 13.2, 7.2 Hz, 1H), 2.31 (s, 3H), 2.01 (m, 2H), 1.69 (dq, *J* = 12.2, 7.4 Hz, 1H).

^{13}C NMR (126 MHz, CDCl$_3$): δ 141.97, 134.30, 130.25, 126.89, 126.12, 124.66, 78.09, 68.79, 33.30, 26.17, 19.39.

HRMS: (EI-TOF) calculated for ($[C_{11}H_{14}O]^+$): 162.1039, found: 162.1041.

FTIR (ATR, cm^{-1}): 2970, 2865, 1600, 1484, 1460, 1363, 1283, 1177, 1059, 931, 748, 723.
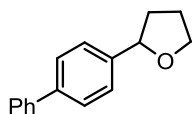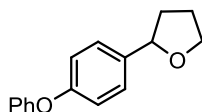

2-([1,1´-biphenyl]-4-yl)tetrahydrofuran (13). Prepared according to the general procedure (72 hours) from 4-chloro-1,1´-biphenyl and THF.   The title compound was isolated via flash chromatography (gradient 100/0 – 90/10 hexanes/ethyl acetate) as a clear oil (38.6 mg, 0.172 mmol, 86% yield).

^{1}H NMR (501 MHz, CDCl$_3$): δ 7.60 – 7.56 (m, 4H), 7.45 – 7.41 (m, 4H), 7.34 (t, *J* = 7.4 Hz, 1H), 4.95 (t, *J* = 7.2 Hz, 1H), 4.15 – 4.11 (m, 1H), 3.99 – 3.94 (m, 1H), 2.40 – 2.33 (m, 1H), 2.10 – 1.99 (m, 2H), 1.90 – 1.82 (m, 1H).

^{13}C NMR (126 MHz, CDCl$_3$): δ 142.66, 141.15, 140.22, 128.86, 127.99, 127.22, 127.21, 126.23, 80.59, 68.85, 34.75, 26.23.

HRMS: (ESI-TOF) calculated for ($[C_{16}H_{16}O + H]^+$): 225.1274 , found: 225.1275.

FTIR (ATR, cm^{-1}): 3028, 2972, 2865, 1599, 1485, 1448, 1405, 1349, 1305, 1178, 1059, 1020, 1007, 917, 833, 761, 734, 695.

2-(4-phenoxyphenyl)tetrahydrofuran (14). Prepared according to the general procedure (70 hours) from 1-chloro-4-phenoxybenzene and THF. The title compound was isolated via flash chromatography (gradient 100/0 – 90/10 hexanes/ethyl acetate) as a clear oil (36.8 mg, 0.153 mmol, 77% yield).

^{1}H NMR (501 MHz, CDCl$_3$): δ 7.36 – 7.28 (m, 4H), 7.09 (t, *J* = 7.4 Hz, 1H), 6.99 (t, *J* = 8.2 Hz, 4H), 4.86 (t, *J* = 7.2 Hz, 1H), 4.10 (q, *J* = 7.2 Hz, 1H), 3.93 (q, *J* = 7.9 Hz, 1H), 2.31 (td, *J* = 12.3, 7.1 Hz, 1H), 2.09 – 1.97 (m, 2H), 1.85 – 1.78 (m, 1H).

^{13}C NMR (126 MHz, CDCl$_3$): δ 157.57, 156.35, 138.37, 129.82, 127.32, 123.19, 119.01, 118.79, 80.49, 68.75, 34.69, 26.23.

**HRMS:** (ESI-TOF) calculated for ($[C_{16}H_{16}O_2 + H]^+$): 241.1223 , found: 241.1222.

FTIR (ATR, cm^{-1}): 2973, 2871, 1588, 1505, 1487, 1287, 1229, 1164, 1094, 1056, 1013, 919, 868, 837, 748, 691.
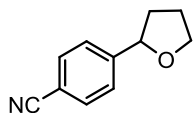
4-(tetrahydrofuran-2-yl)benzonitrile (15). Prepared according to the general procedure (68 hours) from 4-chlorobenzonitrile and THF. The title compound was isolated via flash chromatography (gradient 100/0 − 70/30 hexanes/ethyl acetate) as a clear oil (29.4 mg, 0.170 mmol, 83% yield with 2% unknown impurity). Spectroscopic data matched those previously reported *(23)*.

^{1}H NMR (501 MHz, CDCl$_3$): δ 7.62 (d, *J* = 8.3 Hz, 2H), 7.43 (d, *J* = 8.1 Hz, 2H), 4.93 (t, *J* = 7.2 Hz, 1H), 4.12 − 4.05 (m, 1H), 3.96 (q, *J* = 7.4 Hz, 1H), 2.38 (dq, *J* = 13.1, 7.0 Hz, 1H), 2.08 − 1.94 (m, 2H), 1.74 (dq, *J* = 12.3, 7.8 Hz, 1H).

^{13}C NMR (126 MHz, CDCl$_3$): δ 149.36, 132.32, 126.29, 119.12, 110.94, 79.97, 69.11, 34.86, 26.07.
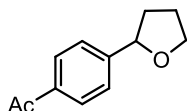
1-(4-(tetrahydrofuran-2-yl)phenyl)ethan-1-one (16). Prepared according to the general procedure (58 h) from 4-chloroacetophenone and THF. The title compound was isolated via flash chromatography (gradient 100/0 − 75/25 hexanes/ ethyl acetate) as a clear oil (30.1 mg, 0.158 mmol, 79% yield). Spectroscopic data matched those previously reported *(12)*.

^{1}H NMR (501 MHz, CDCl$_3$): δ 7.92 (d, *J* = 8.4 Hz, 2H), 7.42 (d, *J* = 8.5 Hz, 2H), 4.95 (t, *J* = 7.2 Hz, 1H), 4.14 − 4.08 (m, 1H), 3.98 − 3.94 (m, 1H), 2.59 (s, 3H), 2.37 (dq, *J* = 13.4, 6.7 Hz, 1H), 2.01 (p, *J* = 6.8 Hz, 2H), 1.77 (dq, *J* = 12.3, 7.7 Hz, 1H).

^{13}C NMR (126 MHz, CDCl$_3$): δ 197.98, 149.33, 136.17, 128.60, 125.72, 80.27, 69.02, 34.85, 26.78, 26.10.
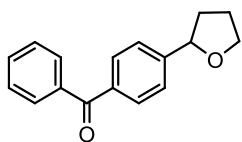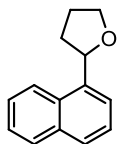

phenyl(4-(tetrahydrofuran-2-yl)phenyl)methanone (17). Prepared according to the general procedure (36 hours) from (4-chlorophenyl)(phenyl)methanone and THF. The title compound was isolated via flash chromatography (gradient 100/0 − 80/20 hexanes/ethyl acetate) as a clear oil (38.3 mg, 0.152 mmol, 76% yield).

^{1}H NMR (501 MHz, CDCl$_3$): δ 7.83 − 7.74 (m, 4H), 7.59 (t, *J* = 7.4 Hz, 1H), 7.51 − 7.42 (m, 4H), 4.98 (t, *J* = 7.2 Hz, 1H), 4.13 (q, *J* = 6.9 Hz, 1H), 3.98 (q, *J* = 7.1 Hz, 1H), 2.40 (dt, *J* = 12.4, 6.5 Hz, 1H), 2.04 (p, *J* = 6.9 Hz, 2H), 1.82 (dq, *J* = 12.3, 7.7 Hz, 1H).

^{13}C NMR (126 MHz, CDCl$_3$): δ 196.62, 148.64, 137.91, 136.54, 132.45, 130.42, 130.16, 128.39, 125.52, 80.36, 69.06, 34.87, 26.16.

**HRMS:** (ESI-TOF) calculated for ([C$_{17}$H$_{16}$O$_2$ + H]$^+$): 253.1223, found: 253.1223.

FTIR (ATR, cm^{-1}): 2973, 2868, 1654, 1607, 1598, 1577, 1446, 1409, 1307, 1274, 1175, 1147, 1060, 1017, 1000, 937, 921, 846, 790, 745, 698.

2-(naphthalene-1-yl)tetrahydrofuran (18). Prepared according to the general procedure (72 hours) from 1-chloronaphthalene and THF. The title compound was isolated via flash chromatography (gradient 100/0 − 90/10 hexanes/ethyl acetate) as a clear oil (31 mg, 0.156 mmol, 66% yield). Spectroscopic data matched those previously reported *(24)*.

^{1}H NMR (501 MHz, CDCl$_3$): δ 7.99 (d, *J* = 8.1 Hz, 1 H), 7.87 (d, *J* = 7.8 Hz, 1H), 7.76 (d, *J* = 8.2 Hz, 1H), 7.64 (d, *J* = 7.1 Hz, 1H), 7.53 − 7.45 (m, 3H), 5.65 (t, *J* = 6.9 Hz, 1H), 4.27 − 4.22 (q, *J* = 7.6 Hz, 1H), 4.06 − 4.02 (q, *J* = 7.6 Hz, 1H), 2.60 − 2.54 (m, 1H), 2.12 − 1.99 (m, 2H), 1.95 − 1.89 (m, 1H).

^{13}C NMR (126 MHz, CDCl$_3$): δ 139.46, 133.85, 130.46, 128.92, 127.55, 125.89, 125.63, 125.50, 123.55, 121.94, 78.06, 68.89, 33.93, 26.09.
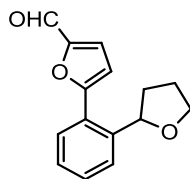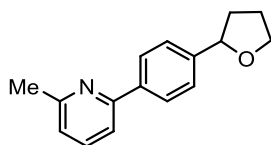

5-(2-(tetrahydrofuran-2-yl)phenyl)furan-2-carbaldehyde (19). Prepared according to the general procedure (63 hours) from 5-(2-chlorophenyl)furan-2-carbaldehyde and THF. The title compound was isolated via flash chromatography (TEA treated silica, gradient 90/10 − 70/30 hexanes/ethyl acetate) as a yellow oil (35.4 mg, 0.146 mmol, 73% yield).

^{1}H NMR (501 MHz, CDCl$_3$): δ 9.66 (s, 1H), 7.67 (d, *J* = 7.9 Hz, 1H), 7.63 − 7.61 (dd, *J* = 7.7, 1.1 Hz, 1H), 7.45 − 7.42 (td, *J* = 7.8, 1.1 Hz, 1H), 7.34 − 7.31 (m, 2H), 6.74 (d, *J* = 3.7 Hz, 1H), 5.31 (t, *J* = 7.0 Hz, 1H), 4.19 − 4.17 (m, 1H), 3.95 − 3.91(q, *J* = 7.3 Hz, 1H), 2.50 − 2.43 (m, 1H), 2.01 (p, *J* = 7.1 Hz, 2H), 1.84 − 1.77 (m, 1H).

^{13}C NMR (126 MHz, CDCl$_3$): broad peak at 122.98 was identified by HSQC; δ 177.35, 159.46, 152.45, 142.46, 130.09, 128.91, 127.30, 126.86, 126.21, 122.98, 111.17, 78.00, 69.14, 34.69, 26.13.

HRMS: (ESI-TOF) calculated for ($[C_{15}H_{14}O_3 + H]^+$): 243.1016, found: 243.1017.

FTIR (ATR, cm^{-1}): 2948, 2867, 1669, 1564, 1513, 1460, 1440, 1388, 1352, 1277, 1242, 1198, 1117, 1054, 1024, 969, 921, 803, 760, 685.
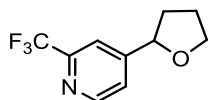

2-methyl-6-(4-(tetrahydrofuran-2-yl)phenyl)pyridine (20). Prepared according to the general procedure (72 hours) from 2-(4-chlorophenyl)-6-methylpyridine and THF. The title compound was isolated via flash chromatography (100/0 − 80/20 hexanes/ethyl acetate) as a clear oil (42.6 mg, 0.170 mmol, 85% yield after correcting for 4% biaryl impurity).

^{1}H NMR (501 MHz, CDCl$_3$): δ 7.96 (d, *J* = 8.1 Hz, 2H), 7.64 (t, *J* = 7.7 Hz, 1H), 7.53 (d, *J* = 7.8 Hz, 1H), 7.44 (d, *J* = 8.2 Hz, 2H), 7.10 (d, *J* = 7.5 Hz, 1H), 4.98 (t, *J* = 7.1 Hz, 1H), 4.15 (q, *J* = 7.2 Hz, 1H), 3.98 (q, *J* = 7.4 Hz, 1H), 2.64 (s, 3H), 2.37 (dq, *J* = 13.0, 6.7 Hz, 1H), 2.12 − 1.98 (m, 2H), 1.84 (dq, *J* = 12.1, 7.7 Hz, 1H).

^{13}C NMR (126 MHz, CDCl$_3$): δ 158.43, 156.95, 144.26, 138.79, 136.95, 127.07, 125.99, 121.59, 117.63, 80.55, 68.85, 34.84, 26.10, 24.89.

HRMS: (ESI-TOF) calculated for ([C$_{16}$H$_{17}$NO + H]$^+$): 240.1383, found: 240.1381.

FTIR (ATR, cm^{-1}): 2972, 2866, 1590, 1577, 1454, 1372, 1303, 1233, 1160, 1061, 1017, 921, 845, 788, 743.

4-(tetrahydrofuran-2-yl)-2-(trifluoromethyl)pyridine (21). Prepared according to the general procedure (72 hours) from 4-chloro-2-(trifluoromethyl)pyridine and THF. The crude reaction mixture was diluted with ethyl ether (20 mL) and washed with sat. CuSO$_4$ (aq) (20 mL). The aqueous phase was extracted with ethyl ether (20 mL) and the combined ethereal layers were dried over Na$_2$SO$_4$, filtered and concentrated under reduced pressure. The title compound was isolated via flash chromatography (gradient 100/0 − 80/20 hexanes/ethyl acetate) as a clear oil (33.9 mg, 0.156 mmol, 78% yield).

^{1}H NMR (501 MHz, CDCl$_3$): δ 8.66 (d, J = 5.0 Hz, 1H), 7.65 (s, 1H), 7.44 (d, J = 4.9 Hz, 1H), 4.97 (t, J = 7.2 Hz, 1H), 4.15 − 4.06 (m, 1H), 4.04 − 3.94 (m, 1H), 2.44 (dtd, J = 13.0, 7.4, 5.8 Hz, 1H), 2.10 − 1.94 (m, 2H), 1.77 (dq, J = 12.4, 7.6 Hz, 1H).

^{13}C NMR (126 MHz, CDCl$_3$): δ 155.16, 150.07, 148.48 (q, J = 34.4 Hz), 123.23, 121.74 (q, J = 274.2 Hz), 117.41 (q, J = 2.8 Hz), 78.87, 69.26, 34.53, 25.98.

^{19}F NMR (282 MHz, CDCl$_3$): δ − 67.98 (s).

HRMS: (ESI-TOF) calculated for ([C$_{10}$H$_{10}$F$_3$NO + H]$^+$): 218.0787, found: 218.0787.

FTIR (ATR, cm^{-1}): 2980, 2876, 1609, 1428, 1324, 1279, 1247, 1175, 1132, 1114, 1081, 1067, 995, 934, 854, 760, 729, 688, 665.
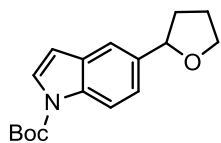

***tert*-butyl 5-(tetrahydrofuran-2-yl)-1H-indole-1-carboxylate (22).** Prepared according to the general procedure (73 hours) from *tert*-butyl 5-chloro-1H-indole-1-carboxylate and THF. The title compound was isolated via flash chromatography (gradient 100/0 − 90/10 hexanes/ethyl acetate) as a clear oil (39.7 mg, 0.138 mmol, 69% yield).

^{1}H NMR (501 MHz, CDCl$_3$): δ 8.08 (d, J = 8.4 Hz, 1H), 7.58 (d, J = 3.6 Hz, 1H), 7.54 (s, 1H), 7.29 − 7.24 (m, 1H), 6.54 (d, J = 3.6 Hz, 1H), 4.99 (t, J = 7.1 Hz, 1H), 4.14 (q, J = 6.9 Hz, 1H), 3.96 (q, J = 7.7 Hz, 1H), 2.35 (td, J = 12.2, 6.9 Hz, 1H), 2.10 − 1.97 (m, 2H), 1.84 (dq, J = 12.0, 7.5 Hz, 1H), 1.67 (s, 9H).

^{13}C NMR (126 MHz, CDCl$_3$): δ 149.91, 137.99, 134.57, 130.70, 126.30, 122.30, 118.00, 115.09, 107.48, 83.72, 81.07, 68.81, 35.13, 28.35, 26.22.

HRMS: (ESI-TOF) calculated for ([C$_{17}$H$_{21}$NO$_3$ + H]$^+$): 288.1594, found: 288.1594.

FTIR (ATR, cm^{-1}): 2975, 2868, 1728, 1582, 1537, 1471, 1439, 1357, 1334, 1284, 1254, 1217, 1193, 1158, 1128, 1080, 1060, 1041, 1021, 923, 886, 853, 818, 765, 724.
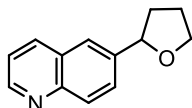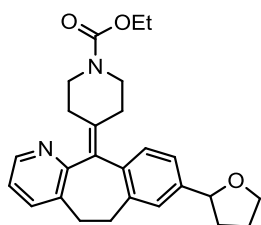
6-(tetrahydrofuran-2-yl)quinoline (23). Prepared according to the general procedure (74 hours) from 6-chloroquinoline and THF. The title compound was isolated via flash chromatography (70/25/5 hexanes/ethyl acetate/triethylamine) as a clear oil (19.2 mg, 0.096 mmol, 48% yield).

^{1}H NMR (501 MHz, CDCl$_3$): δ 8.89 (dd, J = 4.2, 1.7 Hz, 1H), 8.14 (d, J = 8.2 Hz, 1H), 8.08 (d, J = 8.7 Hz, 1H), 7.79 (s, 1H), 7.67 (dd, J = 8.7, 1.9 Hz, 1H), 7.39 (dd, J = 8.3, 4.2 Hz, 1H), 5.09 (t, J = 7.2 Hz, 1H), 4.24 – 4.13 (m, 1H), 4.07 – 3.96 (m, 1H), 2.43 (dq, J = 13.0, 6.8 Hz, 1H), 2.06 (p, J = 6.9 Hz, 2H), 1.88 (dq, J = 12.3, 7.7 Hz, 1H).

^{13}C NMR (126 MHz, CDCl$_3$): δ 150.24, 147.93, 142.00, 136.18, 129.69, 128.21, 127.81, 123.87, 121.38, 80.52, 69.07, 34.82, 26.21.

HRMS: (ESI-TOF) calculated for ([C$_{13}$H$_{13}$NO + H]$^+$): 200.1070, found: 200.1070.

FTIR (ATR, cm^{-1}): 2971, 2867, 1594, 1571, 1499, 1461, 1366, 1338, 1320, 1177, 1117, 1058, 922, 887, 835, 798, 770.


ethyl 4-(8-(tetrahydrofuran-2-yl)-5,6-dihydro-11H-benzo[5,6]cyclohepta[1,2-b]pyridin-11-ylidene)piperidine-1-carboxylate (24). Prepared according to the general procedure (75 hours) from ethyl 4-(8-chloro-5,6-dihydro-11H-benzo[5,6]cyclohepta[1,2-b]pyridin-11-ylidene)piperidine-1-carboxylate and THF. The title compound was isolated via flash chromatography (silica treated with triethylamine, 60/30/10 hexanes/ethylacetate/triethylamine) as a yellow oil (78.8 mg, 0.186 mmol, 93% yield after correcting for 6 mol % triethylamine). ^{13}C NMR showed a mixture of rotamers. HSQC and HMBC spectra can be seen in the NMR data section.

^{1}H NMR (501 MHz, CDCl$_3$): δ 8.36 (d, J = 4.6 Hz, 1H), 7.41 (d, J = 7.6 Hz, 1H), 7.19 – 7.00 (m, 4H), 4.80 (t, J = 6.5 Hz, 1H), 4.12 (q, J = 7.0 Hz, 2H), 4.05 (q, J = 7.1 Hz, 1H), 3.89 (q, J = 7.9 Hz, 1H), 3.79 (s, 2H), 3.43 – 3.30 (m, 2H), 3.10 (dq, J = 12.9, 5.9 Hz, 2H), 2.82 (dt, J = 11.8, 7.6 Hz, 2H), 2.46 (t, J = 10.3 Hz, 1H), 2.36 (s, 2H), 2.27 (tt, J = 14.0, 5.3 Hz, 2H), 1.97 (tt, J = 13.9, 6.9 Hz, 2H), 1.84 – 1.72 (m, 1H), 1.23 (td, J = 7.0, 1.5 Hz, 3H).

^{13}C NMR (126 MHz, CDCl$_3$): Rotamers observed in ^{13}C NMR. Peaks correlated to same proton by HSQC in parentheses. δ 157.72, 155.58, 146.56, 142.48, 142.45, 137.56, (137.44, 137.42), 136.70, 135.24, 133.78, (129.41, 129.28), (126.62, 126.33), (123.75, 123.41), 122.14, (80.58, 80.55), 68.70, 61.35, 44.97, 44.92, 34.38, 34.37, 32.04, 31.82, 31.77, 30.80, 30.61, 26.18, 14.77.

HRMS: (ESI-TOF) calculated for ([C$_{26}$H$_{30}$N$_2$O$_3$ + H]$^+$): 419.2329, found: 419.2333.

FTIR (ATR, cm^{-1}): 2977, 2868, 1686, 1559, 1435, 1386, 1326, 1277, 1227, 1172, 1114, 1060, 1027, 996, 906, 831, 767, 724.
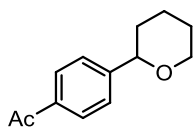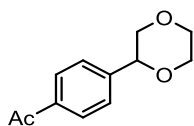
1-(4-(tetrahydro-2H-pyran-2-yl)phenyl)ethan-1-one (25). Prepared according to the general procedure (72 hours) from 4-chloroacetophenone and tetrahydropyran. The title compound was isolated via flash chromatography (gradient 100/0 – 85/15 hexanes/ethyl acetate) as a white solid (23.8 mg, 0.117 mmol, 58% yield).
^{1}H NMR (501 MHz, CDCl3): δ 7.93 (d, *J* = 8.3 Hz, 2H), 7.44 (d, *J* = 8.3 Hz, 2H), 4.48 – 4.29 (m, 1H), 4.16 (dd, *J* = 10.6, 2.8 Hz, 1H), 3.62 (td, *J* = 11.3, 2.7 Hz, 1H), 2.59 (s, 3H), 2.00 – 1.47 (m, 6H).
^{13}C NMR (126 MHz, CDCl3): δ 198.05, 148.90, 136.24, 128.59, 125.95, 79.64, 69.08, 34.29, 26.80, 25.90, 24.05.
HRMS: (ESI-TOF) calculated for ([$C_{13}H_{16}O_2$ + H]$^+$): 205.1223, found: 205.1223.
FTIR (ATR, cm^{-1}): 2939, 2851, 1673, 1605, 1570, 1469, 1444, 1409, 1351, 1306, 1265, 1202, 1180, 1170, 1084, 1043, 1017, 957, 933, 887, 864, 816, 793, 737, 708.
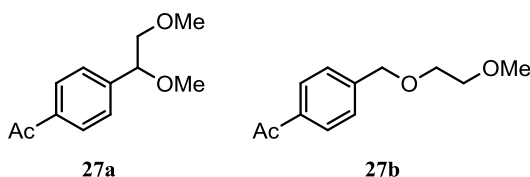

1-(4-(1,4-dioxan-2-yl)phenyl)ethan-1-one (26). Prepared according to the general procedure (74 hours) from 4-chloroacetophenone and 1,4-dioxane. The title compound was isolated as a mixture with 6% biaryl via flash chromatography (gradient 100/0 – 80/20 hexanes/ethyl acetate) as a white solid (29 mg, 0.131 mmol, 66% yield after correcting for 6 mol% biaryl). The ^{1}H NMR yield (78%) against 1-fluoronaphthalene as an external standard was reported.
^{1}H NMR (501 MHz, CDCl3): δ 7.94 (d, *J* = 8.3 Hz, 2H), 7.44 (d, *J* = 8.2 Hz, 2H), 4.68 (dd, *J* = 10.1, 2.5 Hz, 1H), 4.00 – 3.84 (m, 3H), 3.81 (dd, *J* = 11.5, 2.0 Hz, 1H), 3.73 (td, *J* = 11.4, 3.2 Hz, 1H), 3.45 – 3.37 (m, 1H), 2.59 (s, 3H)
^{13}C NMR (126 MHz, CDCl3): δ 197.83, 143.58, 136.86, 128.61, 126.38, 77.52, 72.36, 67.11, 66.47, 26.79.
HRMS: (ESI-TOF) calculated for ([$C_{12}H_{14}O_3$ + H]$^+$): 207.1016, found: 207.1012.
FTIR (ATR, cm^{-1}): 2872, 1681, 1605, 1570, 1463, 1409, 1358, 1267, 1231, 1129, 1113, 1069, 1043, 1022, 1011, 992, 959, 918, 888, 860, 839, 817, 738, 717.

Prepared according to the general procedure (72 hours) from 4-chloroacetophenone and 1,2-dimethoxyethane. The title compounds were isolated as a mixture (1.35:1 27a:27b) via flash chromatography (gradient 100/0 – 70/30 hexanes/ethyl acetate) as a clear oil (38 mg, 0.182 mmol, 91% combined yield). Pure samples of each regioisomer were obtained after additional flash chromatography (80/20 hexanes/ethyl acetate) by collecting a fraction from each tail of the chromatogram peak.
1-(4-(1,2-dimethoxyethyl)phenyl)ethan-1-one (27a)
^{1}H NMR (501 MHz, CDCl3): δ 7.96 (d, *J* = 8.3 Hz, 2H), 7.44 (d, *J* = 8.2 Hz, 2H), 4.45 (dd, *J* = 7.7, 3.7 Hz, 1H), 3.59 (dd, *J* = 10.4, 7.7 Hz, 1H), 3.44 (dd, *J* = 10.4, 3.7 Hz, 1H), 3.39 (s, 3H), 3.31 (s, 3H), 2.61 (s, 3H).

13C NMR (126 MHz, CDCl₃): δ 197.90, 144.58, 137.04, 128.72, 127.30, 82.72, 76.91, 59.50, 57.43, 26.84.

HRMS: (ESI-TOF) calculated for ($[C_{12}H_{16}O_3 + H]^+$): 209.1172, found: 209.1168.

FTIR (ATR, cm⁻¹): 2927, 1684, 1608, 1411, 1359, 1267, 1102, 834.

1-(4-((2-methoxyethoxy)methyl)phenyl)ethan-1-one (27b)

¹H NMR (501 MHz, CDCl₃): δ 7.94 (d, J = 8.3 Hz, 2H), 7.45 (d, J = 8.3 Hz, 2H), 4.64 (s, 2H), 3.67 – 3.63 (m, 2H), 3.62 – 3.57 (m, 2H), 3.41 (s, 3H), 2.60 (s, 3H).

¹³C NMR (126 MHz, CDCl₃): δ 198.00, 143.93, 136.55, 128.64, 127.57, 72.79, 72.10, 69.91, 59.30, 26.83.

HRMS: (ESI-TOF) calculated for ($[C_{12}H_{16}O_3 + H]^+$): 209.1172, found: 209.1173.

FTIR (ATR, cm⁻¹): 2890, 1680, 1609, 1412, 1357, 1265, 1096, 816.
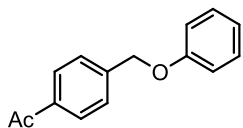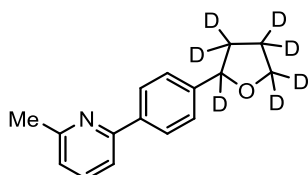

1-(4-(phenoxymethyl)phenyl)ethan-1-one (28). Prepared according to the general procedure (72 hours) from 4-chloroacetophenone and anisole. The title compound was isolated via flash chromatography (gradient 100/0 – 80/20 hexanes/ethyl acetate) as a white solid (21.4 mg, 0.095 mmol, 47% yield).

¹H NMR (501 MHz, CDCl₃): δ 7.98 (d, J = 8.2 Hz, 2H), 7.54 (d, J = 8.2 Hz, 2H), 7.34 – 7.27 (m, 2H), 6.98 (app. t, J = 8.5 Hz, 3H), 5.14 (s, 2H), 2.61 (s, 3H).

¹³C NMR (126 MHz, CDCl₃): δ 197.87, 158.54, 142.66, 136.77, 129.71, 128.80, 127.28, 121.39, 114.95, 69.31, 26.83.

HRMS: (ESI-TOF) calculated for ($[C_{15}H_{14}O_2 + H]^+$): 227.1067, found: 227.1065.

FTIR (ATR, cm⁻¹): 2924, 1682, 1598, 1584, 1485, 1462, 1412, 1382, 1353, 1303, 1265, 1237, 1172, 1080, 1031, 1016, 993, 956, 874, 824, 811, 754, 691.

2-methyl-6-(4-(tetrahydrofuran-2-yl-d7)phenyl)pyridine (32). Prepared according to the general procedure (72 hours) from 2-(4-chlorophenyl)-6-methylpyridine and THF-d₈. A pure fraction of the title compound was isolated via flash chromatography (100/0 – 80/20 hexanes/ethyl acetate) as a clear oil for deuterium labeling experiments.

¹H NMR (501 MHz, CDCl₃): δ 7.94 (d, J = 8.1 Hz, 2H), 7.62 (t, J = 7.7 Hz, 1H), 7.50 (d, J = 7.8 Hz, 1H), 7.42 (d, J = 8.1 Hz, 2H), 7.08 (d, J = 7.6 Hz, 1H), 2.62 (s, 3H).

²H NMR (77 MHz, THF-h8): δ 4.77 (s, 1D), 3.95 (s, 1D), 3.75 (s, 1D), 2.22 (s, 1D), 1.86 (s, 2D), 1.62 (s, 1D).

¹³C NMR (126 MHz, CDCl₃): δ 158.44 , 156.96 , 144.26 , 138.74 , 137.02 , 127.10 , 126.02 , 121.63 , 117.69 , 80.35 – 79.54 (m), 68.44 – 67.40 (m), 34.18 – 33.45 (m), 25.47 – 25.00 (m), 24.88 .

HRMS: (ESI-TOF) calculated for ($[C_{16}H_{10}D_7NO + H]^+$): 247.1822, found: 247.1820.

FTIR (ATR, cm⁻¹): 2961, 2235, 2113, 1591, 1577, 1454, 1305, 1238, 1188, 1162, 1101, 1049, 1013, 965, 926, 841, 786, 745.
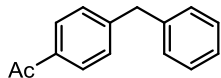
1-(4-benzylphenyl)ethan-1-one (38). Prepared according to the general procedure (72 hours) from 4-chloroacetophenone and toluene. The title compound was obtained in 60% yield by ^{1}H NMR against 1-fluoronaphthalene as an external standard. Crude ^{1}H NMR spectrum was in agreement with the literature *(25)*. The identity of the product was confirmed by HRMS.
<u>HRMS:</u> (ESI-TOF) calculated for ($[C_{15}H_{14}O + H]^+$): 211.1117, found: 211.1116.
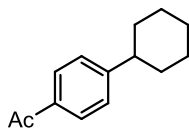
4-cyclohexylacetophenone (39). A ½-dram borosilicate vial (Fisher part number: 03-338AA) equipped with a PTFE-coated stir bar was brought into a N_2-filled glove box. The vial was charged with K_3PO_4 (21 mg, 0.1 mmol, 2 equiv.), a 0.40 M solution of 4-chloroacetophenone in benzene (0.125 mL, 0.05 mmol, 1 equiv.), a 2.5 M solution of cyclohexane in benzene (0.200 mL, 0.5 mmol, 10 eq), a pre-stirred 2 mM solution of Ir[dF(CF$_3$)ppy]$_2$(dtbbpy)PF$_6$ (0.500 mL, 1 µmol, 0.02 equiv.) and a pre-stirred solution containing Ni(cod)$_2$ (1.4 mg, 5 µmol, 0.1 equiv.) and 4,4′-di-*tert*-butyl-2,2′-bipyridine (2.0 mg, 7.5 µmol, 0.15 equiv.) in benzene (0.425 mL). The vial was capped with a Teflon septum cap and sealed with electrical tape. The vial was removed from the glove box, set to stir (800 rpm) and irradiated with a 25 W blue LED array (0.5 cm away, with cooling fan to keep the reaction at room temperature). After 72 hours, the crude mixture was analyzed by GC-FID relative to 1-fluoronapthalene as an external standard to give the title compound (41% yield). The identity of the product was confirmed by GC retention time against authentic product purchased from Sigma Aldrich.

IV. Synthesis and Characterization of Other Materials
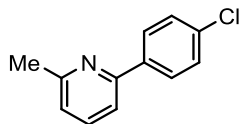
2-(4-chlorophenyl)-6-methylpyridine (30–Cl**).** Synthesis adapted from a reported procedure *(26)*. A mixture containing (4-chlorophenyl)boronic acid (0.45 g, 3.1 mmol), 2-bromo-6-methylpyridine (0.50 g, 2.9 mmol), K_3PO_4 (0.82 g**,** 3.9 mmol) and ethylene glycol (30 mL) was heated to 80 ºC and set to stir. $Pd(OAc)_2$ (6.5 mg, 0.029 mmol) was added and the reaction was left to stir over night. The reaction mixture was combined with brine (30 mL) and extracted with diethyl ether (4 × 30 mL). The organic extracts were dried over $MgSO_4$, filtered and concentrated under reduced pressure. The title compound was isolated via flash chromatography (70/30 hexanes/ethyl acetate) as a white solid (0.59 g, 2.52 mmol, 87% yield). Spectroscopic data matched those previously reported *(27)*.

^{1}H NMR (501 MHz, CDCl$_3$): δ 7.93 (d, *J* = 8.5 Hz, 2H), 7.64 (t, *J* = 7.7 Hz, 1H), 7.49 (d, *J* = 7.8 Hz, 1H), 7.43 (d, *J* = 8.6 Hz, 2H), 7.11 (d, *J* = 7.6 Hz, 1H), 2.62 (s, 3H).
**^{13}C NMR (126 MHz, CDCl$_3$):** δ 158.65, 155.78, 138.28, 137.18, 134.97, 128.98, 128.40, 122.05, 117.53, 24.87.
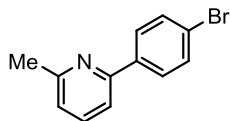
2-(4-bromophenyl)-6-methylpyridine (30–Br**).** Synthesis adapted from a reported method *(26)*. A mixture containing (4-bromophenyl)boronic acid (4.57 g, 22.7 mmol), 2-bromo-6-methylpyridine (3.44 g, 20.0 mmol), K_3PO_4 (5.65 g, 26.6 mmol) and ethylene glycol (100 mL) was heated to 80 ºC and set to stir. $Pd(OAc)_2$ (45 mg, 26.6 mmol) was added and the reaction was left to stir over night. The reaction mixture was combined with brine (100 mL) and extracted with diethyl ether (4 × 70 mL). The organic extracts were dried over $MgSO_4$, filtered and concentrated under reduced pressure. The title compound was isolated via flash chromatography (gradient 100/0 − 70/30 hexanes/ethyl acetate) as a white solid (1.1 g, 4.43 mmol, 22% yield). Spectroscopic data matched those previously reported *(28)*.

^{1}H NMR (501 MHz, CDCl$_3$): δ 7.87 (d, *J* = 8.6 Hz, 2H), 7.64 (t, *J* = 7.7 Hz, 1H), 7.58 (d, *J* = 8.6 Hz, 2H), 7.49 (d, *J* = 7.8 Hz, 1H), 7.12 (d, *J* = 7.6 Hz, 1H), 2.62 (s, 3H).
^{13}C NMR (126 MHz, CDCl$_3$): δ 158.67, 155.81, 138.68, 137.20, 131.93, 128.71, 123.31, 122.11, 117.51, 24.85.
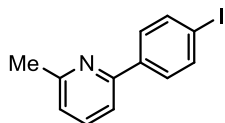
2-(4-iodophenyl)-6-methylpyridine (30–I**).** Synthesis adapted from reported procedures *(29,30)*. An oven dried Schlenk flask was charged with a PTFE stir bar, 2-(4-chlorophenyl)-6-methylpyridine (**30**–Cl) (0.87 g, 4.27 mmol), Pd-Xphos G2 (0.0170 g, 0.022 mmol), Xphos (0.0220g, 0.046 mmol), tetrahydroxydiboron (1.15 g, 12.78 mmol) and potassium acetate (1.26 g, 12.83 mmol). The Schlenk flask was equipped with a reflux condenser and evacuated and

backfilled with nitrogen. Degassed ethanol (30 mL) was added and the reaction mixture was refluxed for 3 hours and was cooled to room temperature. The mixture was diluted with water (10 mL) and extracted with ethyl acetate (3 × 10 mL). The organic extracts were dried over $MgSO_4$ and concentrated under reduced pressure. The resulting crude product was purified by flash chromatography (gradient 100/0 – 85/15 DCM/methanol) to give (4-(6-methylpyridin-2-yl)phenyl)boronic acid (0.5549 g, 2.60 mmol, 61% yield) as a tan solid which was used without any further purification.

An oven dried 3-neck flask was equipped with a PTFE stir bar and a reflux condenser. The flask was charged with (4-(6-methylpyridin-2-yl)phenyl)boronic acid (0.1041 g, 0.49 mmol), potassium carbonate (0.1698 g, 1.23 mmol) and iodine (0.2156 g, 0.85 mmol). The flask was evacuated and backfilled with nitrogen. Acetonitrile (2 mL) was added to the flask and the mixture was heated at reflux for 8 hours. After this period, the flask was cooled to room temperature. The mixture was diluted with water (10 mL) and extracted with ethyl acetate (3 × 10 mL). The organic extracts were dried over $MgSO_4$, concentrated under reduced pressure and the purified by flash chromatography (gradient 100/0 – 85/15 hexanes/ethyl acetate) to give the title compound as a brown solid (85 mg, 0.29 mmol, 59% yield).

^{1}H NMR (501 MHz, CDCl3): δ 7.79 (d, J = 8.5 Hz, 2H), 7.73 (d, J = 8.5 Hz, 2H), 7.65 (t, J = 7.7 Hz, 1H), 7.50 (d, J = 7.8 Hz, 1H), 7.13 (d, J = 7.6 Hz, 1H), 2.63 (s, 3H).

^{13}C NMR (126 MHz, CDCl3): δ 158.59, 155.81, 139.03, 137.94, 137.40, 128.94, 122.28, 117.63, 95.28, 24.75.

HRMS: (ESI-TOF) calculated for ($[C_{12}H_{10}IN + H]^+$): 295.9931, found: 295.9924.

FTIR (ATR, cm^{-1}): 2910, 1592, 1573, 1558, 1488, 1453, 1373, 1230, 1166, 1102, 1079, 1058, 1002, 863, 841, 830, 780, 738, 716.
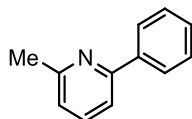
2-methyl-6-phenylpyridine. Synthesis adapted from a reported method *(26)*. A mixture containing phenylboronic acid (0.1340 g, 1.1 mmol), 2-bromo-6-methylpyridine (0.1720 g, 1.0 mmol), K_3PO_4 (0.2820 g, 1.3 mmol) and ethylene glycol (3 mL) was heated to 80 ℃ and set to stir. $Pd(OAc)_2$ (1.1 mg, 5.0 μmol) was added and the reaction was left to stir over night. The reaction mixture was combined with brine (10 mL) and extracted with diethyl ether (4 × 10 mL). The organic extracts were dried over $MgSO_4$, filtered and concentrated under reduced pressure. The title compound was isolated via flash chromatography (80/20 hexanes/ethyl acetate) as a white solid (0.1690 g, 1.0 mmol, 99% yield). Spectroscopic data matched those previously reported *(31)*.

^{1}H NMR (501 MHz, CDCl3): δ 7.98 (d, J = 7.5 Hz, 2H), 7.64 (t, J = 7.7 Hz, 1H), 7.52 (d, J = 7.8 Hz, 1H), 7.47 (t, J = 7.5 Hz, 2H), 7.40 (t, J = 7.3 Hz, 1H), 7.10 (d, J = 7.6 Hz, 1H), 2.64 (s, 3H).

^{13}C NMR (126 MHz, CDCl3): δ 158.48, 157.10, 139.90, 137.01, 128.82, 128.81, 127.13, 121.73, 117.76, 24.91.
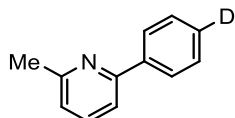
2-methyl-6-(phenyl-4-d)pyridine (31). Synthesis adapted from a reported method *(32)*. In a nitrogen filled glove a Schlenk flask equipped with a PTFE-coated stir bar was charged with 2-(iodophenyl)-6-methylpyridine (**30**–I) (59 mg, 0.2 mmol) and CuCl (20 mg, 0.2 mmol). The flask was sealed and removed from the glove box, then degassed methanol-d4 (1.5 mL) was added and the mixture was set to stir and cooled to 0 ºC with an ice bath. To the reaction mixture was added NaBD$_4$ (50 mg, 1.2 mmol) in three portions over 30 min. The reaction mixture was warmed to room temperature, quenched with saturated aqueous K$_2$CO$_3$ (5 mL) and extracted with diethyl ether (3 × 5 mL). The organic phase was separated, dried over MgSO$_4$ and concentrated under reduced pressure to give the title compound as a clear oil (30.6 mg, 0.180 mmol, 90% yield).

^{1}H NMR (501 MHz, CDCl$_3$): δ 7.98 (d, *J* = 8.3 Hz, 2H), 7.64 (t, *J* = 7.7 Hz, 1H), 7.52 (d, *J* = 7.8 Hz, 1H), 7.46 (d, *J* = 8.1 Hz, 2H), 7.10 (d, *J* = 7.6 Hz, 1H), 2.63 (s, 3H).
^{2}H NMR (77 MHz, THF-h8): δ 7.34 (s, 1D).
^{13}C NMR (126 MHz, CDCl$_3$): δ 158.50 , 157.13 , 139.94 , 137.01 , 128.71 , 128.43 (d, *J* = 24.5 Hz), 127.13 , 121.72 , 117.77 , 24.93
HRMS: (ESI-TOF) calculated for ([C$_{12}$H$_{10}$DN + H]$^+$): 171.1027, found: 171.1028.
FTIR (ATR, cm^{-1}): 2922, 1588, 1573, 1451, 1390, 1372, 1303, 1232, 1182, 1159, 1108, 1079, 1025, 995, 863, 791, 742, 728, 705.
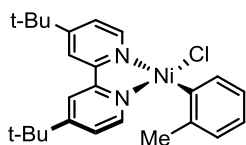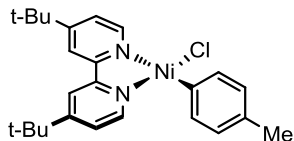

[(dtbbpy)Ni(*o*-tolyl)Cl] (33). In a nitrogen filled glove box a reaction tube equipped with a PTFE-coated stir bar was charged with Ni(cod)$_2$ (550 mg, 2.0 mmol), 4,4′-di-*tert*-butyl-2,2′-pyridine (537 mg, 2.0 mmol) and THF (5 mL). The resulting deep purple solution was left to stir for 1 hour at ambient temperature. To the reaction tube was added 2-chlorotoluene (12 mL, 103 mmol) and left to stir for 20 min. The resulting dark red solution was removed from the glove box and triturated with pentane. The precipitate was collected on a frit, rinsed with pentane and residual solvent was removed under high vacuum to give the title compound as a light red powder (700 mg, 1.54 mmol, 77% yield) with a small amount of residual aryl chloride as an impurity. The title compound was used in quenching and stoichiometric oxidation experiments without further purification.

^{1}H NMR (501 MHz, CD$_2$Cl$_2$): δ 9.03 (d, *J* = 5.9 Hz, 1H), 7.85 (s, 1H), 7.80 (d, *J* = 1.6 Hz, 1H), 7.57 – 7.50 (m, 2H), 7.15 (d, *J* = 6.2 Hz, 1H), 7.10 (dd, *J* = 6.2, 1.9 Hz, 1H), 6.83 – 6.75 (m, 3H), 3.05 (s, 3H), 1.42 (s, 9H), 1.34 (s, 9H).
^{13}C NMR (126 MHz, CD$_2$Cl$_2$): δ 164.08, 163.07, 156.43, 153.04, 151.49, 151.12, 149.46, 142.80, 135.89, 127.64, 124.10, 123.74, 123.39, 122.91, 117.99, 117.19, 35.89, 35.80, 30.58, 30.35, 25.33.
HRMS: (ESI-TOF) calculated for ([C$_{25}$H$_{31}$ClN$_2$Ni – Cl + MeCN]$^+$): 458.2101, found: 458.2102.
FTIR (ATR, cm^{-1}): 2961, 1614, 1546, 1480, 1409, 1365, 1251, 1202, 1120, 1041, 1071, 899, 847, 736.
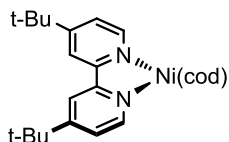
[(dtbbpy)Ni(*o*-tolyl)Cl] (34). In a nitrogen filled glove box a reaction tube equipped with a PTFE-coated stir bar was charged with Ni(cod)$_2$ (550 mg, 2.0 mmol), 4,4′-di-*tert*-butyl-2,2′-pyridine (537 mg, 2.0 mmol) and THF (5 mL). The resulting deep purple solution was left to stir for 1 hour at ambient temperature. To the reaction tube was added 4-chlorotoluene (6 mL, 51.5 mmol) and left to stir for 20 min. The resulting dark red solution was triturated with pentane and the precipitate was collected on a frit, rinsed with pentane and residual solvent was removed under high vacuum to give the title compound as a light red powder (621 mg, 1.37 mmol, 68% yield). The title compound was used in stoichiometric oxidation experiments without further purification.

^{1}H NMR (501 MHz, CD$_2$Cl$_2$): δ 9.00 (d, *J* = 5.2 Hz, 1H), 7.83 (s, 1H), 7.79 (s, 1H), 7.50 (d, *J* = 4.2 Hz, 1H), 7.36 (d, *J* = 5.6 Hz, 1H), 7.32 (d, *J* = 7.8 Hz, 2H), 7.11 (d, *J* = 5.9 Hz, 1H), 6.79 (d, *J* = 7.5 Hz, 2H), 2.25 (s, 3H), 1.40 (s, 9H), 1.33 (s, 9H).

^{13}C NMR (126 MHz, CD$_2$Cl$_2$): δ 163.54, 162.57, 155.87, 152.58, 151.88, 149.08, 144.50, 135.87, 131.38, 126.81, 123.28, 123.14, 117.35, 116.65, 35.35, 35.29, 30.05, 29.84, 20.32.

Elemental Analysis: calculated for ([C$_{25}$H$_{31}$ClN$_2$Ni] C, 66.19 %; H, 6.89 %; N, 6.17 %; Cl, 7.81 %, found: C, 66.16 %; H, 7.06 %; N, 5.89 %; Cl, 8.39 %.

FTIR (ATR, cm^{-1}): 3048, 2956, 2970, 2863, 1612, 1580, 1541, 1478, 1464, 1407, 1363, 1300, 1279, 1250, 1205, 1163, 1120, 1095, 1053, 1011, 927, 900, 882, 856, 793, 742, 723, 668.


[Ni(dtbbpy)(cod)]. In a nitrogen filled glove box a reaction tube equipped with a PTFE-coated stir bar was charged with Ni(cod)$_2$ (512 mg, 1.86 mmol), 4,4′-di-*tert*-butyl-2,2′-pyridine (500 mg, 1.86 mmol) and ethyl ether (10 mL). The tube was sealed with a Teflon coated septum cap and left to stir over night at ambient temperature. The resulting deep purple solution was concentrated under reduced pressure. Attempts were made to rinse the crude product but it was observed that the solid was completely soluble even in cold pentane. Concentration under reduced pressure gave the title compound as a shiny dark purple solid which was 94% pure by ^{1}H NMR with 4,4′-di-*tert*-butyl-2,2′-pyridine and 1,5-cyclooctadiene as impurities. The title compound was used in quenching experiments without any further purification. Spectroscopic data matched those previously reported *(33)*. The ^{13}C NMR spectrum of the crude material contained unidentified peaks.

^{1}H NMR (501 MHz, THF-d8): δ 9.89 (d, *J* = 6.1 Hz, 2H), 7.89 (d, *J* = 1.7 Hz, 2H), 7.42 (dd, *J* = 6.1, 2.0 Hz, 2H), 3.64 (s, 4H), 2.83 – 2.61 (m, 4H), 1.80 (q, *J* = 7.8 Hz, 4H), 1.39 (s, 18H).

^{13}C NMR (126 MHz, THF-d8): δ 150.88, 149.97, 146.92, 121.18, 118.55, 112.97, 90.48, 81.19, 68.13, 36.19, 32.36, 31.43, 30.48, 26.02.

V. Stoichiometric Experiments with Halide Additives

Procedure for Stoichiometric Experiments with Halide Additives. A threaded 16 × 125 mm borosilicate reaction tube (Kimble part number: 73750-16125) equipped with a PTFE-coated stir bar was brought into a N_2-filled glove box and charged with halide additive (0.2 mmol, 1 equiv.) and K_3PO_4 (85 mg, 0.4 mmol, 2 equiv.). To the reaction tube the following were added successively: a clear solution of 4-halotoluene (0.2 mmol, 1 equiv.) in THF (0.5 mL), a yellow solution of Ir[dF(CF₃)ppy]₂(dtbbpy)PF₆ (4.5 mg, 4 µmol, 0.02 equiv.) in THF (1.5 mL) and a dark purple solution of Ni(cod)₂ (5.5 mg, 20 µmol, 0.1 equiv.) and 4,4′-di-*tert*-butyl-2,2′-bipyridine (8.1 mg, 30 µmol, 0.15 equiv.) in THF (3 mL). The tube was capped with a Teflon septum cap and sealed with electrical tape. The reaction tube was removed from the glove box, set to stir (800 rpm) and irradiated with a 34 W blue LED lamp (2 cm away, with cooling fan to keep the reaction at room temperature) for 72 h. The crude product was analyzed by ^{1}H NMR (10 s delay) and GC-FID relative to 1-fluoronaphthalene as an external standard.
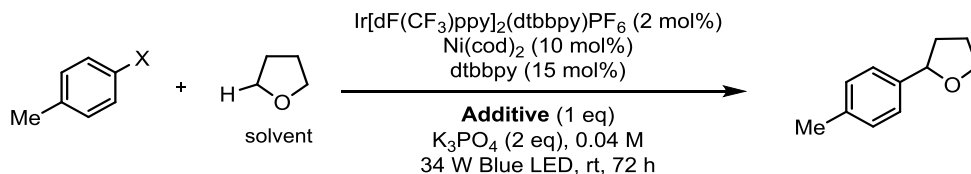
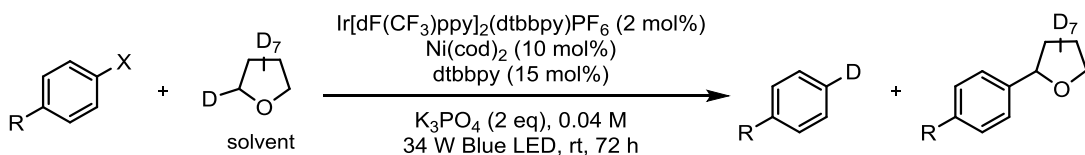| Entry	X	Additive	Yield[a]	Entry	X	Additive	Yield[a]
1	Cl	none	68%[b]	8	Cl	TBACl	65%[c]
2	Br	none	10%	9	Cl	TBABr	63%[b]
3	I	none	5%	10	Cl	TBAI	66%[b]
4	I	TBACl	51%	11	OTf	none	0%
5	I	TBABr	37%	12	OTf	TBACl	10%
6	I	TBAI	6%	13	OTf	TBABr	7%
7	I	TMAF	3%	14	OTf	TBAI	0%
				15	OTf	TBAF	0%

Table S6. Evaluation of halide additives with various *p*-tolyl halides. Reactions were carried out at 0.2 mmol scale. [a] Yield determined by GC-FID using 1-fluoronaphthalene as an external standard. [b] Yield determined by ^{1}H NMR spectroscopy using 1-fluoronaphthalene as an external standard. [c] Reaction was carried out at 0.05 mmol scale.
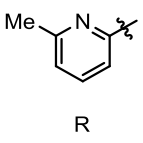
VI. Deuterium Labeling Experiments

Procedure for Deuterium Labeling Experiments. Note: 2-(4-halophenyl)-6-methylpyridines were chosen for these experiments because the products would not evaporate under the high vacuum necessary to remove THF-d$_8$ prior to ^{2}H NMR analysis and the methylpyridine group offered a mass handle for LC-MS analysis. A threaded 16×125 mm borosilicate reaction tube (Kimble part number: 73750-16125) equipped with PTFE-coated stir bar was brought into a N$_2$-filled glove box and charged with 2-(4-halophenyl)-6-methylpyridine (0.05 mmol, 1 equiv.) and K$_3$PO$_4$ (21 mg, 0.1 mmol, 2 equiv.). To the reaction tube the following were added successively: a yellow solution of Ir[dF(CF$_3$)ppy]$_2$(dtbbpy)PF$_6$ (1.1 mg, 1 μmol, 0.02 equiv.) in THF-d$_8$ (0.75 mL) and a dark purple solution of Ni(cod)$_2$ (1.4 mg, 5 μmol, 0.1 equiv.) and 4,4´-di-*tert*-butyl-2,2´-bipyridyl (2.0 mg, 7.5 μmol, 0.15 equiv.) in THF-d$_8$ (0.5 mL). The tube was capped with a Teflon septum cap and sealed with electrical tape. The reaction tube was removed from the glove box,m set to stir (800 rpm) and irradiated with a 34 W blue LED lamp (2 cm away, with cooling fan to keep the reaction at room temperature) for 72 h. The crude reaction mixture was filtered through cotton, concentrated *in vacuo* and left under high vacuum for 30 minutes. The crude product was analyzed by ^{2}H NMR (10 s delay) relative to DMF-d$_7$ as an external standard and by GC-FID relative to 1-fluoronaphthalene as an external standard. The presence of each product was confirmed by LC-MS.
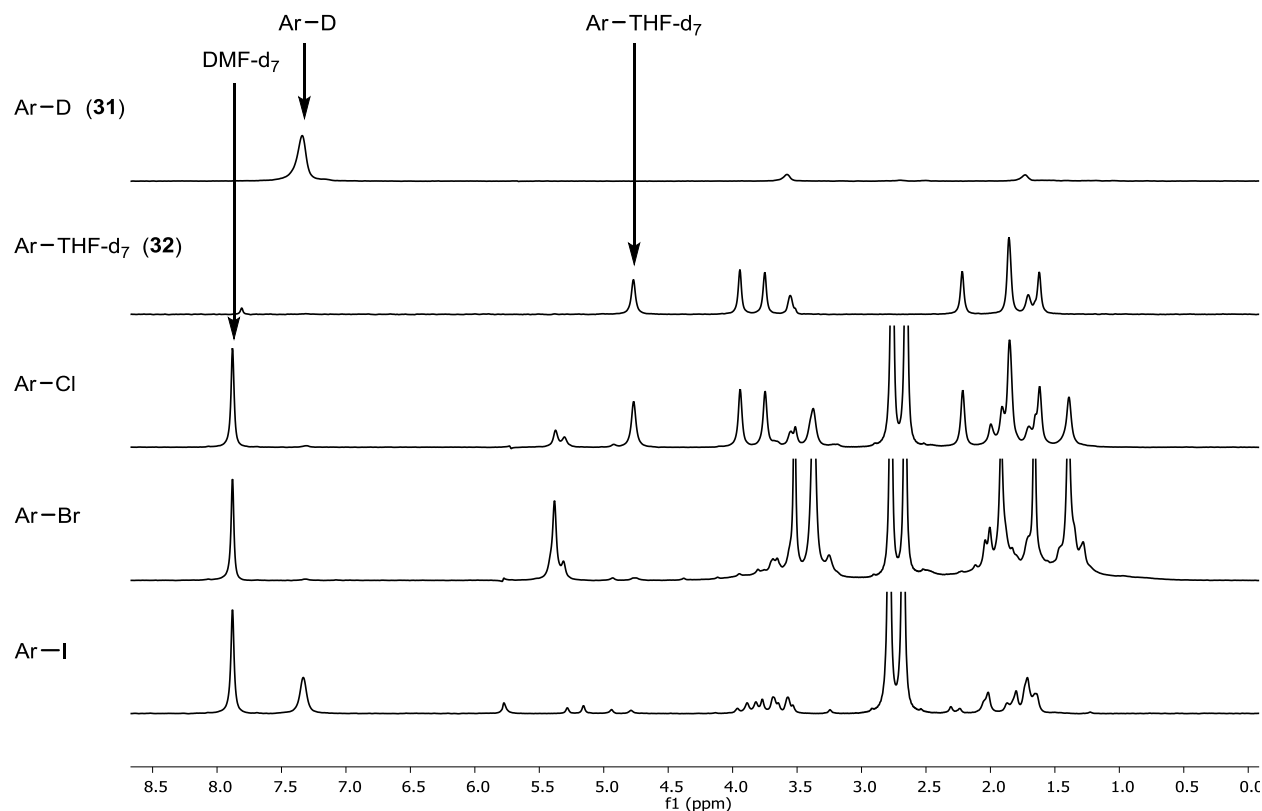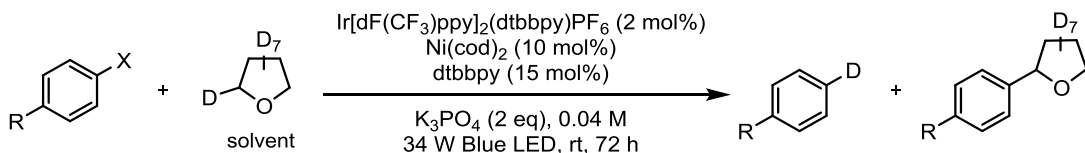

Fig. S1. ^{2}H NMR spectra for authentic products and concentrated reaction mixtures after addition of DMF-d$_7$ as an external standard. The spectra from the top: 2-methyl-6-(phenyl-4-d)pyridine authentic product, 2-methyl-6-(4-(tetrahydrofuran-2-yl-d7)phenyl)pyridine authentic product, reaction of 2-(4-chlorophenyl)-6-methylpyridine, reaction of 2-(4-bromophenyl)-6-methylpyridine, reaction of 2-(4-iodophenyl)-6-methylpyridine.

Reaction scheme conditions:
Ir[dF(CF$_3$)ppy]$_2$(dtbbpy)PF$_6$ (2 mol%)
Ni(cod)$_2$ (10 mol%)
dtbbpy (15 mol%)
K$_3$PO$_4$ (2 eq), 0.04 M
34 W Blue LED, rt, 72 h
solvent

Entry	X	Ar-D Yield	Ar-THF-d$_7$ Yield
1	Cl	3%	**68%**
2	Br	2%	5%
3	I	**66%**	4%

Table S7. Deuterium labeling experiments. Yields determined by ^{2}H NMR using DMF-d$_7$ as an external standard. Reactions were carried out at 0.05 mmol scale.

Reaction scheme conditions:
Ir[dF(CF$_3$)ppy]$_2$(dtbbpy)PF$_6$ (2 mol%)
Ni(cod)$_2$ (10 mol%)
dtbbpy (15 mol%)
K$_3$PO$_4$ (2 eq), 0.04 M
34 W Blue LED, rt, 72 h
solvent

Entry	X	Ar-X Conversion	Ar-D/H Yield	Ar-THF-d$_7$ Yield
1	Cl	98%	4%	**73%**
2	Br	100%	4%	4%
3	I	97%	**70%**	3%

Table S8. Deuterium labeling experiments. Yields and conversion determined by GC-FID using 1-fluoronaphthalene as an external standard. Reactions were carried out at 0.05 mmol scale. The full conversion but low yield observed for entry 2 can be explained in part by the production of large quantities of biaryl which was observed via LC-MS. For additional analysis of byproducts in the reaction of aryl bromides see figure S2 and Table S9.

S22
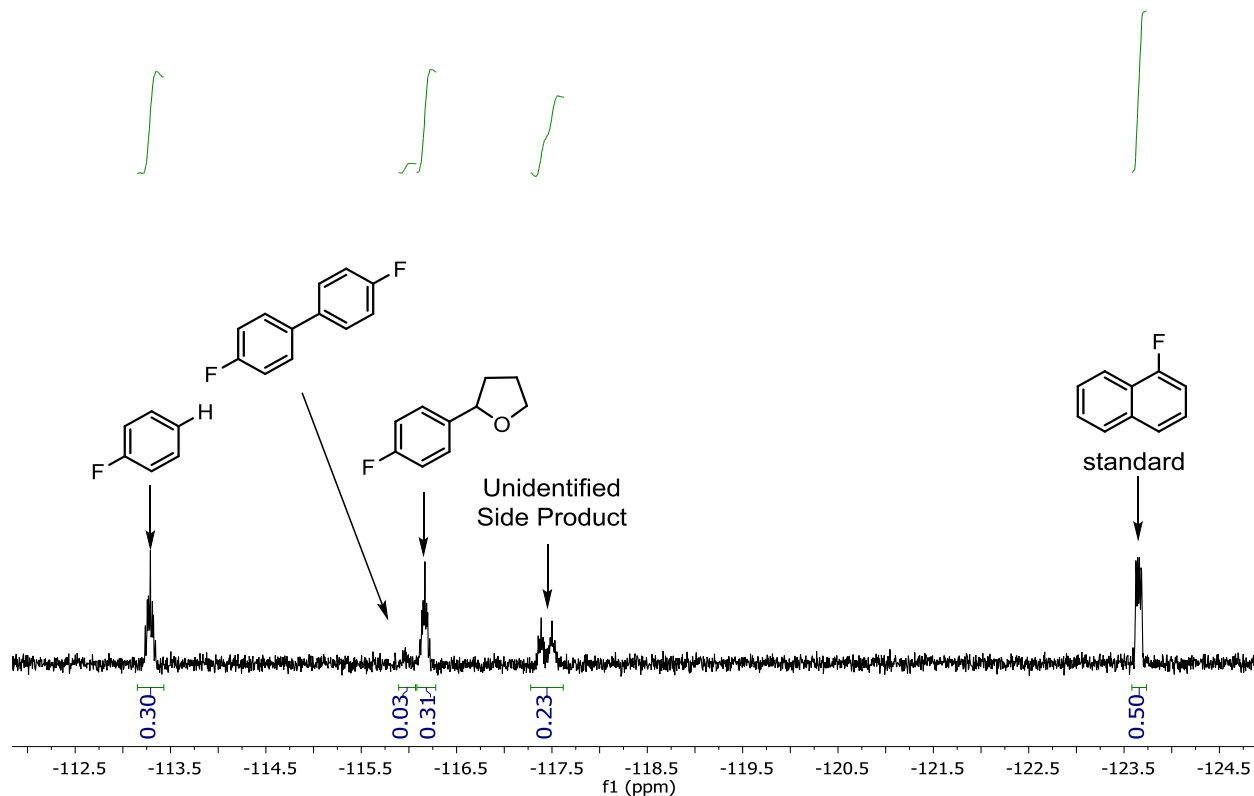
Fig. S2. A comment on the reaction of aryl bromides. The high conversion and low yields observed in reactions of aryl bromides prompted a study of the product distribution. The above ^{19}F NMR corresponds to the crude reaction mixture for Table S9 entry 2 below. Yields and conversion were determined by ^{19}F NMR using 1-fluoronaphthalene as an external standard. With the exception of the peaks at -117.5 ppm all fluorinated products were positively identified by ^{19}F NMR shift and by spiking the crude reaction mixture with a pure sample of each compound. Attempts to isolate a pure sample of the unidentified side product were unsuccessful. Interestingly this product distribution shows a strong dependence on the light source used in the reaction (see Table S9 below).
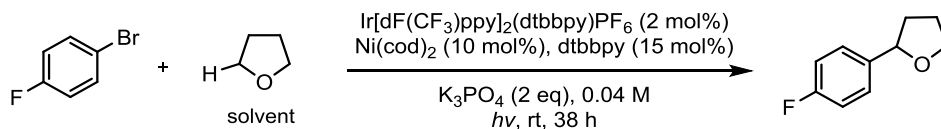
Entry	*hv*	Ar-Br Conv.	Ar-H Yield	Ar-Ar Yield	Unidentified Product Int.	Ar-THF Yield
1	25 W Blue LEDs	78%	0%	21%	5%	**44%**
2	34 W Blue LED	100%	30%	3%	23%	**31%**

Table S9. Reaction of aryl bromides. Reactions were carried out at 0.3 mmol scale. Yields and conversion were determined by ^{19}F NMR using 1-fluoronaphthalene as an external standard.

VII. Halogen Exchange Experiments

Procedure for Halogen Exchange Experiments. A threaded 16×125 mm borosilicate reaction tube (Kimble part number: 73750-16125) equipped with a PTFE-coated stir bar was brought into a N_2-filled glove box and charged with tetrabutylammonium chloride (56 mg, 0.2 mmol, 1 equiv.) and K_3PO_4 (85 mg, 0.4 mmol, 2 equiv.). To the reaction tube the following were added successively: a clear solution of 4-halotoluene (0.2 mmol, 1 equiv.) in THF (0.5 mL), a yellow solution of Ir[dF(CF$_3$)ppy]$_2$(dtbbpy)PF$_6$ (4.5 mg, 4 μmol, 0.02 equiv.) in THF (1.5 mL) and a dark purple solution of Ni(cod)$_2$ (5.5 mg, 20 μmol, 0.1 equiv.) and 4,4′-di-*tert*-butyl-2,2′-bipyridyl (8.1 mg, 30 μmol, 0.15 equiv.) in THF (3 mL). The tube was capped with a Teflon septum cap and sealed with electrical tape. The reaction tube was removed from the glove box, set to stir (800 rpm) and irradiated with a 34 W blue LED lamp (2 cm away, with cooling fan to keep the reaction at room temperature) for 72 h. The crude product was analyzed by ^{1}H NMR (10 s delay) and GC-FID relative to 1-fluoronaphthalene as an external standard.
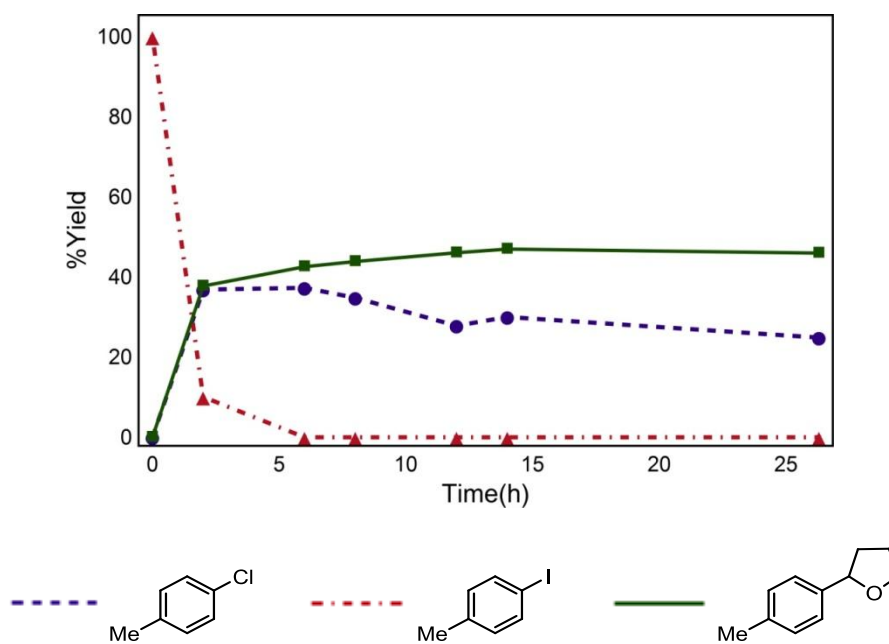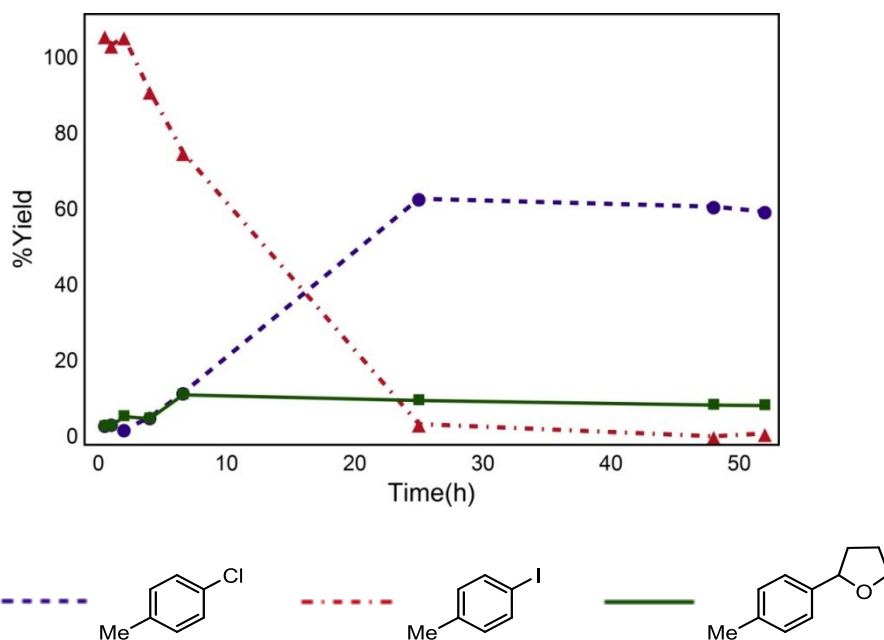

Fig. S3. Halogen exchange time points to 27 hours with 34W blue LED lamps. Yields and conversion determined by GC-FID using 1-fluoronaphthalene as an external standard. Reactions were carried out at 0.1 mmol scale.
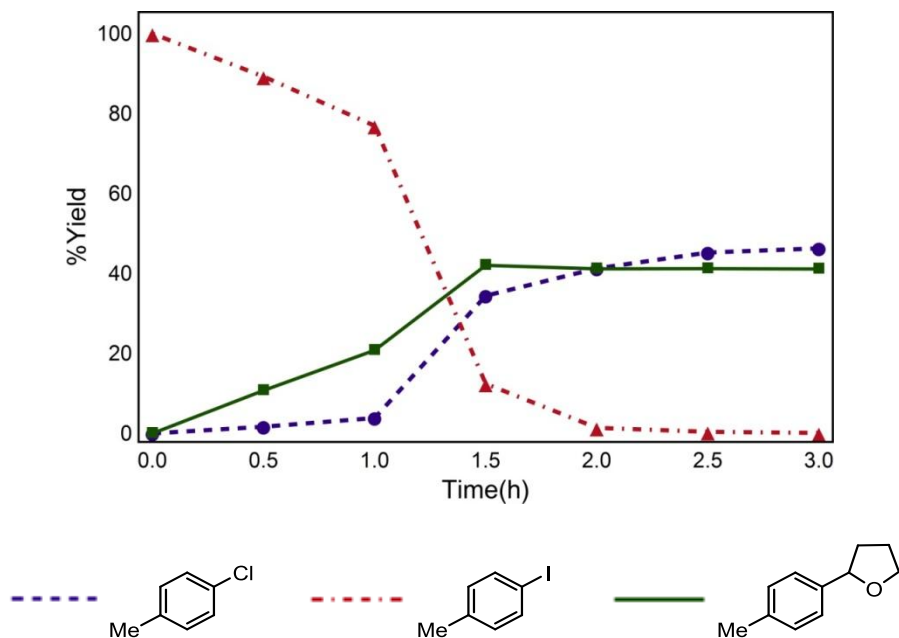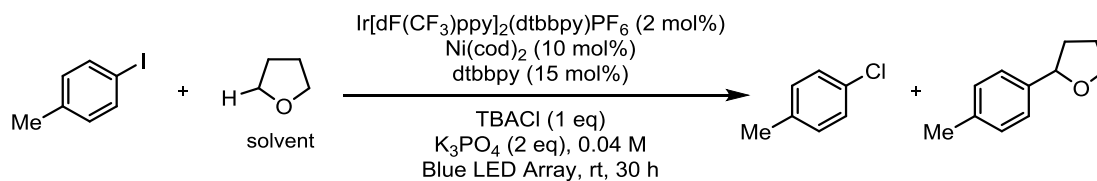
Fig. S4. Halogen exchange time points to 3 hours with 34 W blue LED lamps. Yields and conversion determined by GC-FID using 1-fluoronaphthalene as an external standard. Reactions were carried out at 0.1 mmol scale.

Fig. S5. Halogen exchange time points to 52 hours with 25 W blue LED array. Yields and conversion determined by GC-FID using 1-fluoronaphthalene as an external standard. Reactions were carried out at 0.1 mmol scale. Notice that the formation of THF product is much less efficient under irradiation with the blue LED array but the halogen exchange follows the same trend as with 34 W blue LED lamps.

Reaction scheme: Ir[dF(CF$_3$)ppy]$_2$(dtbbpy)PF$_6$ (2 mol%), Ni(cod)$_2$ (10 mol%), dtbbpy (15 mol%), TBACl (1 eq), K$_3$PO$_4$ (2 eq), 0.04 M, Blue LED Array, rt, 30 h, solvent.

Entry	Deviation	Ar-I Conversion	Ar-Cl Yield	Ar-THF Yield
1	none	60%	**36%**	9%
2	no photocatalyst	11%	**7%**	2%
3	dark	14%	**2%**	1%
4	no Ni(cod)$_2$/dtbbpy	-1%	**0%**	0%
5	no K$_3$PO$_4$	95%	**58%**	16%

Table S10. Halogen exchange controls with 25 W blue LED array. Yields and conversion determined by GC-FID relative to 1-fluoronaphthalene as an external standard. Reactions were carried out at 0.05 mmol scale.

Discussion: The exact mechanism by which exogenous chloride and bromide enable the reaction of aryl iodides is not well understood. This reaction could take place via a common catalytic intermediate (for example [(dtbbpy)Ni(III)(Ar)(I)(Cl)] generated by Ni(I) oxidative addition; stoichiometric oxidation experiments show that such a Ni(III) aryl chloride complex can reductively eliminate aryl chloride or undergo photolysis toward the functionalization reaction) or halogen exchange to make the aryl chloride followed by consumption in the catalytic functionalizaiton reaction. Time point experiments offer one argument against the latter option (Fig. S3 and S4). The reaction of 4-iodotoluene with exogenous chloride is complete after only 3 hours, significantly faster than the reaction of 4-chlorotoluene (72 hours). By analogy it is anticipated that the reaction of aryl iodides with exogenous bromide also proceeds by a mechanism distinct from the reaction of aryl bromides. These observations offers some insight into why, for example, the addition of TBABr to the reaction of 4-iodotoluene surpasses the efficiency of 4-bromotoluene alone (see Table S6).

VIII. Emission Quenching Experiments and Spectroscopic Data

Experimental design. Quenching studies were designed to compare quenching kinetics for the reaction mixture to the individual components of the reaction. An excitation wavelength of 405 nm ($\varepsilon = 4.2 \times 10^3$ M^{-1} cm^{-1}), at the intersection of lamp emission and photocatalyst absorption (Fig. S6), was selected in order to exclude any photolytic processes not native to the synthetic reaction. Experiments were conducted at photocatalyst concentrations similar to the synthetic reaction. Inner filter effects were quantified and corrected by linear absorption measurements.
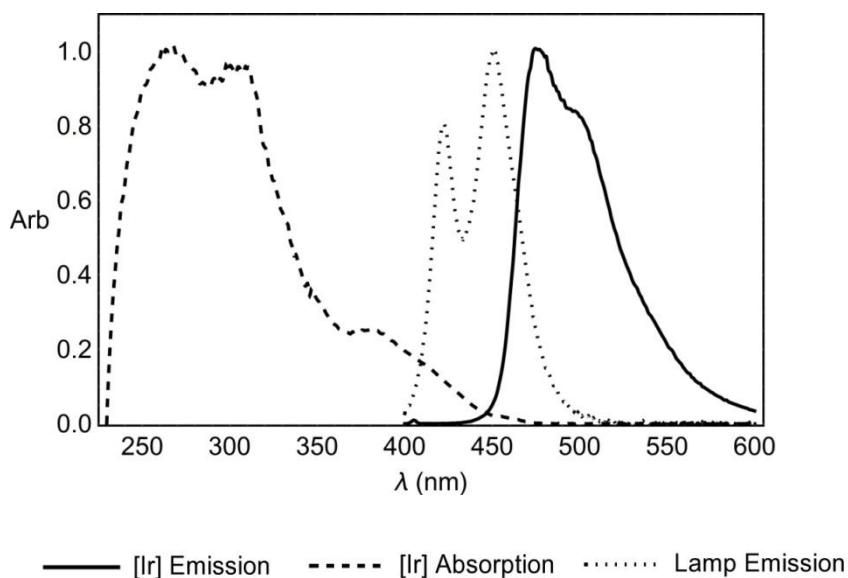
Fig. S6. Normalized absorption, emission and lamp emission data. Electronic absorption (dashed) and emission (solid) spectra of $Ir[dF(CF_3)ppy]_2(dtbbpy)PF_6$ displayed with emission spectrum for 34W blue LED lamp.

Linear Absorption Data. Linear absorption spectra were collected on an Agilent 8453 Spectrophotometer. All reagents were dispensed in stock solutions prepared volumetrically inside a nitrogen filled glove box. In a typical experiment, THF and an appropriate amount of analyte dispensed in THF were added to screw-top 1.0 cm quartz cuvette. The cuvette was then sealed with a septum cap and electrical tape, removed from the glovebox and a spectrum was collected. All Ni(dtbbpy)(cod)/aryl halide mixtures were stirred until the reaction mixture had changed from deep purple to ruby red. Complete consumption of Ni(dtbbpy)(cod) was confirmed by linear absorption measurements which showed the disappearance of the broad visible absorption of Ni(dtbbpy)(cod) (Fig. S12, $\lambda_{max} = 562$ nm) and the appearance of an absorption spectrum consistent with that of the independently prepared oxidative adduct (Fig. S8, $\lambda_{max} = 469$ nm).   In some cases baseline drifting was observed due to the use of a separate cuvette for the blank (air sensitivity of quenchers and photocatalyst quenching by oxygen precluded titration via syringe). Baseline drift was corrected by setting the absorbance at 900 nm equal to zero where applicable.
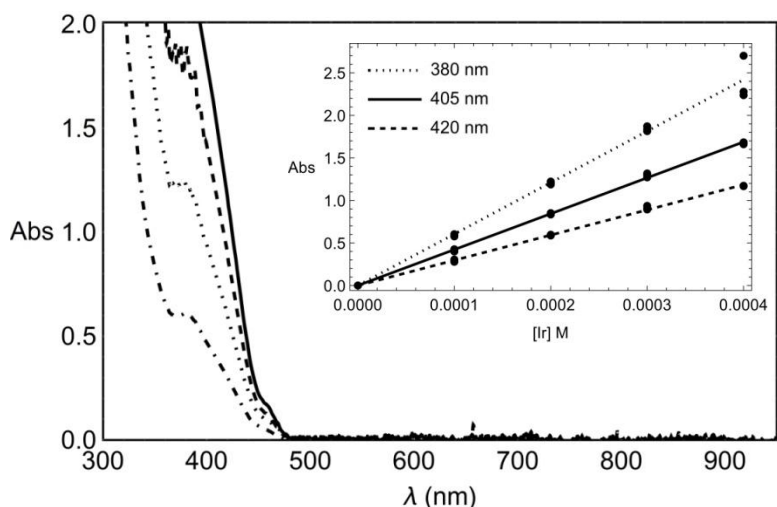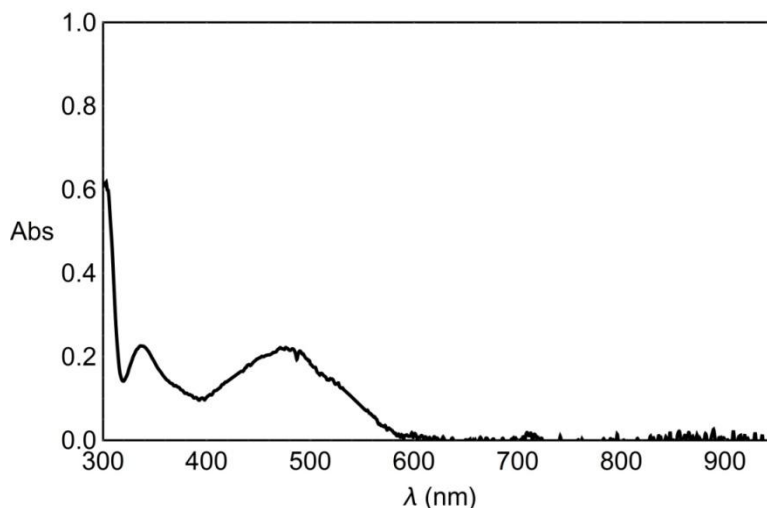
Fig. S7. Electronic absorption spectra of Ir[dF(CF$_3$)ppy]$_2$(dtbbpy)PF$_6$ in THF at various concentrations around those employed in quenching experiments: dot dashed 1.0×10^{-4} M, dotted 2.0×10^{-4} M, dashed 3.0×10^{-4} M, solid 4.0×10^{-4} M. In the inset calibration curves at various wavelengths: Ir[dF(CF$_3$)ppy]$_2$(dtbbpy)PF$_6$ absorption maximum at 380 nm ($\varepsilon = 6.1 \times 10^3$ M^{-1} cm^{-1}), excitation wavelength used in quenching experiments at 405 nm ($\varepsilon = 4.2 \times 10^3$ M^{-1} cm^{-1}), emission band of 34W blue LED lamp at 420 nm ($\varepsilon = 3.0 \times 10^3$ M^{-1} cm^{-1}).
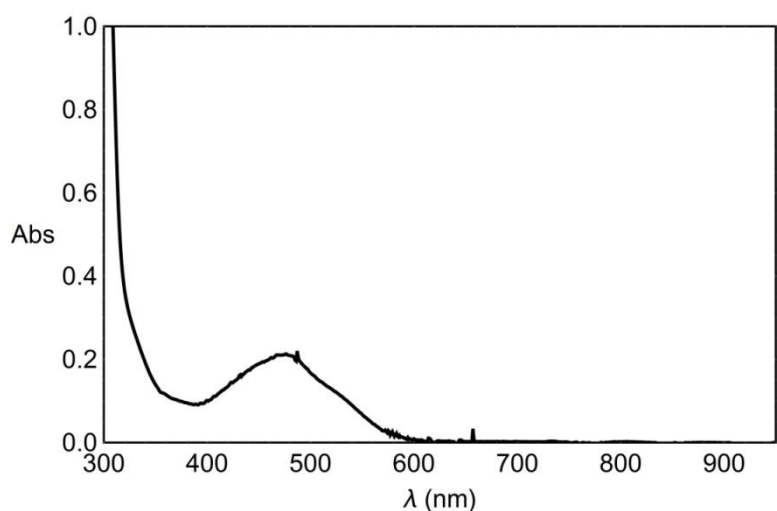
Fig. S8. Electronic absorption spectrum of (dtbbpy)Ni (*o*-tolyl)Cl (6.68×10^{-5} M) in THF. The visible region of the spectrum is dominated by a single band at 469 nm ($\varepsilon = 3.0 \times 10^3$ M^{-1} cm^{-1}). Optical densities of the quenching experiment mixtures at the excitation (405 nm, $\varepsilon = 1.9 \times 10^3$ M^{-1} cm^{-1}) and emission (478 nm, $\varepsilon = 3.0 \times 10^3$ M^{-1} cm^{-1}) wavelengths were used to account for inner filter effects.
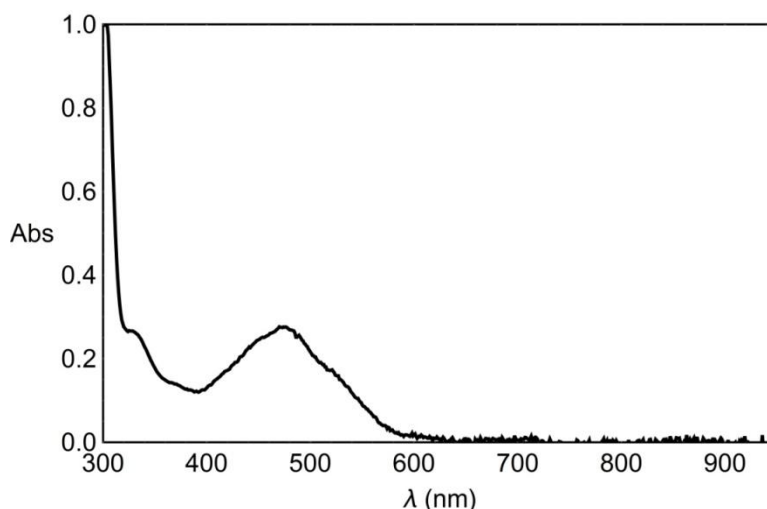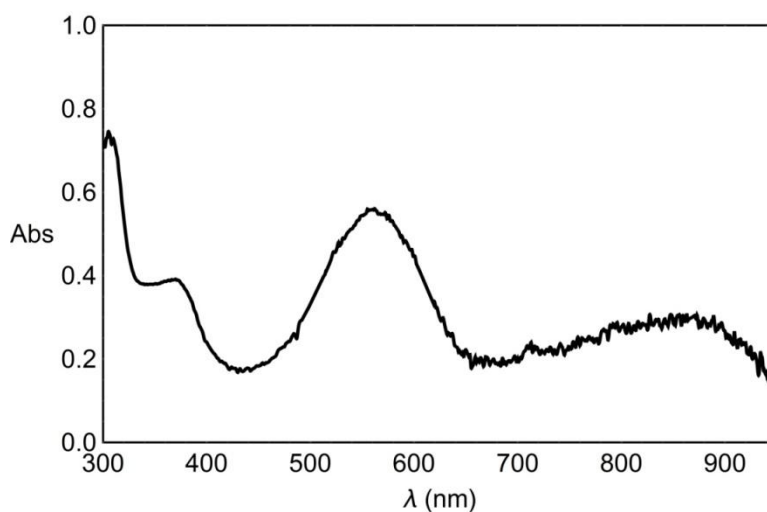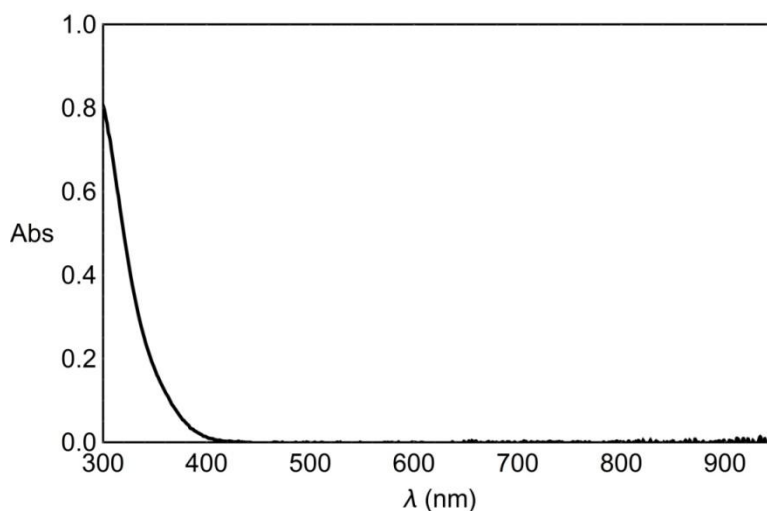
Fig. S9. Electronic absorption spectrum of Ni(dtbbpy)(cod) (6.68×10^{-5} M) and 2-chlorotoluene (6.68×10^{-4} M) mixture in THF. The visible region of the spectrum is dominated by a single band at 476 nm ($\varepsilon = 3.7 \times 10^3$ M^{-1} cm^{-1}). Optical densities of the quenching experiment mixtures at the excitation (405 nm, $\varepsilon = 2.1 \times 10^3$ M^{-1} cm^{-1}) and emission (478 nm, $\varepsilon = 3.7 \times 10^3$ M^{-1} cm^{-1}) wavelengths were used to account for inner filter effects.


Fig. S10. Electronic absorption spectrum of Ni(dtbbpy)(cod) (6.68×10^{-5} M) and 2-bromotoluene (6.68×10^{-4} M) mixture in THF. The visible region of the spectrum is dominated by a single band at 471 nm ($\varepsilon = 3.2 \times 10^3$ M^{-1} cm^{-1}). Optical densities of the quenching experiment mixtures at the excitation (405 nm, $\varepsilon = 1.8 \times 10^3$ M^{-1} cm^{-1}) and emission (478 nm, $\varepsilon = 3.2 \times 10^3$ M^{-1} cm^{-1}) wavelengths were used to account for inner filter effects.
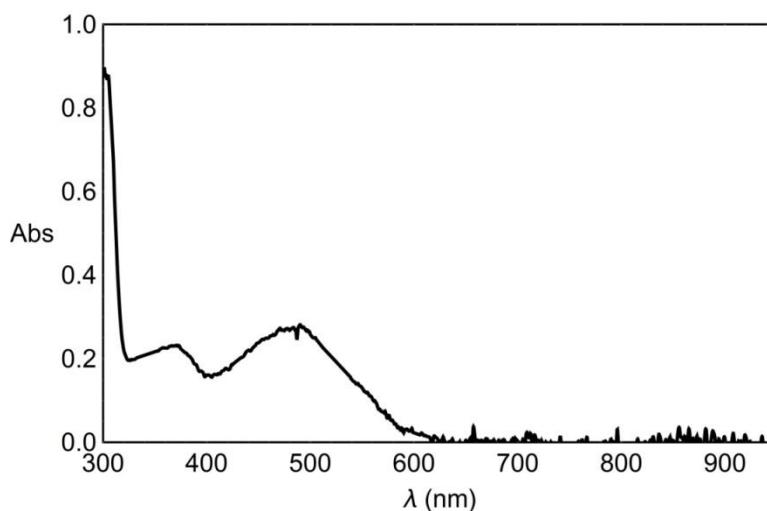
Fig. S11. Electronic absorption spectrum of Ni(dtbbpy)(cod) (6.68×10^{-5} M) and 2-iodotoluene (6.68×10^{-4} M) mixture in THF. The visible region of the spectrum is dominated by a single band at 490 nm ($\varepsilon = 3.7 \times 10^3$ M^{-1} cm^{-1}). Optical densities of the quenching experiment mixtures at the excitation (405 nm, $\varepsilon = 2.5 \times 10^3$ M^{-1} cm^{-1}) and emission (478 nm, $\varepsilon = 3.7 \times 10^3$ M^{-1} cm^{-1}) wavelengths were used to account for inner filter effects.

Fig. S12. Electronic absorption spectrum of Ni(dtbbpy)(cod) (6.68×10^{-5} M) in THF. The visible region of the spectrum is dominated by a band at 562 nm. Optical densities of the quenching experiment mixtures at the excitation (405 nm, $\varepsilon = 4.2 \times 10^3$ M^{-1} cm^{-1}) and emission (478 nm, $\varepsilon = 4.1 \times 10^3$ M^{-1} cm^{-1}) wavelengths were used to account for inner filter effects.
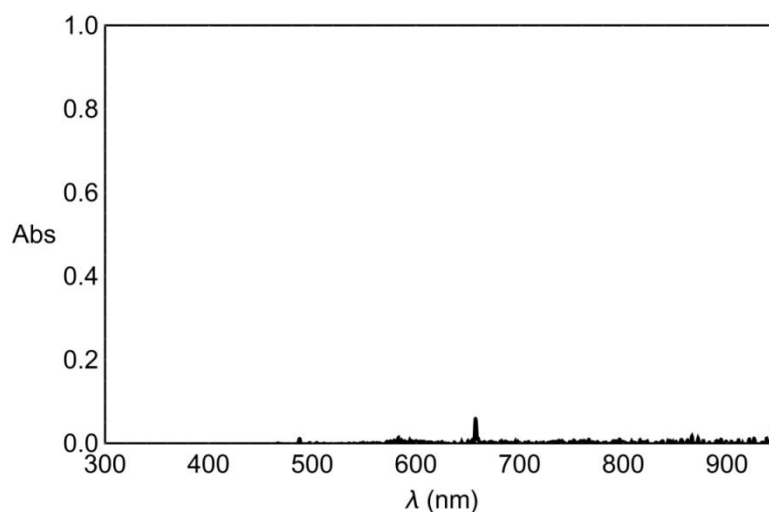
Fig. S13. Electronic absorption spectrum of Ni(cod)$_2$ (6.68×10^{-5} M) in THF. The visible region of the spectrum shows no absorbance.   Emission quenching data with Ni(cod)$_2$ were not corrected for inner filter effects.
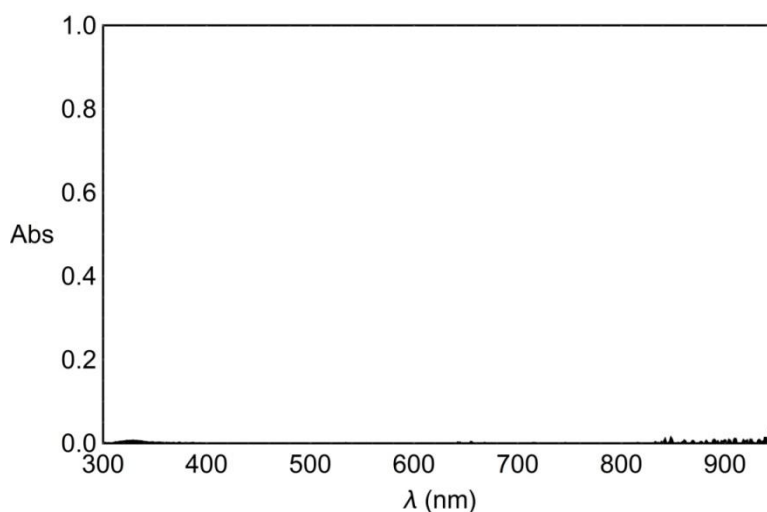
Fig. S14. Linear absorption spectrum of TBACl (6.68×10^{-5} M) in THF. The spectrum shows no absorbance. Emission quenching data with TBACl were not corrected for inner filter effects.
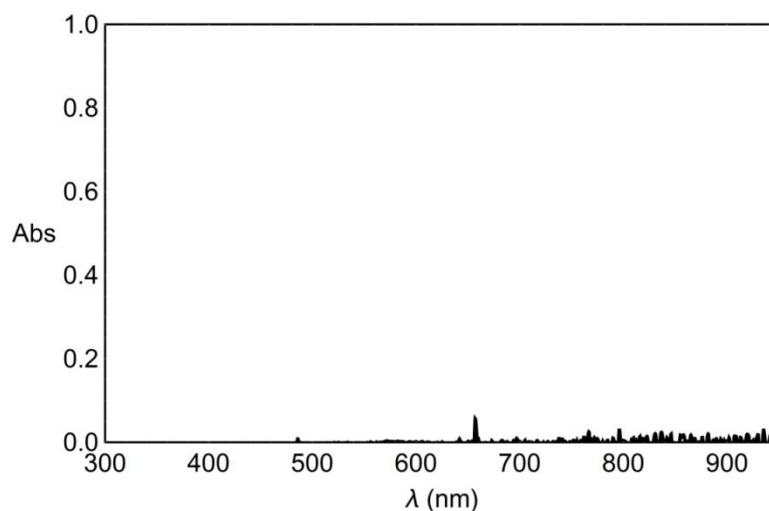
Fig. S15. Linear absorption spectrum of TBABr (6.68×10^{-5} M) in THF. The spectrum shows no absorbance. Emission quenching data with TBABr were not corrected for inner filter effects.

Fig. S16. Linear absorption spectrum of TBAI (6.68×10^{-5} M) in THF. The spectrum shows no absorbance. Emission quenching data with TBAI were not corrected for inner filter effects.

Emission Quenching Data. Emission spectra were collected on an Agilent Cary Eclipse Fluorescence Spectrophotometer with excitation and emission slit widths of 2.5 nm. Samples were excited at 405 nm (Ir[dF(CF$_3$)ppy]$_2$(dtbbpy)PF$_6$, $\varepsilon = 4.2 \times 10^3$ M^{-1} cm^{-1}) and emission was monitored at 478 nm. All reagents were dispensed in stock solutions prepared volumetrically inside a nitrogen filled glove box. All experiments were carried out with the same reagent ratios as the synthetic reaction (eg. 10 mol % [Ni] relative to aryl halides). For each compound and mixture which displayed quenching, data were collected in triplicate (with exception of Ni(cod)$_2$ which was collected in duplicate) and each control was collected in duplicate or a single run. For halide quenching experiments TBAPF$_6$ was added to maintain constant ionic strength. Base was excluded from quenching experiments in order to prevent scattering due to inhomogeneous mixtures. Exclusion of base was reasonable because the synthetic reaction produces product in the absence of base. For experiments with Ni(cod)$_2$ and dtbbpy a mixing time dependence for quenching was observed. It was determined that this effect was a result of the slow ligation of nickel coupled with the highly colored, deep purple, nature of the complex. This issue was addressed by employing the isolated Ni(dtbbpy)(cod) complex in all experiments. All Ni(dtbbpy)(cod)/aryl halide mixtures were stirred until the reaction mixture had changed from deep purple to ruby red. Complete consumption of Ni(dtbbpy)(cod) was confirmed by linear absorption measurements which showed the disappearance of the broad absorption of Ni(dtbbpy)(cod) (Fig, S12, λ_{max} = 562 nm) and the appearance of an absorption spectrum consistent with that of the independently prepared oxidative adduct (Fig. S8, λ_{max} = 469 nm).

In a typical experiment, THF, a 3.00 mM solution of Ir[dF(CF$_3$)ppy]$_2$(dtbbpy)PF$_6$ in THF (167 μL, 0.50 μmol, 1.67×10^{-4} M after dilution to 3 mL total volume) and an appropriate amount quencher dispensed in THF were added to screw-top 1.0 cm quartz cuvette in a nitrogen filled glove box. The cuvette was then sealed with a septum cap and electrical tape, removed from the glovebox and an emission spectrum was collected. In cases where quencher absorbed at excitation or emission wavelengths, a linear absorption spectrum of each sample was also collected using the 1.67×10^{-4} M solution of Ir[dF(CF$_3$)ppy]$_2$(dtbbpy)PF$_6$ in THF ([Q] = 0 entry) as the black.

Inner Filter Effect Corrections. Inner filter effects (IFEs) produce a decrease in emission intensity with positive deviation from linearity which gives the appearance of a mixed quenching model. For quenchers that showed absorbance at the excitation or emission wavelengths, a correction factor based on optical density measurements was applied to the raw emission data *(34)*. For samples with optical density at the emission (OD_{Em}) and excitation (OD_{Ex}) wavelength, primary IFEs due to a decrease in the intensity of incident light and secondary IFEs due to absorption of emitted photons are given by $10^{-0.5 OD_{Ex}}$ and $10^{-0.5 OD_{Em}}$ respectively. Therefore, the corrected phosphorescence intensity is give by

$$I_{Corrected} = I10^{0.5(OD_{Ex} + OD_{Em})} \qquad (Eq. 1)$$

where *I* is the observed emission intensity and *I$_{Corrected}$* is the IFE corrected emission intensity *(34)*. The sample without any quencher added was used as the blank in linear absorption measurements. Optical density at the excitation wavelength due to photocatalyst is the same in each sample. Thus the corrected phosphorescence intensity can be expressed as

$$I10^{0.5(OD_{Ex} + OD_{Em})} = I10^{0.5(OD_{Ex,Ir} + OD_{Ex,Q} + OD_{Em})} = I10^{0.5(OD_{Ex,Ir})}10^{0.5(OD_{Ex,Q} + OD_{Em})}$$

where $OD_{Ex,Ir}$ and $OD_{Ex,Q}$ are optical density at the excitation wave length due to photocatalyst and quencher respectively. When the ratio $\frac{I_0}{I}$ is taken in quenching experiments all primary IFEs due to photocatalyst absorbance are canceled. Note that this correction factor assumes that irradiation and detection take place at the center of the sample cuvette which is reasonable with small slit widths.

Model Selection. The following three representative models for steady state quenching kinetics were considered: Stern-Volmer (Eq. 2 and 3, $K_D = \tau_0 k_q$ is the dynamic quenching constant and $K_S = K_{eq}$ is the static quenching constant), mixed static and dynamic (Eq. 4, $K_D = \tau_0 k_q$ and $K_S = K_{eq}$) and Sphere of Action (Eq. 5, $K_D = \tau_0 k_q, N_A = 6.022 \times 10^{23} \, mol^{-1}$, and $V = $ volume of sphere) *(34)*. Nonlinear quenching models were included based on observed positive deviations from linearity though quenching phenomena such as transient effects could explain these deviations.

$$\frac{I_0}{I} = 1 + K_D[Q] \qquad (Eq.\,2)$$

$$\frac{I_0}{I} = 1 + K_S[Q] \qquad (Eq.\,3)$$

$$\frac{I_0}{I} = (1 + K_D[Q])(1 + K_S[Q]) \qquad (Eq.\,4)$$

$$\frac{I_0}{I} = (1 + K_D[Q])e^{\frac{N_A V[Q]}{1000}} \qquad (Eq.\,5)$$

The general data analysis procedure involved fitting the collected data to each model via linear or nonlinear least squares regression in *Mathematica* 10. For each quencher that displayed IFEs, corrected emission data were used in regression analysis. The best fit model was then determined by residuals analysis and Akaike's Information Criterion (AIC) *(35,36)*. The corrected AIC (AIC$_C$) value was calculated for each model and used to calculate evidence ratios with the linear model set to 1. Note that the evidence ratio is a measure of how different models fit the same data set (eg. with the linear model set to 1 an evidence ratio for the sphere of action of 1000 suggests that the sphere of action model fits 1000 times better) *(36)*. For each quencher the best fit model regression parameters were tabulated. Standard error in each parameter was calculated by fixed regressor bootstrapping (resampled 1000 times).

Mathematica Code. The following code was written in *Mathematica 10*. The code performs least squares regressions and returns a table with fitted functions, AIC$_C$ values, evidence ratios and R^2 values for each model. This code defines a *Mathematica* function which is called according to the following syntax: *quenchFit[data1,"data1"]* where the quenching data array is *data1* and the function takes the array and the name of the array *"data1"* (with quotes added) as arguments.

```
lmodel=b+k*x;
soamodel=(b+Subscript[k,d]*x)*Exp[NV*x/1000];
sdmodel=b+(Subscript[k,d]+Subscript[k,s])*x+Subscript[k,d]*Subscript[k,s]*x^2;
modelNames={"","Stern-Volmer","Sphere of Action","Static + Dynamic"};
Quiet[svStat[data_]:=LinearModelFit[data,x,x];
soaStat[data_]:=NonlinearModelFit[data,{soamodel,Subscript[k,d]>0},{{Subscript[k,d]},{NV},b},x,Method-
>NMinimize];
sdStat[data_]:=NonlinearModelFit[data,{sdmodel,Subscript[k,d]>0},{{Subscript[k,d]},{Subscript[k,s]},b},x,M
ethod->NMinimize];]
dString[name_]:=StringDrop[name,4];
svExpression[name_]:=ToExpression[StringJoin["sv",dString[name]]];
soaExpression[name_]:=ToExpression[StringJoin["soa",dString[name]]];
sdExpression[name_]:=ToExpression[StringJoin["sd",dString[name]]];
modelsExpression[name_]:=ToExpression[StringJoin["models",dString[name]]];
svStatExpression[name_]:=ToExpression[StringJoin["svStat",dString[name]]];
soaStatExpression[name_]:=ToExpression[StringJoin["soaStat",dString[name]]];
sdStatExpression[name_]:=ToExpression[StringJoin["sdStat",dString[name]]];
evdExpression[name_]:=ToExpression[StringJoin["evd",dString[name]]];
aicExpression[name_]:=ToExpression[StringJoin["aic",dString[name]]];
rsqExpression[name_]:=ToExpression[StringJoin["rsq",dString[name]]];
quenchFitExpression[name_]:=ToExpression[StringJoin["quenchFit",dString[name]]];
models[data_,name_]:={modelsExpression[name]={"ModelFits",svExpression[name][x_]=svStat[data]["[Q]
"],soaExpression[name][x_]=soaStat[data]["[Q]"],sdExpression[name][x_]=sdStat[data]["[Q]"]}}
modelStat[data_,name_]:={"Statistics",svStatExpression[name]=svStat[data],soaStatExpression[name]=s
oaStat[data],sdStatExpression[name]=sdStat[data]}
aic[name_]:={aicExpression[name]={"AICc",svStatExpression[name][#]&["AICc"],soaStatExpression[nam
e][#]&["AICc"],sdStatExpression[name][#]&["AICc"]}}
rsq[name_]:={rsqExpression[name]={"R^2",svStatExpression[name][#]&["RSquared"],soaStatExpression[
name][#]&["RSquared"],sdStatExpression[name][#]&["RSquared"]}}
evidenceRatio[AIC1_,AIC2_]:=1/E^(-0.5*(AIC1-AIC2));
evd[name_]:={evdExpression[name]={"EvidenceRatio",evidenceRatio[svStatExpression[name][#]&["AICc"
],svStatExpression[name][#]&["AICc"]],evidenceRatio[svStatExpression[name][#]&["AICc"],soaStatExpres
sion[name][#]&["AICc"]],evidenceRatio[svStatExpression[name][#]&["AICc"],sdStatExpression[name][#]&["
AICc"]]}}
fitTable[name_]:=Grid[Transpose[{modelNames,modelsExpression[name],aicExpression[name],evdExpre
ssion[name],rsqExpression[name]}],Alignment->Left]
quenchFit[data_,name_]:=Quiet[{quenchFitExpression[name]={models[data,name],modelStat[data,name]
,aic[name],rsq[name],evd[name]};Flatten[fitTable[name]]}]
```

The following code was written to perform fixed regressor bootstrap error analysis for model parameters. This code returns a table of bootstrapped parameters and is called according to the following syntax: *soaBootTable[data,n]* and *svBootTable[data,n]* where the experimental quenching data array is *data* and the number of bootstrap iterations is *n* ($n = 1000$ for this work). The standard deviation of the parameters in the table is the estimated standard error. Note that "15" in both sets of code refers to the number of data points.

```
soaBootTable[data_,n_]:=Table[
Values[soaStat[data+Thread[{ConstantArray[0,15],RandomChoice[Flatten[Rest[Transpose[data]]]-
MapThread[soaStat[data],{Flatten[Most[Transpose[data]]]}],15]}]][["BestFitParameters"]],n]

svBootTable[data_,n_]:=Table[
svStat[data+Thread[{ConstantArray[0,15],RandomChoice[Flatten[Rest[Transpose[data]]]-
MapThread[svStat[data],{Flatten[Most[Transpose[data]]]}],15]}]][["BestFitParameters"],n]
```

<u>Data Reported.</u> A summary of the results for quenching experiments can be seen in Table S11. In the following section measured emission intensity versus quencher concentration and the best fit models are plotted for each quencher and control. Both the corrected emission intensity and raw emission intensity without IFE corrections along with best fit models are plotted for quenchers that absorbed at excitation or emission wavelengths. All model fits are shown for each model that displayed nonlinear quenching. For each quencher and control, concentrations and measured emission intensity are tabulated and each quencher that displayed IFEs, the uncorrected emission intensity and optical density at excitation (OD_{405nm}) and emission (OD_{478nm}) wavelengths are tabulated. A model selection summary consisting of AIC_C values, evidence rations and R^2 values for each model are shown for each set of data. Best fit model parameters (y-intercept, K, V) and standard errors (SE) are reported for each quencher. Steady state quenching experiments do not discriminate between dynamic (Eq. 2) and static (Eq. 3) quenching with exception of the sphere the Sphere of Action model (Eq. 5) which mathematically separates K_D. Thus the K is reported rather than k_D or K_{eq}.

Quencher	K (M^{-1})	SE$_K$ (M^{-1})	$K - \text{t} \times \text{SE}_K$ (M^{-1})	$K + \text{t} \times \text{SE}_K$ (M^{-1})
Ni(dtbbpy)(cod) + 2-chlorotoluene	1.2×10^4	3.2×10^2	1.1×10^4	1.3×10^4
Ni(dtbbpy)(o-tolyl)Cl	8.8×10^3	5.4×10^2	7.6×10^3	1.0×10^4
TBACl	1.2×10^{-1}	7.5×10^2	-1.6×10^3	1.6×10^3
Ni(dtbbpy)(cod) + 2-bromotoluene	9.4×10^3	2.9×10^2	8.8×10^3	1.0×10^4
TBABr	7.1×10^{-1}	1.3×10^3	-2.7×10^3	2.7×10^{-1}
Ni(dtbbpy)(cod) + 2-iodotoluene	1.4×10^4	6.5×10^2	1.2×10^4	1.5×10^4
TBAI	1.3×10^4	1.7×10^3	8.9×10^3	1.6×10^4
Ni(dtbbpy)(cod)	1.1×10^4	4.3×10^3	2.1×10^3	2.1×10^4
Ni(cod)$_2$	2.0×10^4	4.7×10^2	1.9×10^4	2.1×10^4

Controls				
4,4′-di-*tert*-butyl-2,2′-bipyridine		No Quenching		
2-chlorotoluene		No Quenching		
2-bromotoluene		No Quenching		
2-iodotoluene		No Quenching		

Table S11. Summary of quenching rate data. The quenching constant K is reported rather than the dyanamic rate constant k_D or equilibrium constant K_{eq}. If one assumes a dynamic quenching mechanism K can be divided by $\tau_0 = 2.3 \times 10^{-6}$ s to arrive at k_D *(14)*. The relatively large standard error for TBACl and TBABr quenching constants is the result of small values of K_D. Consider the logarithmic form of Eq. 5, $\ln\left(\frac{I_0}{I}\right) = ln(1 + K_D[Q]) + \frac{N_A V[Q]}{1000}$. If K_D is small then $ln(1 + K_D[Q]) \approx K_D[Q]$ and $\ln\left(\frac{I_0}{I}\right) \approx K_D[Q] + \frac{N_A V}{1000}[Q] = \left(K_D + \frac{N_A V}{1000}\right)[Q]$ which leads to a large uncertainty in the values of K_D and V. Quenching by Ni(dtbbpy)(cod)/2-chlorotoluene, (dtbbpy)Ni(o-tolyl)Cl, Ni(dtbbpy)(cod)/2-bromotoluene and Ni(dtbbpy)(cod)/2-iodotoluene occurred at similar rates and data fit the Stern-Volmer model. Linear absorption spectra for each mixture compared to spectrum for (dtbbpy)Ni(o-tolyl)Cl suggest that Ni(II) aryl halide complexes are the dominant Ni species in the reaction mixture. Taken together with the controls these data suggest that Ni(II) aryl halide complexes are primarily responsible for quenching in the reaction mixture.

Quencher	V (cm^3)	SE_V (cm^3)	k_D (M^{-1} s^{-1})	SE_{k_D} (M^{-1} s^{-1})
TBACl	2.1×10^{-17}	1.2×10^{-18}	5.3×10^4	3.2×10^8
TBABr	2.5×10^{-17}	1.7×10^{-18}	3.1×10^5	5.4×10^8
TBAI	1.1×10^{-17}	9.7×10^{-19}	5.5×10^9	7.5×10^8

Table S12. Summary of Sphere of Action rate data for halides. The dynamic quenching rate constant k_D is reported. The relatively large standard errors for TBACl and TBABr quenching constants are the result of small values of K_D. See Table S11 for discussion. Quenching of Ir[dF(CF$_3$)ppy]$_2$(dtbbpy)PF$_6$ (1.21 V versus SCE in MeCN) by electron transfer with bromide (1.6 V versus SCE in MeCN) and chloride (2.03 V versus SCE in MeCN) is predicted to be thermodynamically unfavorable *(14,11)*. This accounts for the observed small dynamic quenching rate constants. It is unlikely that the observed quenching with bromide and chloride is due to an electron transfer process. By contrast quenching with iodide (1.06 V versus SCE in MeCN) by electron transfer is predicted to be favorable and the resulting dynamic quenching rate constant is large, near the diffusion limit *(11)*.

A
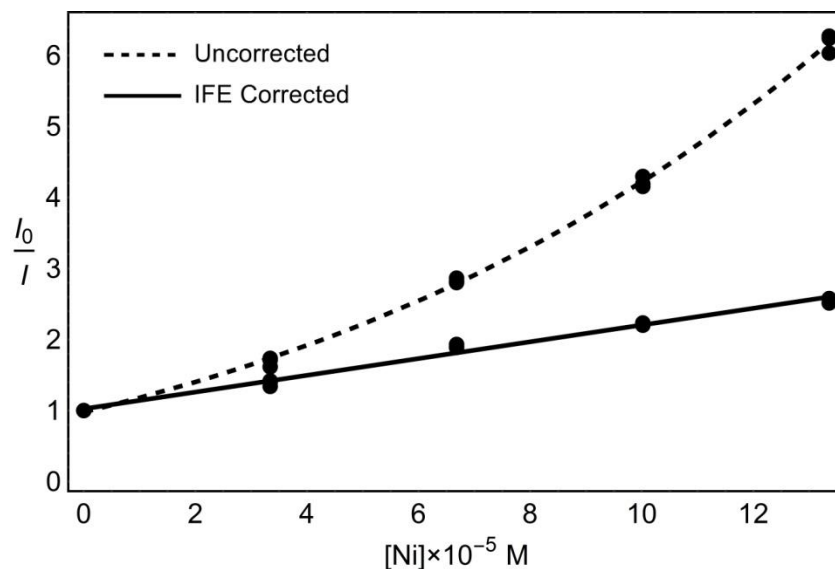
B [Ni] $\times 10^{-5}$ M	I	$OD_{405\ nm}$	$OD_{478\ nm}$
0.00	321.63	0.00	0.00
3.34	187.92	0.06	0.11
6.68	112.27	0.11	0.23
10.02	77.39	0.19	0.36
13.36	51.30	0.28	0.49
0.00	319.47	0.00	0.00
3.34	184.00	0.06	0.11
6.68	114.03	0.11	0.23
10.02	76.23	0.19	0.36
13.36	51.19	0.28	0.49
0.00	314.86	0.00	0.00
3.34	194.70	0.06	0.10
6.68	111.47	0.11	0.23
10.02	73.28	0.20	0.37
13.36	52.19	0.27	0.49

C Model	AIC_C	Evidence Ratio	R^2
Stern-Volmer	-36.2	1.00	0.990
Sphere of Action	-32.4	0.15	0.999
Static + Dynamic	-32.4	0.15	0.999

D Best Fit Model	y-int	$SE_{y\text{-}int}$	K (M^{-1})	SE_K (M^{-1})
Stern-Volmer	1.03	0.03	1.21×10^4	3.22×10^2

Fig. S17. Ir[dF(CF$_3$)ppy]$_2$(dtbbpy)PF$_6$ emission quenching by Ni(dtbbpy)(cod) and 2-chlorotoluene reaction mixture in THF. [**A**] Plot of data with and without inner filer effect corrections and best fit models. [**B**] Emission quenching and linear absorption data. [**C**] Model fitting results summary. [**D**] Best fit model and parameter error estimates.

A
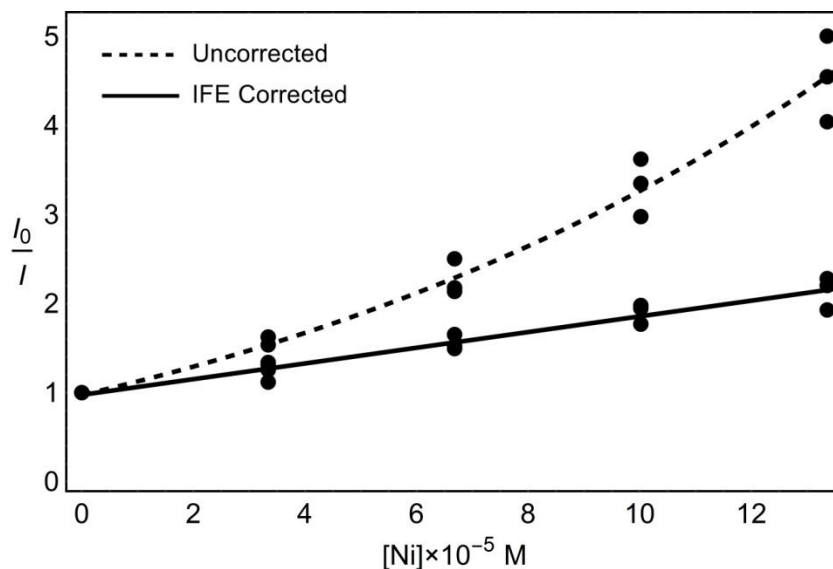
B	[Ni] $\times 10^{-5}$ M	I	$OD_{405\text{ nm}}$	$OD_{478\text{ nm}}$
	0.00	315.95	0.00	0.00
	3.34	194.54	0.08	0.10
	6.68	126.22	0.14	0.22
	10.02	87.22	0.20	0.32
	13.36	63.15	0.26	0.42
	0.00	317.36	0.00	0.00
	3.34	237.00	0.09	0.07
	6.68	148.49	0.13	0.18
	10.02	106.59	0.19	0.26
	13.36	78.50	0.27	0.37
	0.00	320.36	0.00	0.00
	3.34	208.59	0.08	0.10
	6.68	147.24	0.13	0.18
	10.02	95.66	0.18	0.29
	13.36	70.44	0.24	0.39

C	Model	AIC_C	Evidence Ratio	R^2
	Stern-Volmer	-19.2	1	0.95
	Sphere of Action	-15.4	0.15	0.99
	Static + Dynamic	-14.8	0.11	0.99

D	Best Fit Model	y-int	$SE_{\text{y-int}}$	K (M^{-1})	SE_K (M^{-1})
	Stern-Volmer	0.97	0.04	8.82×10^3	5.42×10^2

Fig. S18. Ir[dF(CF$_3$)ppy]$_2$(dtbbpy)PF$_6$ emission quenching by (dtbbpy)Ni(o-tolyl)Cl in THF. [**A**] Plot of data with and without inner filer effect corrections and best fit models. [**B**] Emission quenching and linear absorption data. [**C**] Model fitting results summary. [**D**] Best fit model and parameter error estimates.

A
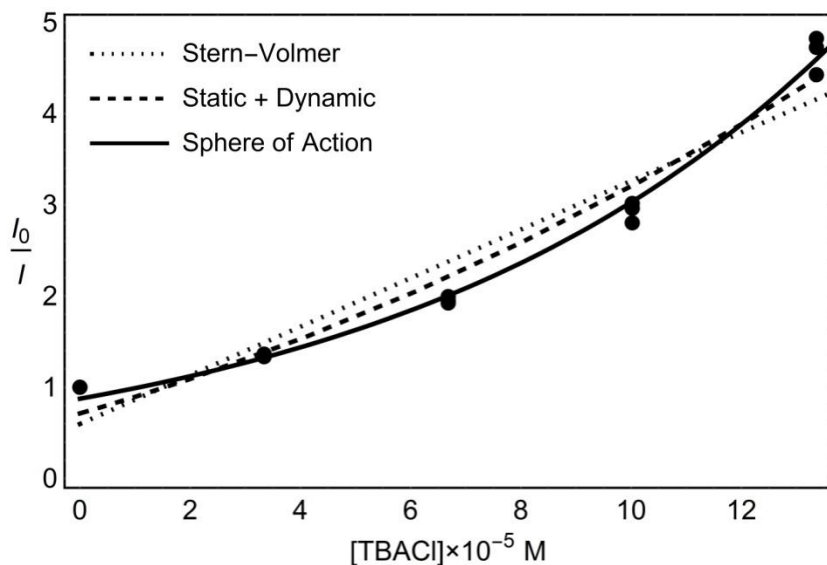
B

[TBACl] $\times 10^{-5}$ M	I
0.00	316.59
3.34	237.17
6.68	162.52
10.02	112.95
13.36	71.51
0.00	316.92
3.34	232.54
6.68	158.91
10.02	107.01
13.36	67.06
0.00	316.69
3.34	235.81
6.68	164.56
10.02	105.01
13.36	65.63

C

Model	AIC_C	Evidence Ratio	R^2
Stern-Volmer	22.6	1	0.91
Sphere of Action	-9.0	7.2×10^6	0.99
Static + Dynamic	14.4	59.1	0.99

D

Best Fit Model	y-int	$SE_{y\text{-int}}$	V (cm^3)	SE_V (cm^3)	K (M^{-1})	SE_K (M^{-1})
Sphere of Action	0.87	0.04	2.06×10^{-17}	1.24×10^{-18}	1.22×10^{-1}	7.49×10^2

Fig. S19. Ir[dF(CF$_3$)ppy]$_2$(dtbbpy)PF$_6$ emission quenching by TBACl in THF. [**A**] Plot of data with and all model fits. [**B**] Emission quenching data. [**C**] Model fitting results summary. [**D**] Best fit model and parameter error estimates.

A

B
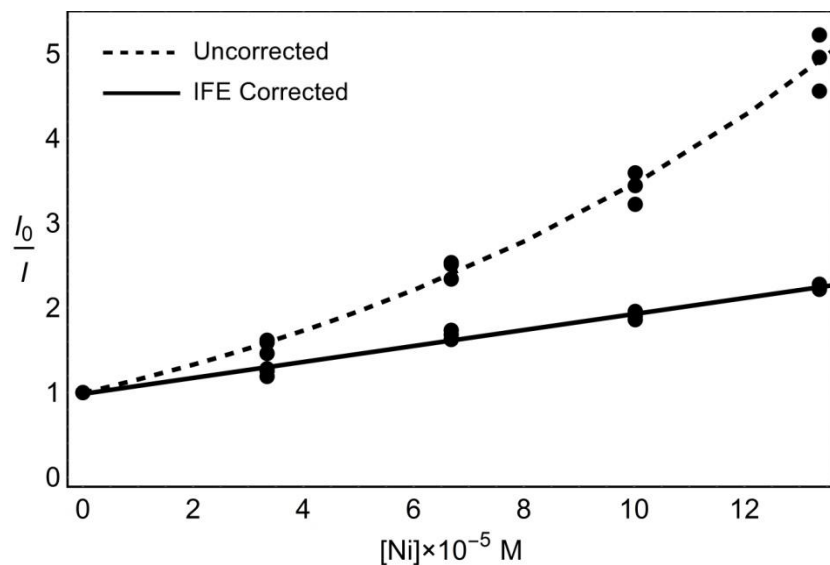
[Ni] $\times 10^{-5}$ M	I	$OD_{405 \text{ nm}}$	$OD_{478 \text{ nm}}$
0.00	319.27	0.00	0.00
3.34	200.64	0.10	0.10
6.68	125.99	0.14	0.21
10.02	88.83	0.22	0.33
13.36	61.14	0.28	0.44
0.00	283.24	0.00	0.00
3.34	193.70	0.07	0.11
6.68	121.04	0.11	0.21
10.02	87.88	0.16	0.32
13.36	62.12	0.21	0.42
0.00	322.06	0.00	0.00
3.34	199.08	0.09	0.11
6.68	128.19	0.12	0.20
10.02	93.49	0.18	0.31
13.36	64.95	0.26	0.44

C

Model	AIC_C	Evidence Ratio	R^2
Stern-Volmer	-37.1	1	0.99
Sphere of Action	-33.3	0.15	0.99
Static + Dynamic	-29.2	0.02	0.99

D

Best Fit Model	y-int	$SE_{\text{y-int}}$	K (M^{-1})	SE_K (M^{-1})
Stern-Volmer	0.98	0.02	9.43×10^3	2.94×10^2

Fig. S20. Ir[dF(CF$_3$)ppy]$_2$(dtbbpy)PF$_6$ emission quenching by Ni(dtbbpy)(cod) and 2-bromotoluene reaction mixture in THF. [**A**] Plot of data with and without inner filer effect corrections and best fit models. [**B**] Emission quenching and linear absorption data. [**C**] Model fitting results summary. [**D**] Best fit model and parameter error estimates.

A
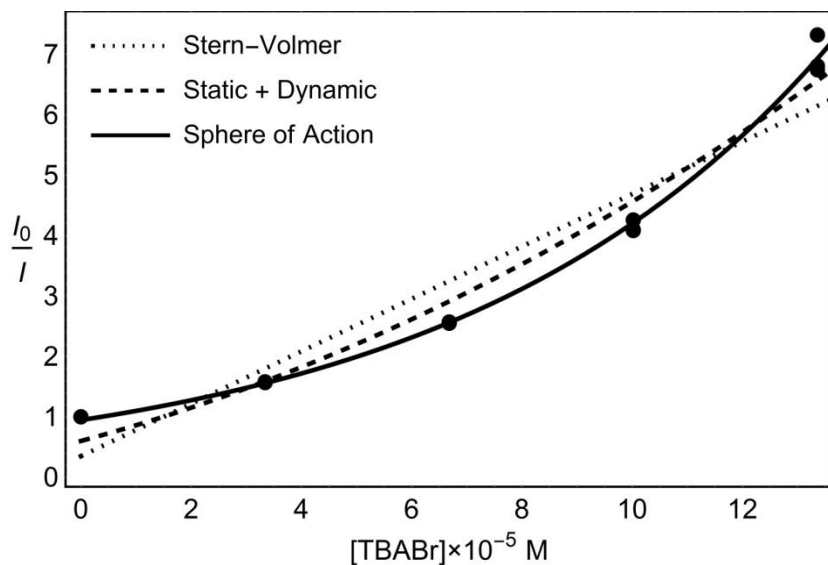
B

[TBABr] $\times 10^{-5}$ M	I
0.00	319.83
3.34	204.06
6.68	124.55
10.02	78.32
13.36	47.42
0.00	311.86
3.34	198.64
6.68	122.33
10.02	76.13
13.36	45.81
0.00	312.31
3.34	197.72
6.68	121.53
10.02	73.33
13.36	42.67

C

Model	AIC_C	Evidence Ratio	R^2
Stern-Volmer	36.8	1	0.91
Sphere of Action	-7.3	3.9×10^9	0.99
Static + Dynamic	24.8	410	0.99

D

Best Fit Model	y-int	$SE_{y\text{-}int}$	V (cm^3)	SE_V (cm^3)	K (M^{-1})	SE_K (M^{-1})
Sphere of Action	0.95	0.03	2.47×10^{-17}	1.69×10^{-18}	7.09×10^{-1}	1.25×10^3

Fig. S21. Ir[dF(CF$_3$)ppy]$_2$(dtbbpy)PF$_6$ emission quenching by TBABr in THF. [**A**] Plot of data with and all model fits. [**B**] Emission quenching data. [**C**] Model fitting results summary. [**D**] Best fit model and parameter error estimates.

A
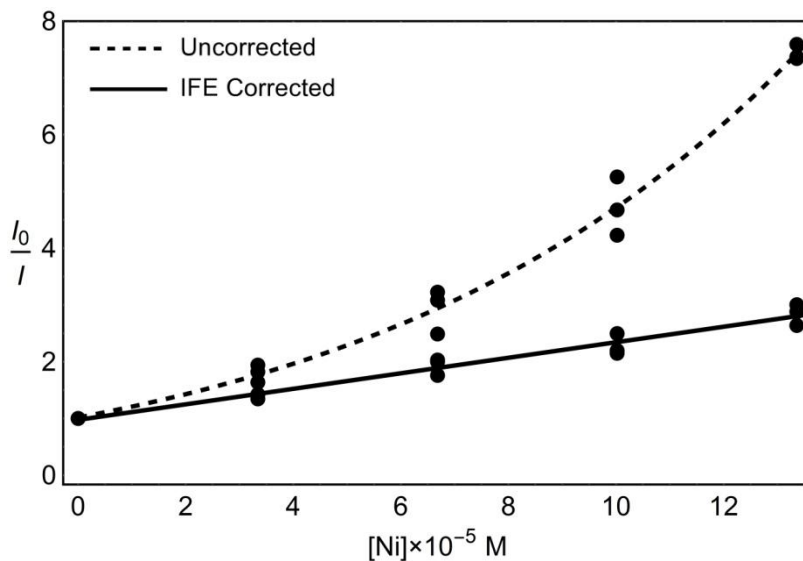
B [Ni] $\times 10^{-5}$ M	I	$OD_{405\ nm}$	$OD_{478\ nm}$
0.00	316.51	0.00	0.00
3.34	193.10	0.07	0.10
6.68	127.22	0.12	0.18
10.02	60.22	0.25	0.39
13.36	42.96	0.30	0.51
0.00	323.53	0.00	0.00
3.34	166.67	0.13	0.14
6.68	100.29	0.15	0.25
10.02	69.23	0.28	0.37
13.36	42.63	0.37	0.43
0.00	309.48	0.00	0.00
3.34	169.71	0.08	0.13
6.68	100.36	0.13	0.25
10.02	73.19	0.23	0.36
13.36	42.17	0.34	0.54

C Model	AIC_C	Evidence Ratio	R^2
Stern-Volmer	-12.9	1	0.97
Sphere of Action	-9.1	0.15	0.99
Static + Dynamic	-9.4	0.17	0.99

D Best Fit Model	y-int	$SE_{y\text{-int}}$	$K\ (M^{-1})$	$SE_K\ (M^{-1})$
Stern-Volmer	0.98	0.05	1.37×10^4	6.47×10^2

Fig. S22. Ir[dF(CF$_3$)ppy]$_2$(dtbbpy)PF$_6$ emission quenching by Ni(dtbbpy)(cod) and 2-iodotoluene reaction mixture in THF. [**A**] Plot of data with and without inner filer effect corrections and best fit models. [**B**] Emission quenching and linear absorption data. [**C**] Model fitting results summary. [**D**] Best fit model and parameter error estimates.

A
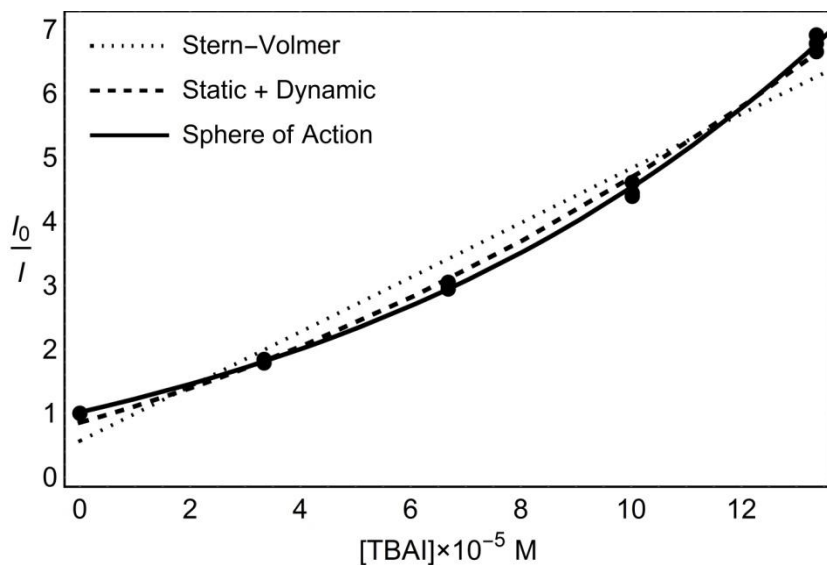
B	[TBAI] $\times 10^{-5}$ M	I
	0.00	318.25
	3.34	172.57
	6.68	106.77
	10.02	71.60
	13.36	47.81
	0.00	307.32
	3.34	171.90
	6.68	104.38
	10.02	69.95
	13.36	45.31
	0.00	312.54
	3.34	171.06
	6.68	102.50
	10.02	67.77
	13.36	45.19

C Model	AIC_C	Evidence Ratio	R^2
Stern-Volmer	23.6	1	0.96
Sphere of Action	-22.8	1.2×10^{10}	0.99
Static + Dynamic	-0.4	1.7×10^5	0.99

D Best Fit Model	y-int	$SE_{y\text{-int}}$	V (cm^3)	SE_V (cm^3)	K (M^{-1})	SE_K (M^{-1})
Sphere of Action	1.02	0.04	1.14×10^{-17}	9.67×10^{-19}	1.26×10^4	1.72×10^3

Fig. S23. Ir[dF(CF$_3$)ppy]$_2$(dtbbpy)PF$_6$ emission quenching by TBAI in THF. [**A**] Plot of data with and all model fits. [**B**] Emission quenching data. [**C**] Model fitting results summary. [**D**] Best fit model and parameter error estimates.

A
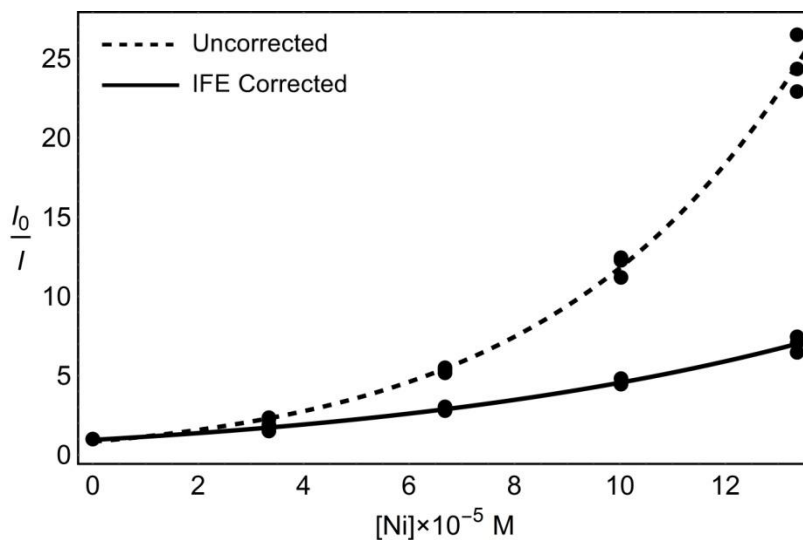
B [Ni] $\times 10^{-5}$ M	I	$OD_{405\,nm}$	$OD_{478\,nm}$
0.00	309.01	0.00	0.00
3.34	136.60	0.13	0.12
6.68	57.50	0.30	0.27
10.02	25.18	0.45	0.43
13.36	13.48	0.56	0.54
0.00	317.14	0.00	0.00
3.34	134.73	0.16	0.13
6.68	57.60	0.25	0.26
10.02	25.48	0.41	0.41
13.36	11.97	0.55	0.55
0.00	312.80	0.00	0.00
3.34	164.50	0.11	0.09
6.68	60.41	0.25	0.25
10.02	27.94	0.40	0.40
13.36	12.85	0.55	0.53

C Model	AIC_C	Evidence Ratio	R^2
Stern-Volmer	37.8	1	0.92
Sphere of Action	23.5	459	0.99
Static + Dynamic	27.3	69	0.99

D Best Fit Model	y-int	$SE_{y\text{-int}}$	V (cm^3)	SE_V (cm^3)	K (M^{-1})	SE_K (M^{-1})
Sphere of Action	0.95	0.10	1.29×10^{-17}	2.82×10^{-23}	1.14×10^4	4.30×10^3

Fig. S24. Ir[dF(CF$_3$)ppy]$_2$(dtbbpy)PF$_6$ emission quenching by Ni(dtbbpy)(cod) in THF. [**A**] Plot of data with and without inner filer effect corrections and best fit models. [**B**] Emission quenching and linear absorption data. [**C**] Model fitting results summary. [**D**] Best fit model and parameter error estimates.

A
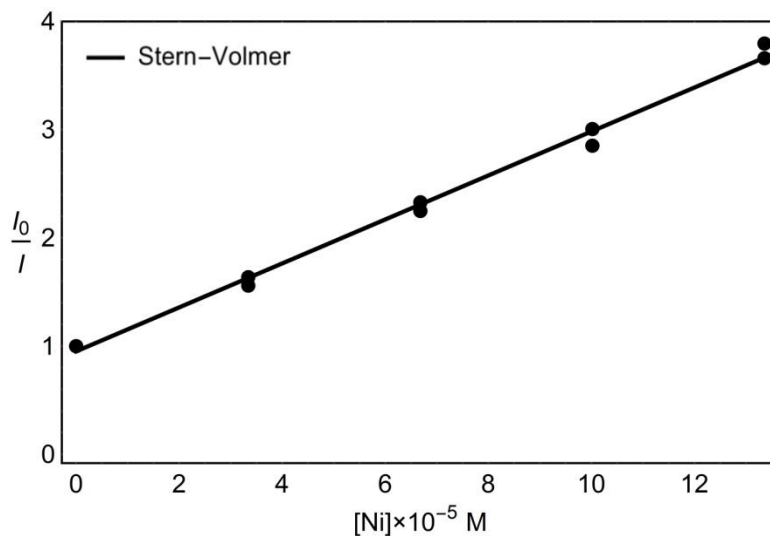
B	$[\text{Ni(cod)}_2] \times 10^{-5}$ M	I
	0.00	288.82
	3.34	176.42
	6.68	123.99
	10.02	96.10
	13.36	76.11
	0.00	293.27
	3.34	188.18
	6.68	130.43
	10.02	102.86
	13.36	80.14

C	Model	AIC_C	Evidence Ratio	R^2
	Stern-Volmer	-14.7	1	0.99
	Sphere of Action	-8.7	0.05	0.99
	Static + Dynamic	-13.1	0.4	0.99

D	Best Fit Model	y-int	$SE_{\text{y-int}}$	K (M^{-1})	SE_K (M^{-1})
	Stern-Volmer	0.95	0.04	2.03×10^4	4.73×10^2

Fig. S25. Ir[dF(CF$_3$)ppy]$_2$(dtbbpy)PF$_6$ emission quenching by Ni(cod)$_2$ in THF. [**A**] Plot of data and best fit model. [**B**] Emission quenching data. [**C**] Model fitting results summary. [**D**] Best fit model and parameter error estimates.

A
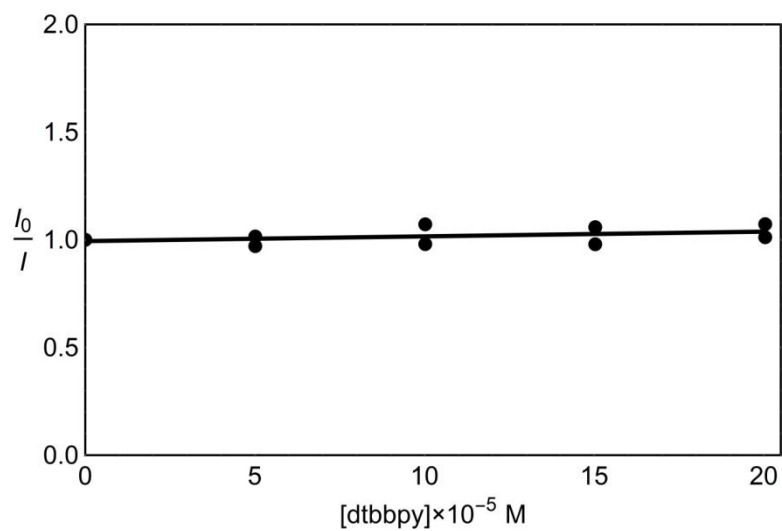
B	$[\text{dtbbpy}] \times 10^{-5}$ M	I
	0.00	283.66
	5.01	292.27
	10.02	289.44
	15.03	289.71
	20.04	280.34
	0.00	298.77
	5.01	294.19
	10.02	278.77
	15.03	282.28
	20.04	278.56

Fig. S26. Ir[dF(CF$_3$)ppy]$_2$(dtbbpy)PF$_6$ emission quenching by dtbbpy in THF. [**A**] Plot of data and best fit model. [**B**] Emission quenching data.

A
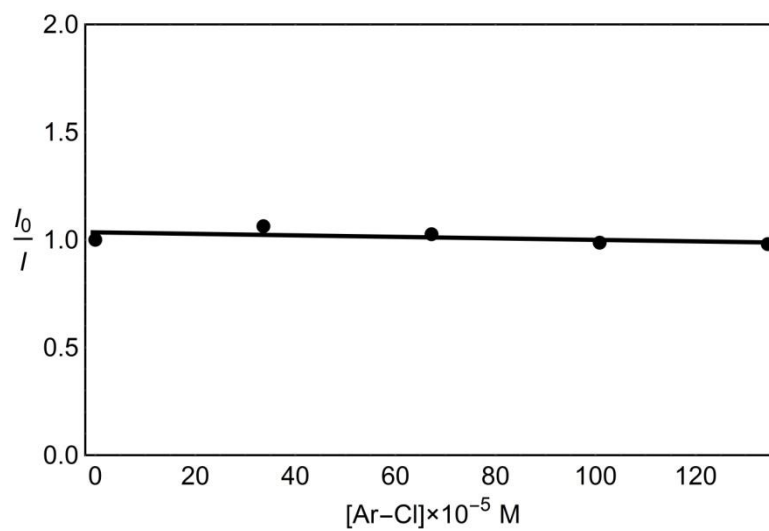
[Ar-Cl] × 10^{-5} M	I
B	
0.00	309.90
33.60	291.46
67.20	302.00
100.80	314.15
134.40	316.25

Fig. S27. Ir[dF(CF$_3$)ppy]$_2$(dtbbpy)PF$_6$ emission quenching by 2-chlorotoluene in THF. [**A**] Plot of data and best fit model. [**B**] Emission quenching data.

A
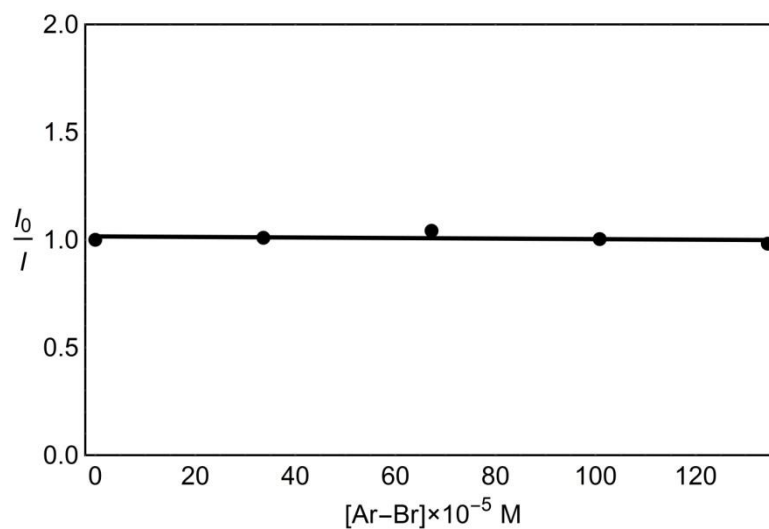
$[\text{Ar-Br}] \times 10^{-5}$ M	I
0.00	318.29
33.60	315.32
67.20	305.55
100.80	317.20
134.40	324.12

B appears at the left margin of the table.

Fig. S28. Ir[dF(CF$_3$)ppy]$_2$(dtbbpy)PF$_6$ emission quenching by 2-bromotoluene in THF. [**A**] Plot of data and best fit model. [**B**] Emission quenching data.

A
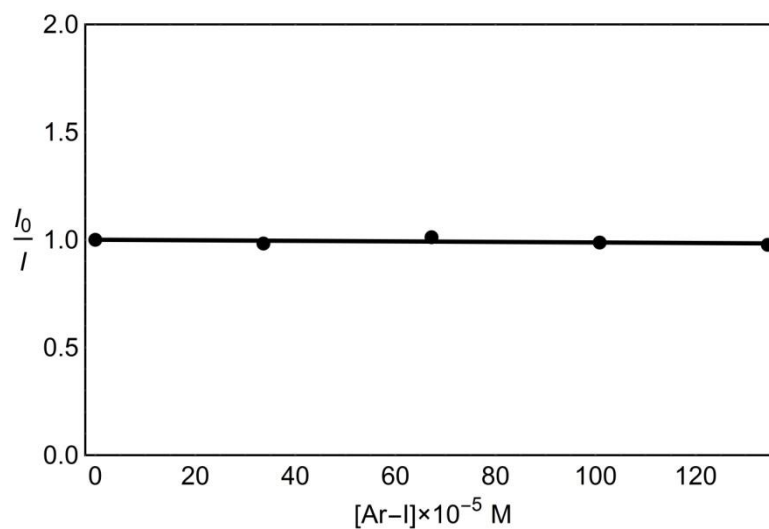
[Ar-I] × 10^{-5} M	I
B 0.00	318.94
33.60	324.51
67.20	315.10
100.80	322.99
134.40	326.63

Fig. S29. Ir[dF(CF$_3$)ppy]$_2$(dtbbpy)PF$_6$ emission quenching by 2-iodotoluene in THF. [**A**] Plot of data and best fit model. [**B**] Emission quenching data.

A
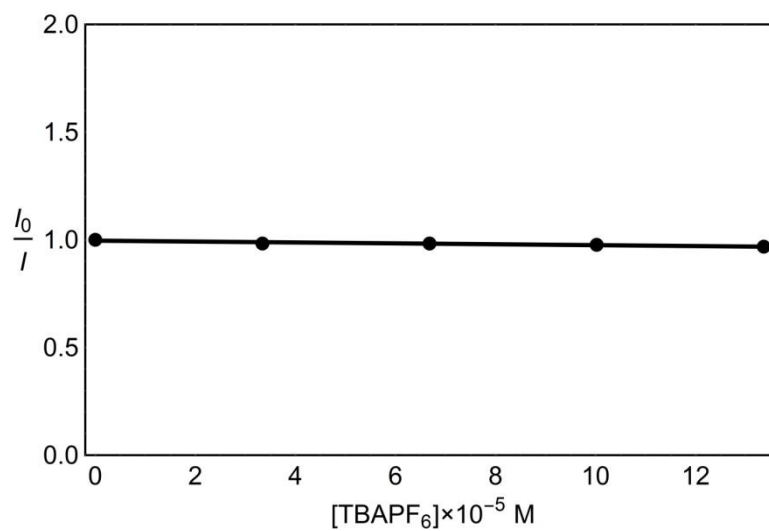
B	$[\text{TBAPF}_6] \times 10^{-5}$ M	I
	0.00	302.27
	3.34	307.57
	6.68	307.64
	10.02	309.46
	13.36	312.20

Fig. S30. Ir[dF(CF$_3$)ppy]$_2$(dtbbpy)PF$_6$ emission quenching by TBAPF$_6$ in THF. [**A**] Plot of data and best fit model. [**B**] Emission quenching data.

IX. Stoichiometric Oxidation Experiments

Representative Procedure for Stoichiometric Oxidation Experiments. A threaded 20 × 125 mm borosilicate reaction tube (Fisher part number: 14-959-37A) equipped with PTFE-coated stir bar was brought into a N_2-filled glove box and charged with (dtbbpy)Ni(p-tolyl)Cl (11 mg, 0.025 mmol, 1 equiv.), 4,4'-di-*tert*-butyl-2,2'-bipyridine (6.7 mg, 0.025 mmol, 1 equiv.) and K_3PO_4 (10.6 mg, 0.05 mmol, 2 equiv.) followed by THF (9 mL) to give a ruby red solution. To a two dram vial was added tris(4-bromophenyl)ammoniumyl hexachloroantimonate ([TBPA]$SbCl_6$, 20 mg, 0.025 mmol, 1 equiv.) followed by THF (3.5 mL) to give a turquoise solution. The reaction tube and vial were capped with Teflon septum caps, sealed with electrical tape and removed from the glove box. The (dtbbpy)Ni(p-tolyl)Cl solution was placed in a acetone/dry ice bath and set to stir (800 rpm) for 15 min. The [TBPA]$SbCl_6$ solution was cooled in a acetone/dry ice bath. The cooled (dtbbpy)Ni(p-tolyl)Cl solution was irradiated with two 34 W blue LED lamps (5 cm away, placed 180º apart). The cooled [TBPA]$SbCl_6$ solution was titrated drop wise via syringe into the (dtbbpy)Ni(p-tolyl)Cl solution. During the titration condensation was washed from the reaction tube with acetone. The reaction mixture y changed from ruby red to light yellow after complete addition of the [TBPA]$SbCl_6$. After addition of [TBPA]$SbCl_6$ was complete the reaction was warmed to room temperature and the crude product was analyzed by GC-FID relative to 1-fluoronaphthalene as an external standard.
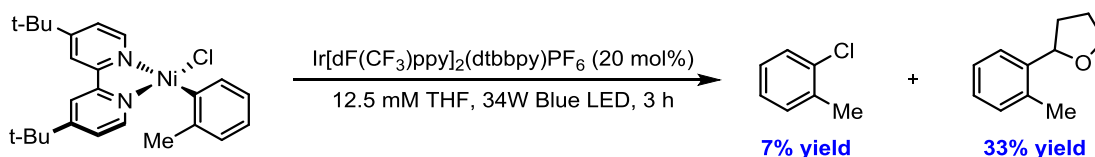
Fig. S31. Evaluation of complex **33** (Ar = 2-methylphenyl) under catalytic conditions. Yields determined by GC-FID using 1-fluoronaphthalene as an external standard. Reaction was carried out at 0.05 mmol scale.

34 (Ar = *p*-tolyl)
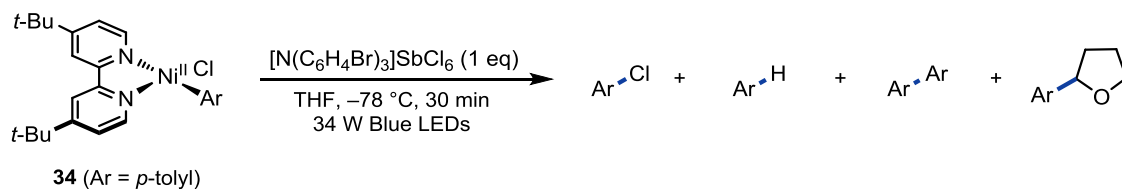
Entry	Conditions	Yield Ar-Cl	Yield Ar-H	Yield Ar-Ar	Yield Ar-THF
1	2 mM THF	12%	51%	0%	**14%**
2	**dtbbpy** (1 eq), **K₃PO₄** (2 eq), 2 mM THF	6%	37%	32%	**20%**
3	dtbbpy (1 eq), K₃PO₄ (2 eq), **1 mM** THF	8%	53%	0%	**28%**
4	dtbbpy (1 eq), K₃PO₄ (2 eq), 2 mM THF, **no oxidant**	3%	0%	62%	**0%**
5	dtbbpy (1 eq), K₃PO₄ (2 eq), 2 mM THF, **dark**	63%	15%	9%	**0%**
6	**dtbbpy** (1 eq), 2 mM THF	7%	34%	36%	**17%**
7	**K₃PO₄** (2 eq), 2 mM THF	9%	63%	12%	**8%**

Table S13. Stoichiometric reactions of complex **34** (Ar = 4-methylphenyl). Yields determined by GC-FID using 1-fluoronaphthalene as an external standard. Reactions were carried out at 0.025 mmol scale. The presence of product in entry 3 was confirmed by ^{1}H NMR.

33 (Ar = *o*-tolyl)
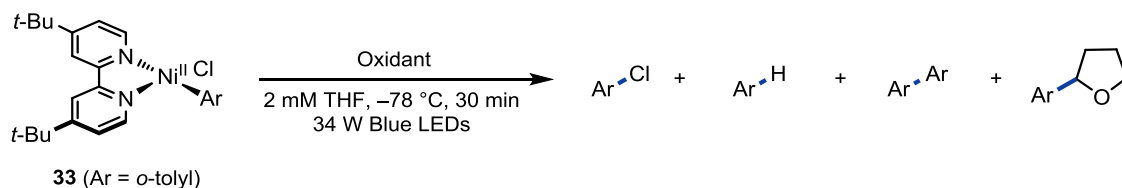
Entry	Conditions	Yield Ar-Cl	Yield Ar-H	Yield Ar-Ar	Yield Ar-THF
1	FcBAr$^F_4$ (1 eq)	12%	40%	2%	**7%**
2	FcBAr$^F_4$ (1 eq), **dark**	50%	3%	0%	**0%**
3	**no oxidant**	5%	2%	0%	**0%**
4	[N(C₆H₄Br)₃]SbCl₆ (1 eq)	9%	40%	0%	**9%**

Table S14. Stoichiometric reactions of complex **33** (Ar = 2-methylphenyl). Yields determined by GC-FID using 1-fluoronaphthalene as an external standard. Reactions were carried out at 0.025 mmol scale. The presence of product in entry 1 was confirmed by ^{1}H NMR. Nickel complex contained trace aryl chloride remaining from synthesis which accounts for the small amount observed in the absence of oxidant.

X. Cyclic Voltammetry Data

Cyclic Voltammetry was performed on a CH Instruments Electrochemical Analyzer (CH1600E). A 1 mM solution of (dtbbpy)Ni(*o*-tolyl)Cl with 0.1 M tetrabutylammonium hexafluorophosphate as a supporting electrolyte in THF was prepared in a nitrogen filled glove box. The solution was removed from the glove box and a cyclic voltammogram was obtained under nitrogen atmosphere using a glassy carbon working electrode, a platinum mesh counter electrode, and a saturated calomel reference electrode. Scan rate = 0.01 Vs^{-1}.
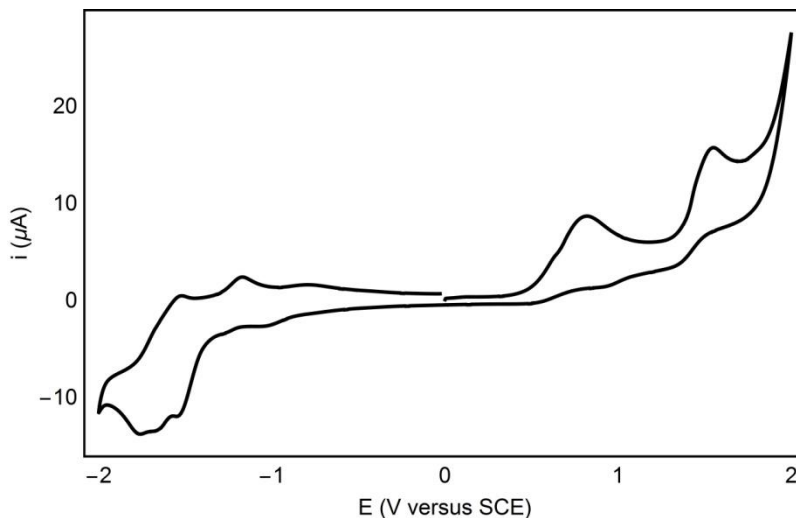
Fig. S32. Cyclic voltammogram of (dtbbpy)Ni(*o*-tolyl)Cl shows an irreversible first oxidation at E_p = 0.85 V versus SCE in THF which corresponds to the Ni^{II}/Ni^{III} redox couple and an irreversible first reduction at E_p = − 1.17 V versus SCE in THF which corresponds to the Ni^{I}/Ni^{II} redox couple. Remaining peaks could not be assigned due to the irreversible nature of the first oxidation and reduction.
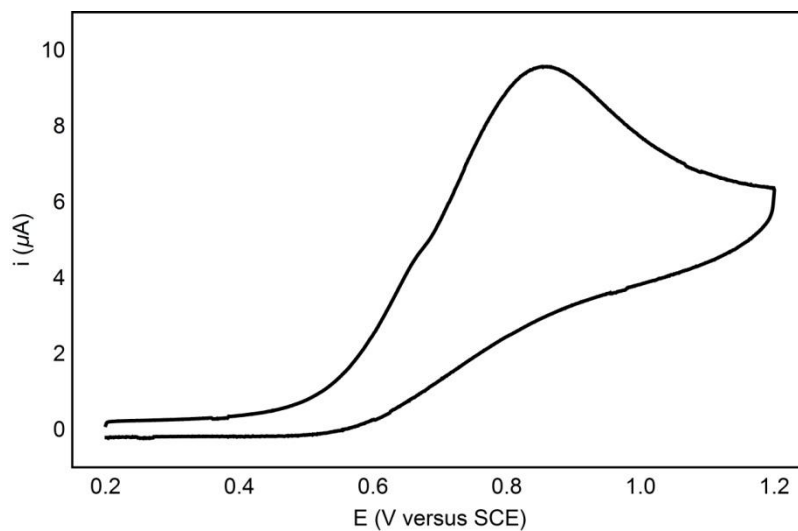
Fig. S33. Cyclic voltammogram of (dtbbpy)Ni(*o*-tolyl)Cl shows an irreversible first oxidation at E_p = 0.85 V versus SCE in THF which corresponds to the Ni^{II}/Ni^{III} redox couple.

XI. LED Emission Spectra

Emission spectra were measured on a digital spectrometer with optical fiber (Ocean Optics USB4000). Spectra were normalized to 1.0 at the emission maximum.
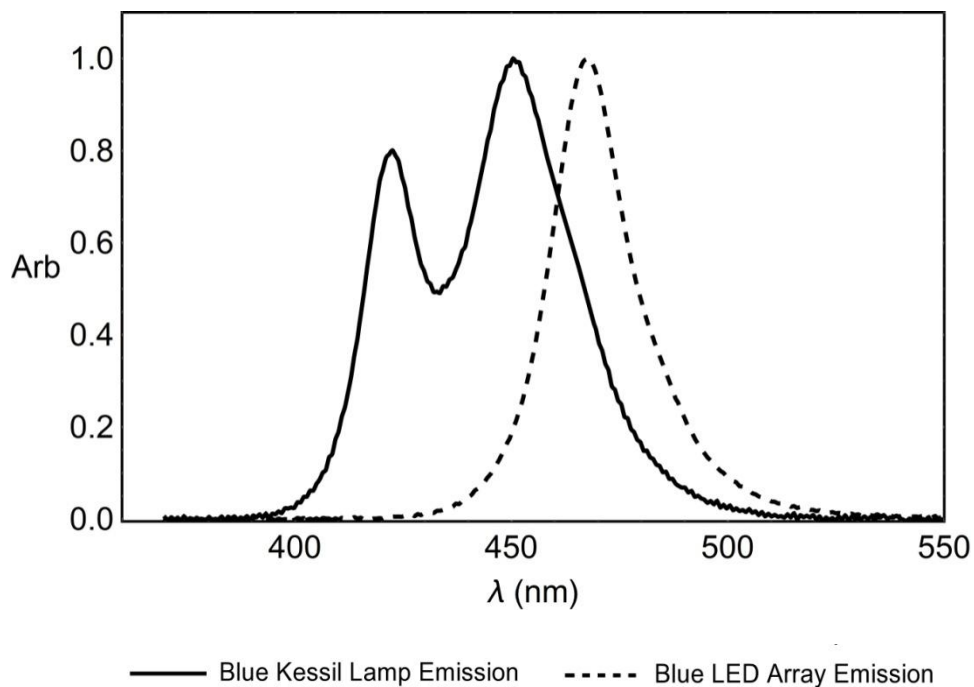
Fig. S34. Emission spectra for light sources. Emission spectrum from a 25W blue LED array shown as dashed line with emission maximum at $\lambda_{max} = 467$ nm. Emission spectrum from a 34 W blue Kessil Lamp shown as solid line with emission maximum at $\lambda_{max} = 450$ nm flanked by a second peak at $\lambda = 422$ nm.

XII. Computational Studies

Calculations were performed on Gaussian 09 D.01 software suite *(37)*. For all calculations the B3LYP hybrid exchange-correlation functional was used. Gas-phase geometry optimization and frequency calculations were carried out using a SDD basis set for Ni and Cl and 6-31G* for all other atoms. Optimization and frequency calculations for thermochemistry were carried out using a SDD basis for Ni and Cl and 6-311++G** for all other atoms with the SMD (THF) solvation model. All frequency calculations gave no imaginary frequencies. Time-dependent DFT (TD-DFT) calculations were carried out on the gas-phase optimized geometry using the TZVP basis set. These levels of theory have adequately reproduced experimental results for Ni(III) trihalides *(9)*.

Ni—Cl Bond (kcal mol^{-1})	
BDE	56
BDFE	47
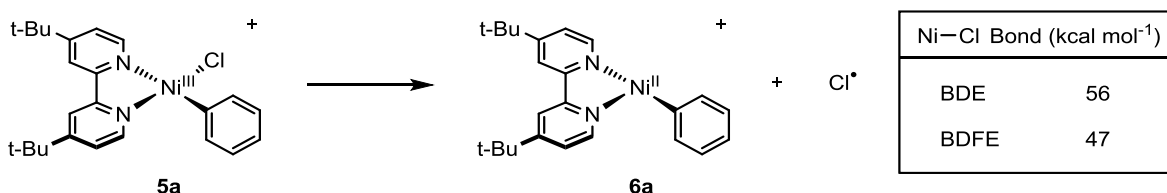
	[Ni^{III}(dtbbpy)(Ph)Cl]$^+$ (**5a**)	[Ni^{II}(dtbbpy)(Ph)]$^+$ (**6a**)	Cl$^\bullet$
Sum of Electronic and Thermal Enthalpies	-1672.382131	-1212.163114	-460.129513
Sum of Electronic and Thermal Free Energies	-1672.471305	-1212.248447	-460.147551

Fig. S35. Computed bond dissociation enthalpy and free energy for [Ni^{III}(dtbbpy)(Ph)Cl]$^+$. Energies are in hartrees.
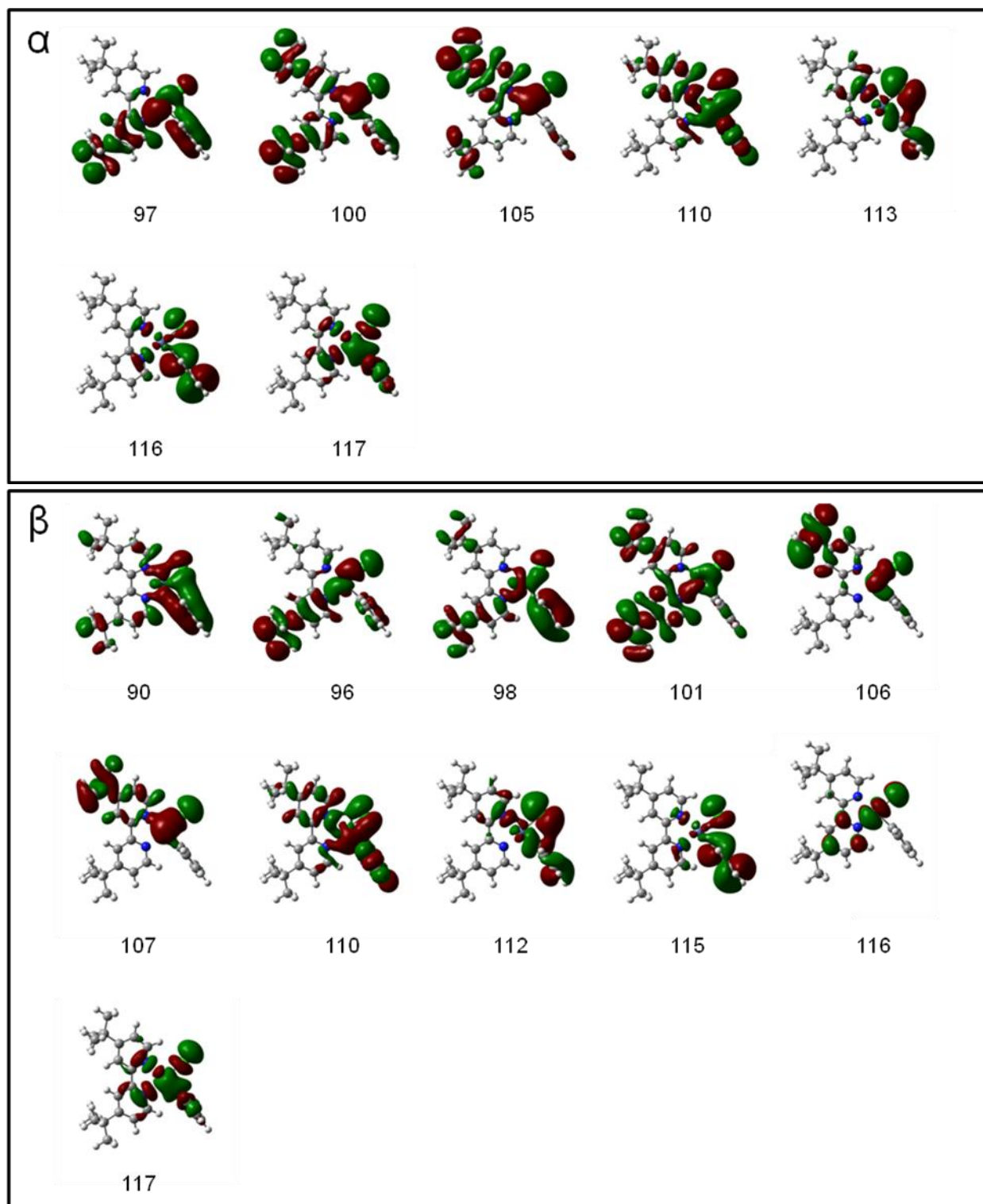
Fig. S36. Relevant molecular orbitals for [Ni(dtbbpy)(Ph)Cl]$^+$ (**5a**).
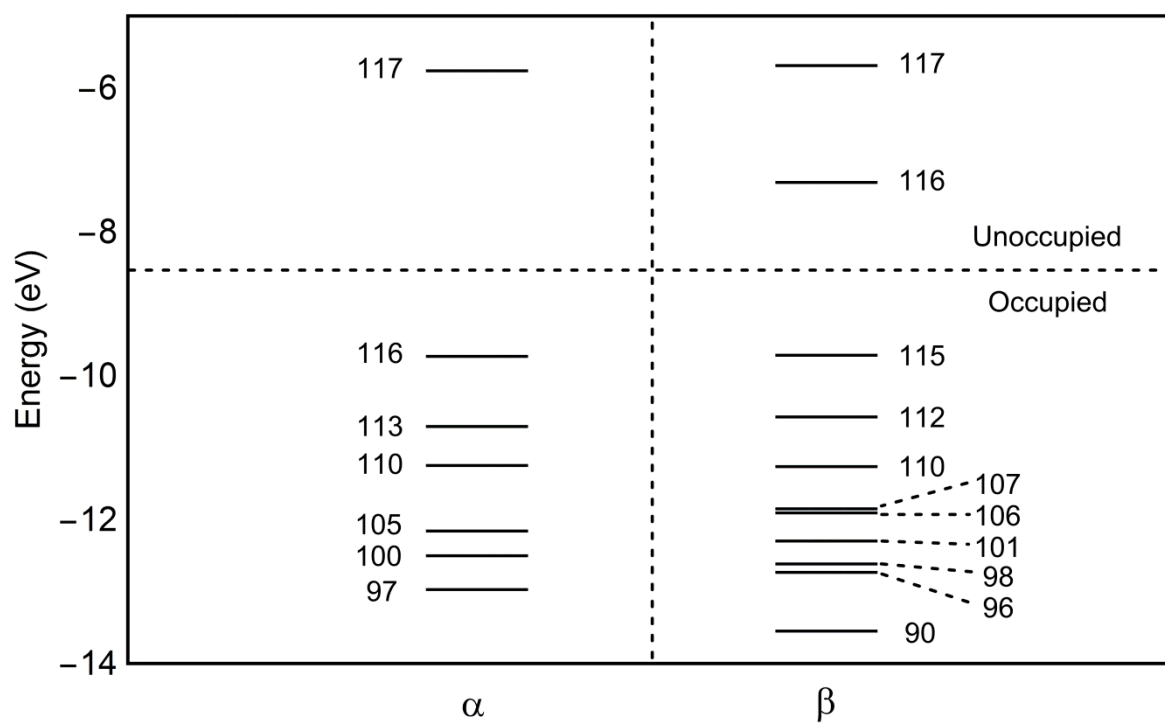
Fig. S37. Energy levels for relevant molecular orbitals of [Ni(dtbbpy)(Ph)Cl]$^+$ (**5a**).

Excited State	λ (nm)	Energy (kcal mol^{-1})	f	Contributions
1	689	46	0.0076	$116\alpha \rightarrow 117\alpha$ (74%) $115\beta \rightarrow 117\beta$ (12%)
2	486	65	0.0049	$113\alpha \rightarrow 117\alpha$ (11%) $109\beta \rightarrow 116\beta$ (28%) $111\beta \rightarrow 116\beta$ (26%) $115\beta \rightarrow 117\beta$ (15%)
3	460	68	0.0092	$109\beta \rightarrow 116\beta$ (10%) $111\beta \rightarrow 116\beta$ (17%) $112\beta \rightarrow 117\beta$ (26%) $115\beta \rightarrow 117\beta$ (18%)
4	401	78	0.0075	$110\alpha \rightarrow 117\alpha$ (29%) $107\beta \rightarrow 117\beta$ (22%) $110\beta \rightarrow 117\beta$ (13%) $115\beta \rightarrow 117\beta$ (10%)
5	396	79	0.0025	$114\alpha \rightarrow 118\alpha$ (40%) $113\beta \rightarrow 118\beta$ (38%)
6	392	80	0.0209	$113\alpha \rightarrow 117\alpha$ (33%) $112\beta \rightarrow 117\beta$ (12%)
7	375	84	0.022	$106\beta \rightarrow 117\beta$ (11%) $107\beta \rightarrow 117\beta$ (19%) $115\beta \rightarrow 117\beta$ (31%)

Table S15. TD-DFT calculated transitions for [Ni(dtbbpy)(Ph)Cl]$^+$ (**5a**). Transitions f > 0.0025 are shown. Orbital contributions ≥ 10% are shown of which Ni–Cl σ → σ* transitions are in red.
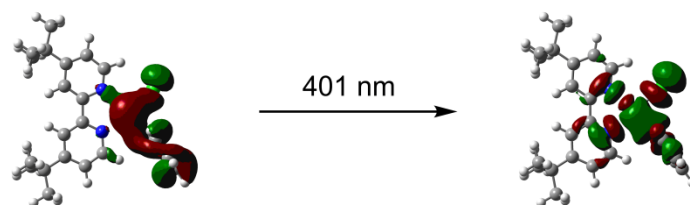
Fig. S38. β Natural transition orbitals for excited state 4 of [Ni(dtbbpy)(Ph)Cl]$^+$ (**5a**). This transition has a large Ni–Cl σ → σ* component.
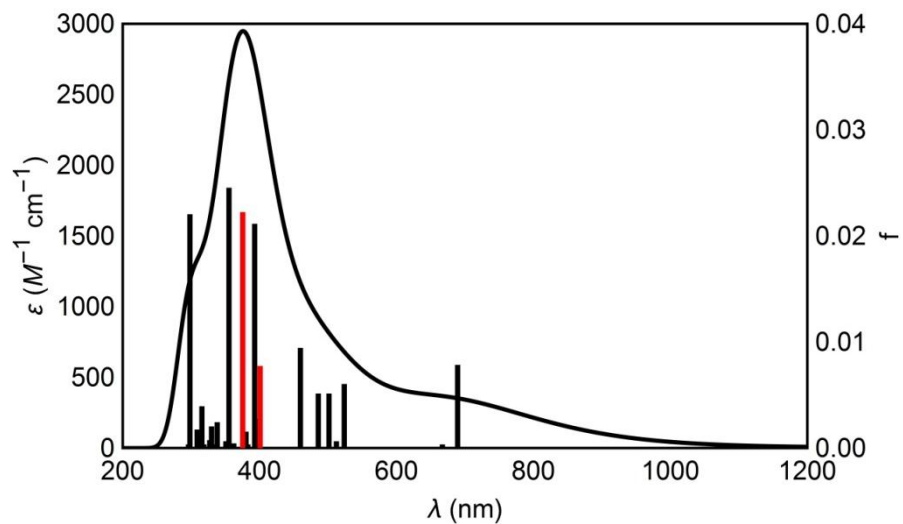
Fig. S39. Calculated absorption spectrum (solid black line) and oscillators (solid bars: first 40 excited states; red bars: transitions with > 10% Ni–Cl, σ → σ* contributions) from TD-DFT calculations on [Ni^{III}(dtbbpy)(Ph)Cl]$^+$ (**5a**).

Table S16. Cartesian coordinates for gas phase geometry-optimized [Ni(dtbbpy)(Ph)Cl]$^+$ (**5a**).

Atom Type	x	y	z
Ni	1.372841	-1.43945	-0.00027
C	-0.40067	0.800178	-0.00016
C	1.815472	1.527248	-0.0005
C	-0.84057	2.118359	-5.3E-05
C	1.424483	2.8596	-0.00042
H	2.861958	1.249373	-0.00066
C	0.063934	3.1956	-0.00019
H	-1.90472	2.316432	0.000144
H	2.194375	3.620584	-0.00055
C	-1.30536	-0.37349	-4.5E-05
C	-2.69349	-0.29578	0.00008
C	-3.48309	-1.46126	0.000136
H	-3.17621	0.673369	0.000118
C	-1.39842	-2.6926	-0.00008
C	-2.79109	-2.67811	0.000032
H	-0.83651	-3.62097	-0.00013
H	-3.31584	-3.62487	0.000065
C	3.304678	-1.20222	0.000046
C	3.948719	-1.05645	-1.22301
C	3.947759	-1.05542	1.223503
C	5.294669	-0.66367	-1.21081
C	5.293717	-0.66267	1.212069
C	5.96061	-0.46609	0.000804
H	5.817458	-0.53229	-2.15405
H	5.815766	-0.5305	2.155609
Cl	1.815653	-3.57132	-0.00031
N	0.934034	0.511864	-0.00036
N	-0.66923	-1.57075	-0.0001
H	3.440285	-1.23875	2.166287
H	7.007554	-0.17794	0.001091
H	3.441987	-1.24057	-2.16603
C	-0.44741	4.639566	-7.7E-05
C	-5.01333	-1.36104	0.000225
C	-1.31069	4.866298	-1.26684
H	-0.72619	4.711586	-2.18034
H	-2.18052	4.201611	-1.30294
H	-1.6833	5.895931	-1.2752
C	-1.31068	4.866181	1.266694
H	-2.18052	4.201501	1.302763
H	-0.72618	4.711396	2.180185

H	-1.68329	5.895812	1.275148
C	0.704831	5.661339	-0.00002
H	1.337261	5.568129	0.890027
H	1.337136	5.568391	-0.89018
H	0.290636	6.674097	0.000149
C	-5.46667	-0.59279	-1.26626
H	-5.06157	0.424456	-1.30213
H	-5.15845	-1.11363	-2.17939
H	-6.55869	-0.51236	-1.27593
C	-5.4666	-0.59221	1.266377
H	-5.15826	-1.11259	2.179738
H	-5.06162	0.425093	1.301724
H	-6.55863	-0.51187	1.276108
C	-5.68377	-2.7479	0.000572
H	-5.42237	-3.33193	-0.88911
H	-5.42204	-3.33163	0.890353
H	-6.77115	-2.62461	0.000739

Table S17. Cartesian coordinates for solution phase geometry-optimized [Ni(dtbbpy)(Ph)Cl]⁺ (**5a**).

Atom Type	x	y	z
Ni	1.387736	-1.40173	-0.04729
C	-0.41112	0.79776	0.018752
C	1.785863	1.565592	0.066009
C	-0.87758	2.103395	0.001578
C	1.369822	2.887001	0.052116
H	2.837541	1.319323	0.091023
C	0.006697	3.192356	0.006246
H	-1.94299	2.277948	-0.02856
H	2.126578	3.658388	0.068864
C	-1.29485	-0.38888	0.002635
C	-2.68122	-0.32784	0.040021
C	-3.45058	-1.50179	0.024073
H	-3.17215	0.633706	0.084945
C	-1.35939	-2.70283	-0.06793
C	-2.74781	-2.70754	-0.03176
H	-0.79764	-3.62729	-0.11202
H	-3.2561	-3.66067	-0.04758
C	3.317891	-1.12225	0.034617
C	4.019104	-0.90184	-1.13971
C	3.901936	-1.07025	1.290013
C	5.371603	-0.55397	-1.04008
C	5.25608	-0.72182	1.369101
C	5.985115	-0.46394	0.208994
H	5.938789	-0.36653	-1.94549
H	5.732561	-0.66401	2.341774
Cl	1.871274	-3.54514	-0.29049
N	0.92631	0.535508	0.041875
N	-0.64492	-1.57458	-0.05027
H	3.342029	-1.28475	2.193351
H	7.03548	-0.20392	0.277562
H	3.549409	-0.98893	-2.11263
C	-0.5298	4.624116	-0.05862
C	-4.98002	-1.42487	0.077963
C	-1.31491	4.794741	-1.38114
H	-0.66826	4.629693	-2.24766
H	-2.15907	4.104351	-1.45185
H	-1.70904	5.812912	-1.44245
C	-1.4722	4.876614	1.140876
H	-2.33252	4.20287	1.144003

H	-0.94285	4.757689	2.090634
H	-1.85347	5.900344	1.092843
C	0.601238	5.664175	-0.01915
H	1.17781	5.604079	0.908154
H	1.289774	5.554107	-0.86149
H	0.171152	6.667157	-0.07526
C	-5.49025	-0.56742	-1.10311
H	-5.1103	0.4565	-1.06383
H	-5.19962	-1.00262	-2.06355
H	-6.58221	-0.51668	-1.07269
C	-5.39707	-0.76474	1.413326
H	-5.04689	-1.34948	2.268872
H	-5.00184	0.249524	1.510056
H	-6.4877	-0.70495	1.46806
C	-5.63148	-2.81534	-0.00677
H	-5.37525	-3.33219	-0.93603
H	-5.34527	-3.45432	0.833413
H	-6.71838	-2.70548	0.020464

Table S18. Cartesian coordinates for solution phase geometry-optimized [Ni(dtbbpy)(Ph)]$^+$ (**6a**).

Atom Type	x	y	z
Ni	1.508441	-1.41945	0.003544
C	-0.27815	0.663075	0.003367
C	1.911993	1.446583	0.03719
C	-0.75959	1.962809	0.001242
C	1.478364	2.765271	0.041951
H	2.964816	1.207896	0.049292
C	0.113385	3.060196	0.022652
H	-1.82754	2.123283	-0.01806
H	2.229243	3.542765	0.058919
C	-1.13203	-0.54308	-0.00497
C	-2.51938	-0.53976	-0.01017
C	-3.23496	-1.7478	-0.0178
H	-3.05	0.40193	-0.0068
C	-1.09187	-2.86098	-0.0104
C	-2.47974	-2.92492	-0.01852
H	-0.49033	-3.76321	-0.00937
H	-2.94784	-3.89863	-0.02412
C	3.371819	-1.33167	-0.00228
C	4.09648	-1.26413	-1.20281
C	4.065259	-1.60522	1.188048
C	5.472987	-1.50396	-1.21891
C	5.442702	-1.84495	1.172055
C	6.146688	-1.79518	-0.03148
H	6.01888	-1.4606	-2.15606
H	5.964868	-2.06313	2.098296
N	1.061534	0.409838	0.017137
N	-0.43017	-1.70028	-0.00363
H	3.538017	-1.63585	2.137849
H	7.216443	-1.97467	-0.04327
H	3.592173	-1.02896	-2.13603
C	-0.43914	4.488567	0.019751
C	-4.76852	-1.73725	-0.01594
C	-1.25492	4.706443	-1.27606
H	-0.63278	4.563237	-2.16413
H	-2.10721	4.025352	-1.34352
H	-1.64326	5.728625	-1.29668
C	-1.35953	4.681744	1.246894
H	-2.21357	3.999966	1.236617
H	-0.81099	4.526464	2.180485

H	-1.75081	5.702922	1.251663
C	0.682255	5.538149	0.08082
H	1.281099	5.440292	0.990527
H	1.352	5.475144	-0.78135
H	0.241544	6.538176	0.082542
C	-5.27667	-0.94699	-1.24411
H	-4.95322	0.09658	-1.22613
H	-4.92603	-1.39688	-2.17739
H	-6.37023	-0.95355	-1.25609
C	-5.26117	-1.04952	1.278942
H	-4.91615	-1.5865	2.167262
H	-4.91397	-0.01579	1.350205
H	-6.35473	-1.03664	1.294781
C	-5.35634	-3.15721	-0.07195
H	-5.05333	-3.6903	-0.97771
H	-5.06512	-3.75707	0.794917
H	-6.44739	-3.09459	-0.07559

XIII. References

(1) Fokin, A. A.; Schreiner P. R. *Chem. Rev.* **2002**, *102*, 1551–1594.

(2) Carey, F. A.; Sundberg, R. J. *Advanced Organic Chemistry Part A: Structure and Mechanisms*; Springer: New York, 2007; 965–1063.

(3) Tasker, S. Z.; Standley, E. A.; Jamison, T. F. *Nature* **2014**, *509*, 299–309.

(4) Ananikov, V. P. *ACS Catal.* **2015**, *5*, 1964–1971.

(5) (a) Tellis, J. C.; Primer, D. N.; Molander, G. A. *Science* **2014**, *345*, 433–436. (b) Weix, D. J. *Acc. Chem. Res.* **2015**, *48*, 1767–1775. (c) Cornella, J.; Edwards, J. T.; Qin, T.; Kawamura, S.; Wang, J.; Pan, C.; Gianatassio, R.; Schmidt, M.; Eastgate, M. D.; Baran, P. S. *J. Am. Chem. Soc.* **2016**, *138*, 2174–2177. (d) Shaw, M. H.; Twilton, J.; MacMillan, D. W. C. *J. Org. Chem.* **2016**, *81*, 6898–6926.

(6) (a) Zuo, Z.; Ahneman, D. T.; Chu, L.; Terrett, J. A.; Doyle, A. G.; MacMillan, D. W. C. *Science* **2014**, *345*, 437–440. (b) Joe, C. L.; Doyle, A. G. *Angew. Chem. Int. Ed.* **2016**, *55*, 4040–4043.   (c) Ahneman, D. T.; Doyle, A. G. *Chem. Sci.* **2016**, DOI: 10.1039/c6sc02815b.

(7) Shaw, M. H.; Shurtleff, V. W.; Terrett, J. A.; Cuthbertson, J. D.; MacMillan, D. W. C. *Science* **2016**, *352*, 1304–1308.

(8) Esswein, A. J.; Nocera, D. G. *Chem. Rev.* **2007**, *107*, 4022–4047.

(9) Hwang, S. J.; Powers, D. C.; Maher, A. G.; Anderson, B. L.; Hadt, R. G.; Zheng, S. L.; Chen, S.; Nocera, D. G. *J. Am. Chem. Soc.* **2015**, *137*, 6472–6475.

(10) Hwang, S. J.; Anderson, B. L.; Powers, D. C.; Maher, A. G.; Hadt, R. G.; Nocera, D. G. *Organometallics* **2015**, *34*, 4766–4774.

(11) Isse, A. A.; Lin C. Y.; Coote, M. L.; Gennaro, A. *J. Phys. Chem. B.* **2011**, *115*, 678–684.

(12) For a leading example of Ni-catalyzed C(sp^3)–H arylation of ethers using aryl boronic acids and a stoichiometric oxidant, see: (a) Liu, D.; Liu, C.; Li, H.; Lei, A. *Angew. Chem. Int. Ed.* **2013**, *52*, 4453–4456. For a leading example of photoredox-catalyzed C(sp^3)–H arylation of benzylic ethers using electron-deficient aryl nitriles, see: (b) Qvortrup, K.; Rankic, D. A.; MacMillan, D. W. C. *J. Am. Chem. Soc.* **2014**, *136*, 626–629.

(13) Luca, O. R.; Gustafson, J. L.; Maddox, S. M.; Fenwick, A. Q.; Smith, D. C. *Org. Chem. Front.* **2015**, *2*, 823–848.

(14) Lowry, M. S.; Goldsmith, J. I.; Slinker, J. D.; Rohl, R.; Pascal, R. A.; Malliaras G. G.; Bernhard, S. *Chem. Mater.* **2005**, *17*, 5712–5719.

(15) Lipinski, C. A.; Lombardo, F.; Dominy, B. W.; Feeney, P. J. *Adv. Drug Deliv. Rev.* **1997**, *23*, 3–25.

(16) Tsou, T. T.; Kochi, J. K. *J. Am. Chem. Soc.* **1979**, *101*, 6319–6332.

(17) Scariano, J. C.; Stewart, L. C. *J. Am. Chem. Soc.* **1983**, *105*, 3609–3614.

(18) Tsou, T. T.; Kochi, J. K. *J. Org. Chem.* **1980**, *45*, 1930–1937.

(19) Sheppard, T. D. *Org. Biomol. Chem.* **2009**, *7*, 1043–1052.

(20) Preliminary studies suggest that nickel, the iridium catalyst, and light are all necessary for halogen exchange (Table S10).

(21) Connelly, N. G.; Geiger, W. E. *Chem. Rev.* **1996**, *96*, 877–910.

(22) Zheng, B.; Tang, F.; Luo, J.; Schultz, J. W.; Rath, N. P.; Mirica, L. M. *J. Am. Chem. Soc.* **2014**, *136*, 6499–6504.

(23) Zuo, Z.; MacMillan, D. W. C. *J. Am. Chem. Soc.* **2014**, *136*, 5257–5260.

(24) Ueno, R.; Shirakawa, E. *Org. Biomol. Chem.* **2014**, *12*, 7469–7473.

(25) Molander, G. A.; Ito, T. *Org. Lett.* **2001**, *3*, 393–396.

(26) Liu, C.; Han, N.; Song, X.; Qin, J. *Eur. J. Org. Chem.* **2010**, *29*, 5548–5551.

(27) Ackermann, L.; LPotukuchi, H.; Kapadi, A. R.; Schulzke, C. *Chem. Eur. J.* **2010**, *16*, 3300–3303.

(28) Zheng, M.; Chen, P.; Wu, W.; Jiang, H. *Chem. Commun.* **2016**, *52*, 84–87.

(29) Molander, G. A.; Trice, S. L. J.; Kennedy, S. M.; Dreher, S. D.; Tudge, M. T. *J. Am. Chem. Soc.* **2012**, *134*, 11667–11673.

(30) Niu, L.; Zhang, H.; Yang, H.; Fu, H. *Synlett*, **2014**, *25*, 995–1000.

(31) Mee, S. P. H.; Lee, V.; Baldwin, J. E. *Chem. Eur. J.* **2005**, *11*, 3294–3308.

(32) Narisada, M.; Horibe, I.; Watanabe, F.; Takeda, K. *J. Org. Chem.* **1989**, *54*, 5308–5313.

(33) Wotal, A. C.; Ribson, R. D.; Weix, D. J. *Organometallics*, **2014**, *33*, 5874–5881.

(34) Lakowicz, J. R. *Principles of Fluorescence Spectroscopy*; Kluwer Academic/Plenum Publishers: New York, 1999.

(35) Akaike, H. *Proceeding of the Second International Symposium on Information Theory*; Petrov, B. N.; Caski, F.; Akedemiai Kiado: Budapest, 1973; 267–281.

(36) Burnham, K. P.; Anderson, D. R. *Sociological Methods & Research* **2004**, *33*, 261–304.

(37) Frisch, M. J.; Trucks, G. W.; Schlegel, H. B.; Scuseria, G. E.; Robb, M. A.; Cheeseman, J. R.; Scalmani, G.; Barone, V.; Mennucci, B.; Petersson, G. A.; Nakatsuji, H.; Caricato, M.; Li, X.; Hratchian, H. P.; Izmaylov, A. F.; Bloino, J.; Zheng, G.; Sonnenberg, J. L.; Hada, M.; Ehara, M.; Toyota, K.; Fukuda, R.; Hasegawa, J.; Ishida, M.; Nakajima, T.; Honda, Y.; Kitao, O.; Nakai, H.; Vreven, T.; Montgomery, J. A., Jr.; Peralta, J. E.; Ogliaro, F.; Bearpark, M.; Heyd, J. J.; Brothers, E.; Kudin, K. N.; Staroverov, V. N.; Keith, T.; Kobayashi, R.; Normand, J.; Raghavachari, K.; Rendell, A.; Burant, J. C.; Iyengar, S. S.; Tomasi, J.; Cossi, M.; Rega, N.; Millam, J. M.; Klene, M.; Knox, J. E.; Cross, J. B.; Bakken, V.; Adamo, C.; Jaramillo, J.; Gomperts, R.; Stratmann, R. E.; Yazyev, O.; Austin, A. J.; Cammi, R.; Pomelli, C.; Ochterski, J. W.; Martin, R. L.; Morokuma, K.; Zakrzewski, V. G.; Voth, G. A.; Salvador, P.; Dannenberg, J. J.; Dapprich, S.; Daniels, A. D.; Farkas, O.; Foresman, J. B.; Ortiz, J. V.; Cioslowski, J.; Fox, D. J. Gaussian 09, revision D.01; Gaussian, Inc.: Wallingford, CT, 2009.

XIV. NMR Spectra

^{1}H NMR (501 MHz, CDCl$_3$): 2-(*p*-tolyl)tetrahydrofuran (10)
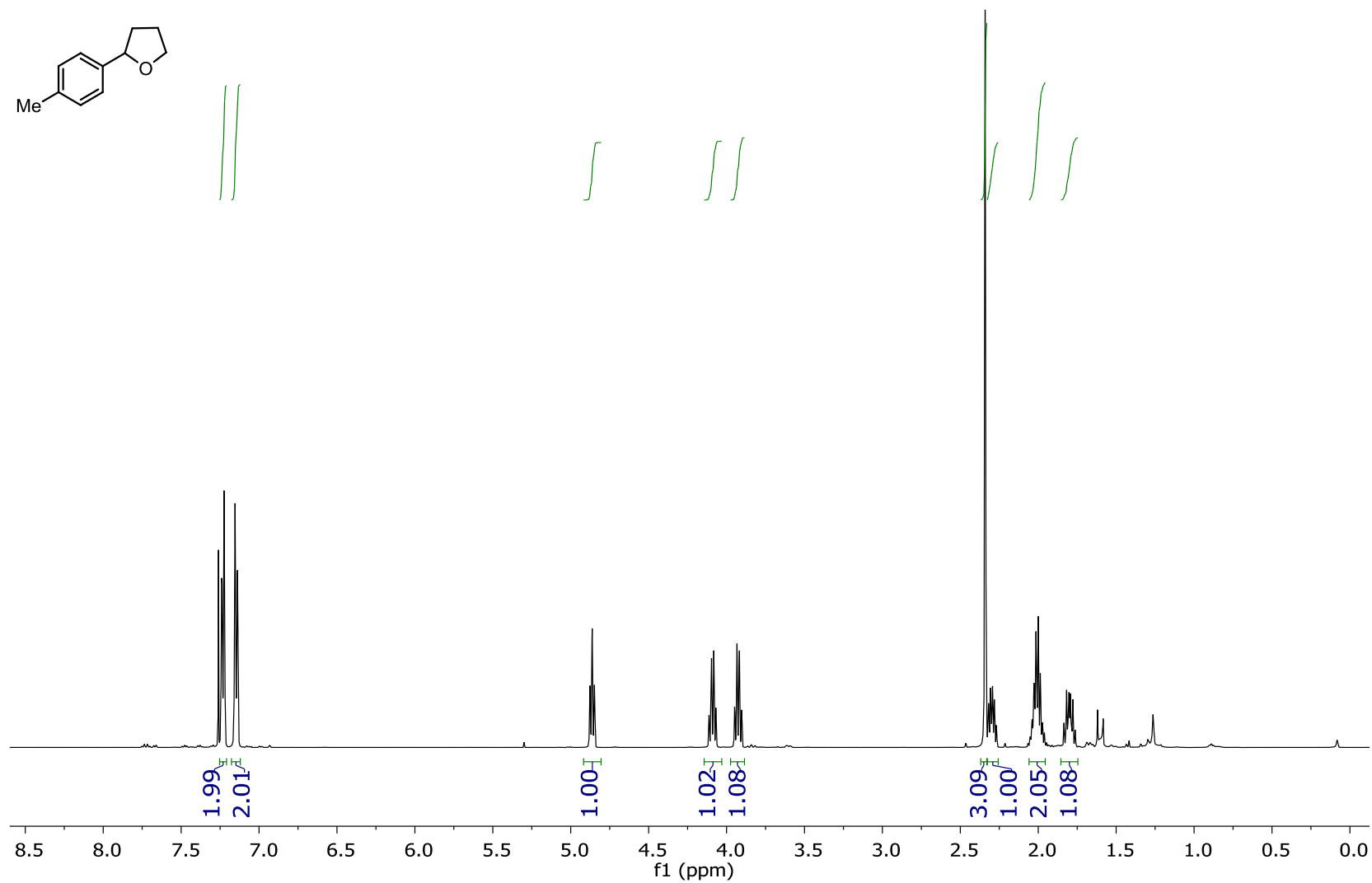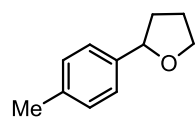
¹³C NMR (126 MHz, CDCl₃): 2-(*p*-tolyl)tetrahydrofuran (10)
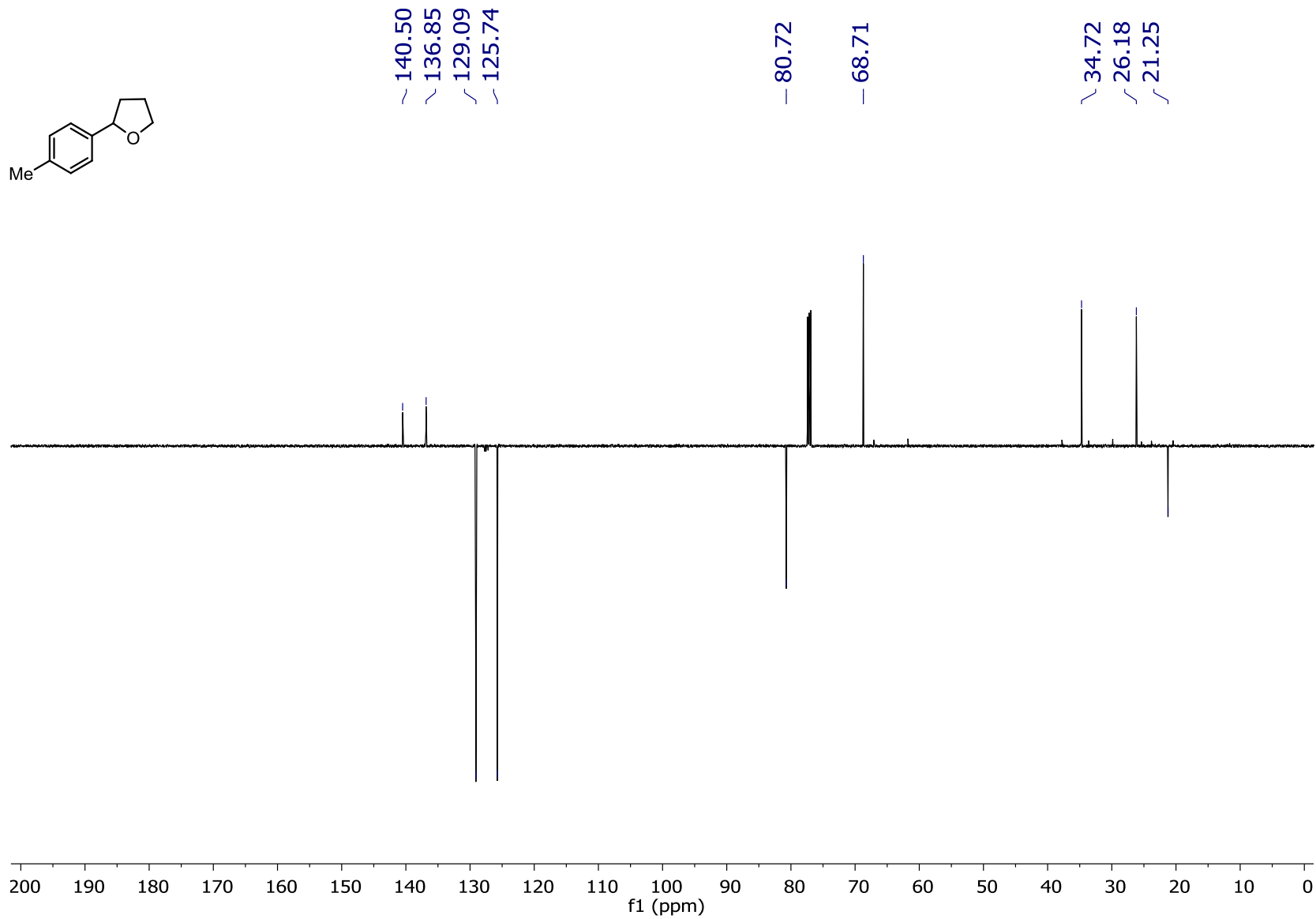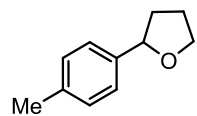
140.50
136.85
129.09
125.74

80.72

68.71

34.72
26.18
21.25

f1 (ppm)

S73

^{1}H NMR (501 MHz, CDCl$_3$): 2-(*m*-tolyl)tetrahydrofuran (11)

¹³C NMR (126 MHz, CDCl₃): 2-(*m*-tolyl)tetrahydrofuran (11)

¹³C NMR (126 MHz, CDCl₃): 2-(*m*-tolyl)tetrahydrofuran (11)

143.48
138.04
128.32
128.00
126.42
122.86
80.84
68.79
34.70
26.19
21.62

Me

230 220 210 200 190 180 170 160 150 140 130 120 110 100 90 80 70 60 50 40 30 20 10 0 -10
f1 (ppm)

S75
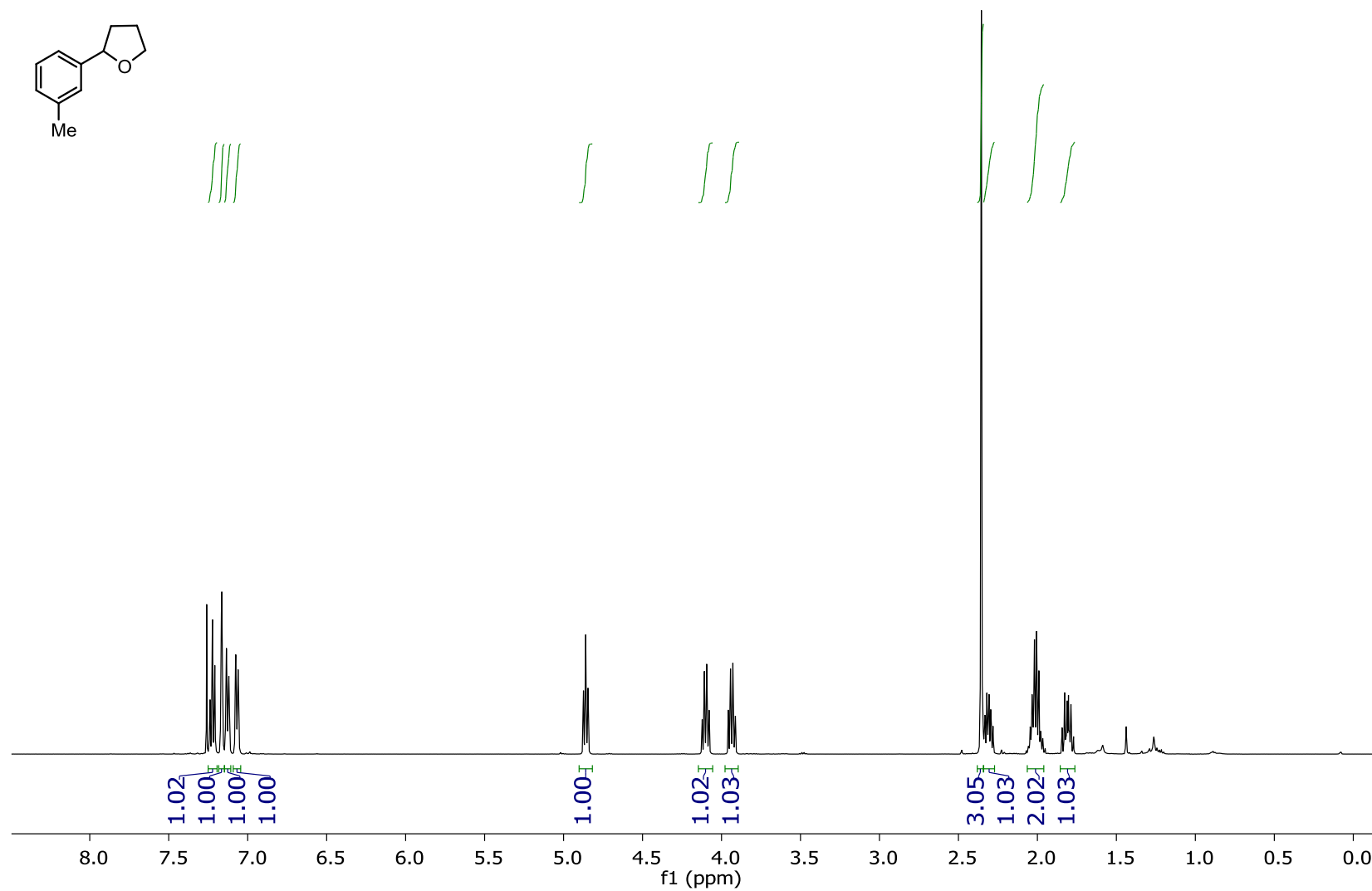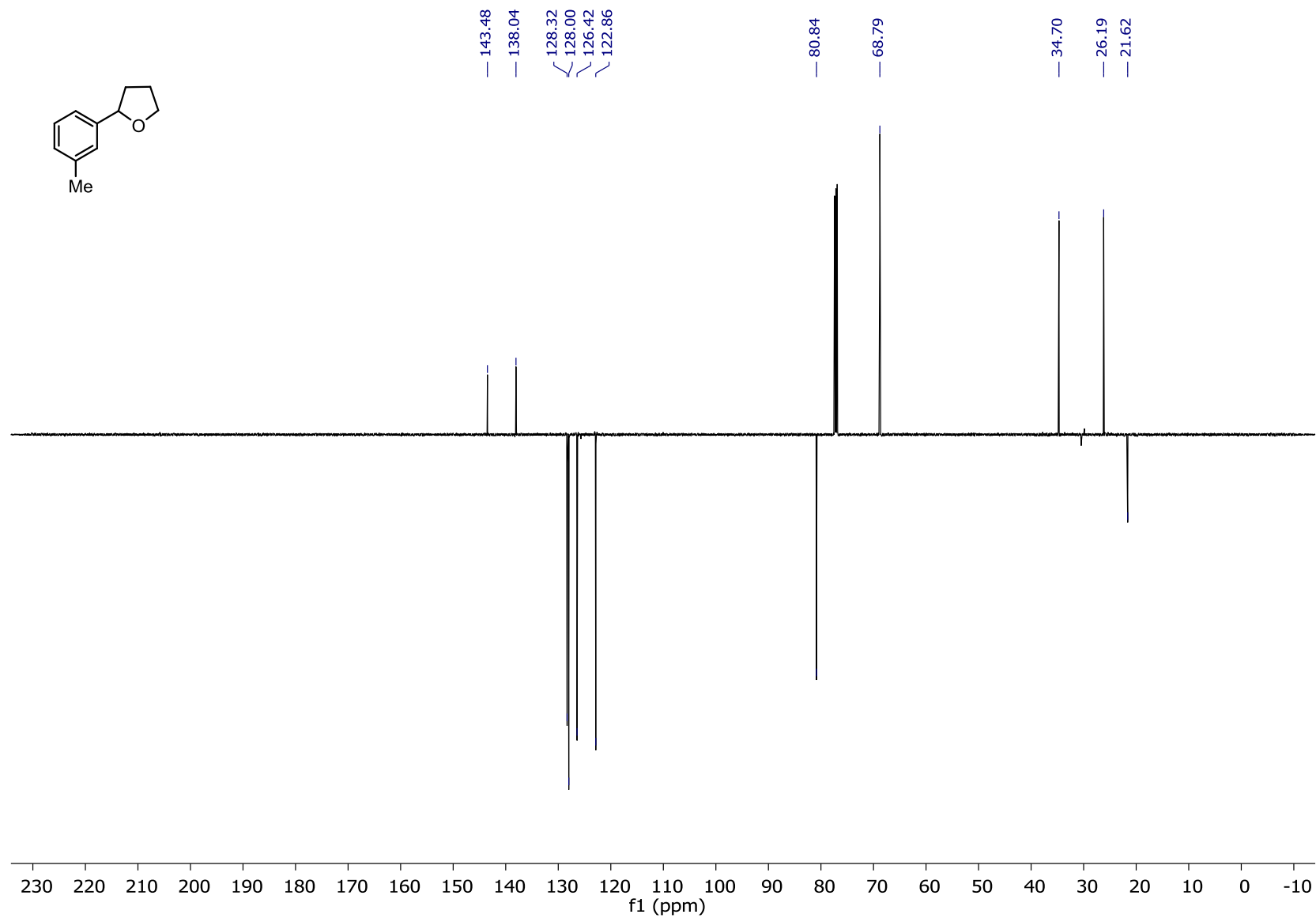
¹H NMR (501 MHz, CDCl₃): 2-(*o*-tolyl)tetrahydrofuran (12)
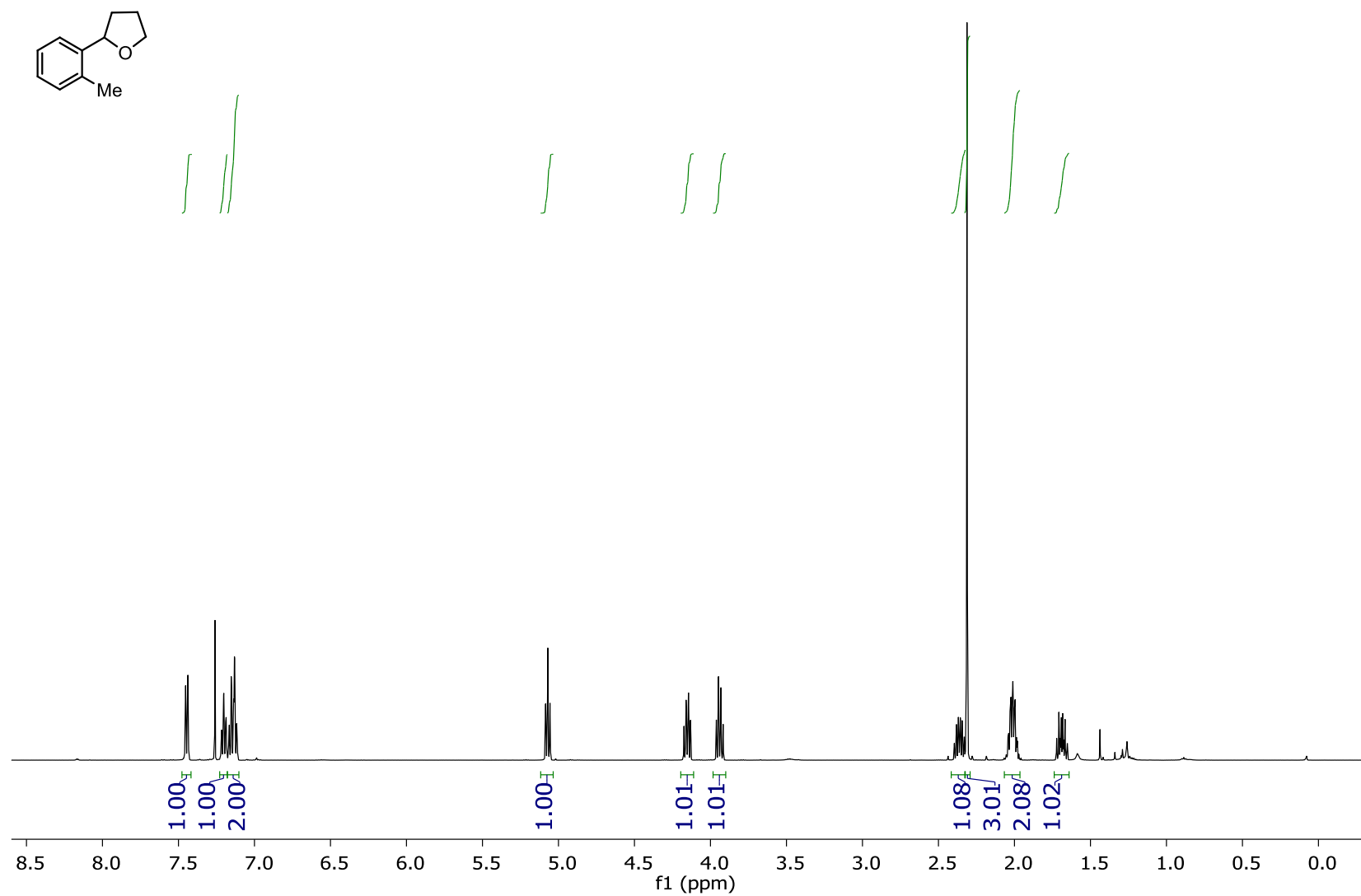
^{13}C NMR (126 MHz, CDCl$_3$): 2-(o-tolyl)tetrahydrofuran (12)

141.97
134.30
130.25
126.89
126.12
124.66
78.09
68.79
33.30
26.17
19.39

f1 (ppm)
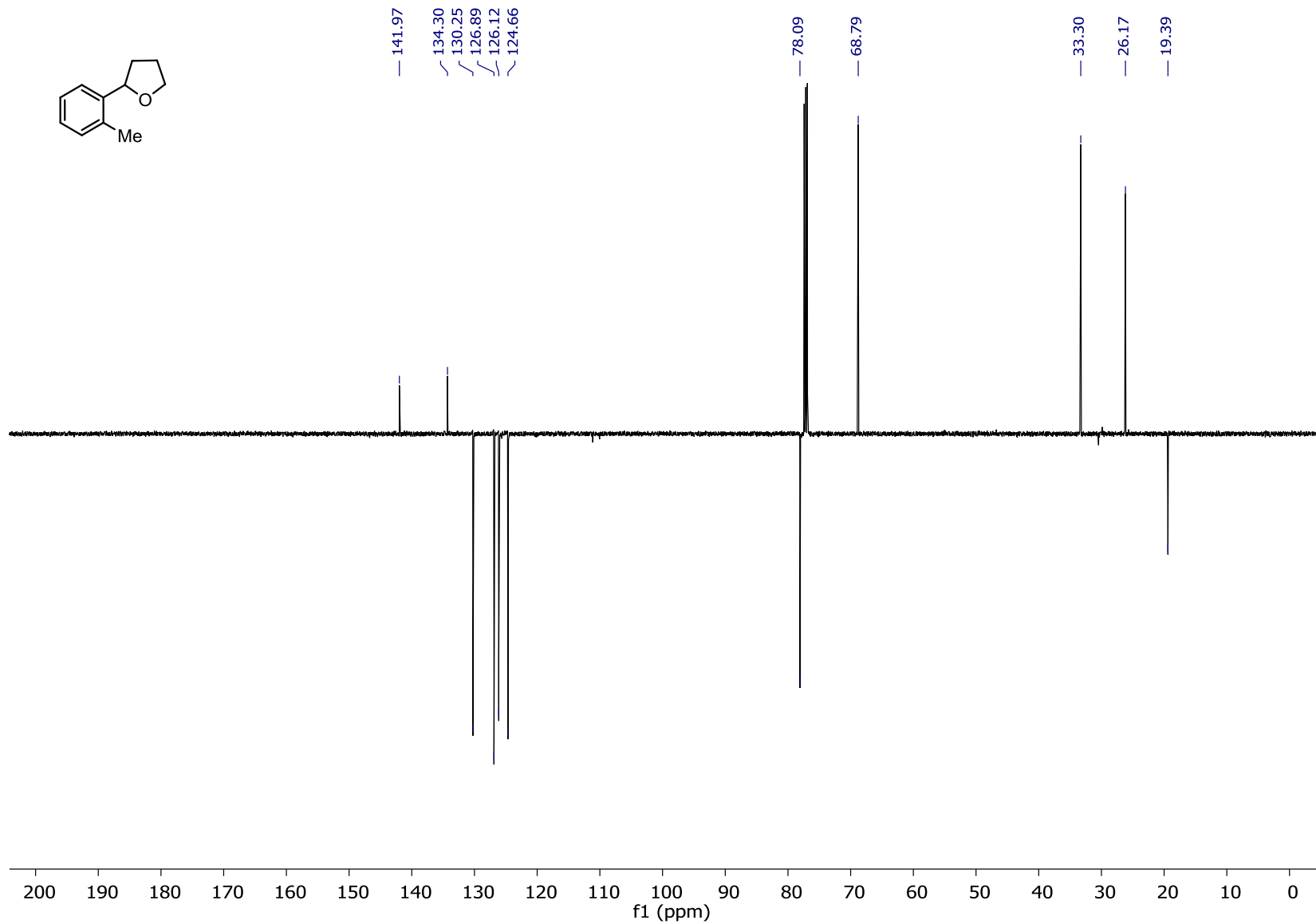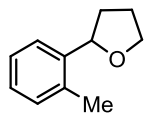
^{1}H NMR (501 MHz, CDCl$_3$): 2-([1,1′-biphenyl]-4-yl)tetrahydrofuran (13)

¹³C NMR (126 MHz, CDCl₃): 2-([1,1´-biphenyl]-4-yl)tetrahydrofuran (13)

^{13}C NMR (126 MHz, CDCl$_3$): 2-([1,1´-biphenyl]-4-yl)tetrahydrofuran (13)

142.66
141.15
140.22
128.86
127.29
127.22
127.21
126.23

80.59

68.85

34.75

26.23

200   190   180   170   160   150   140   130   120   110   100   90   80   70   60   50   40   30   20   10   0
f1 (ppm)
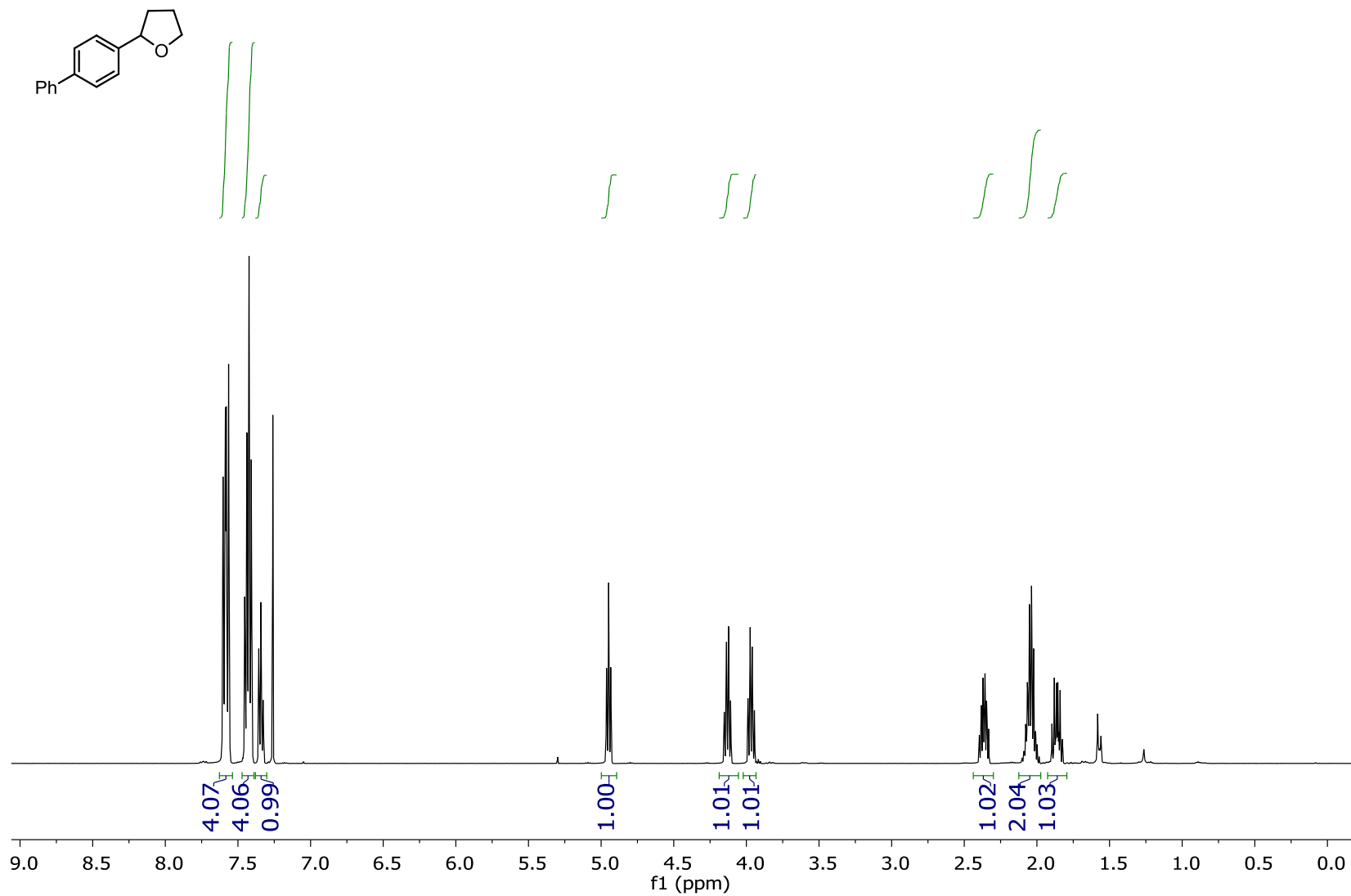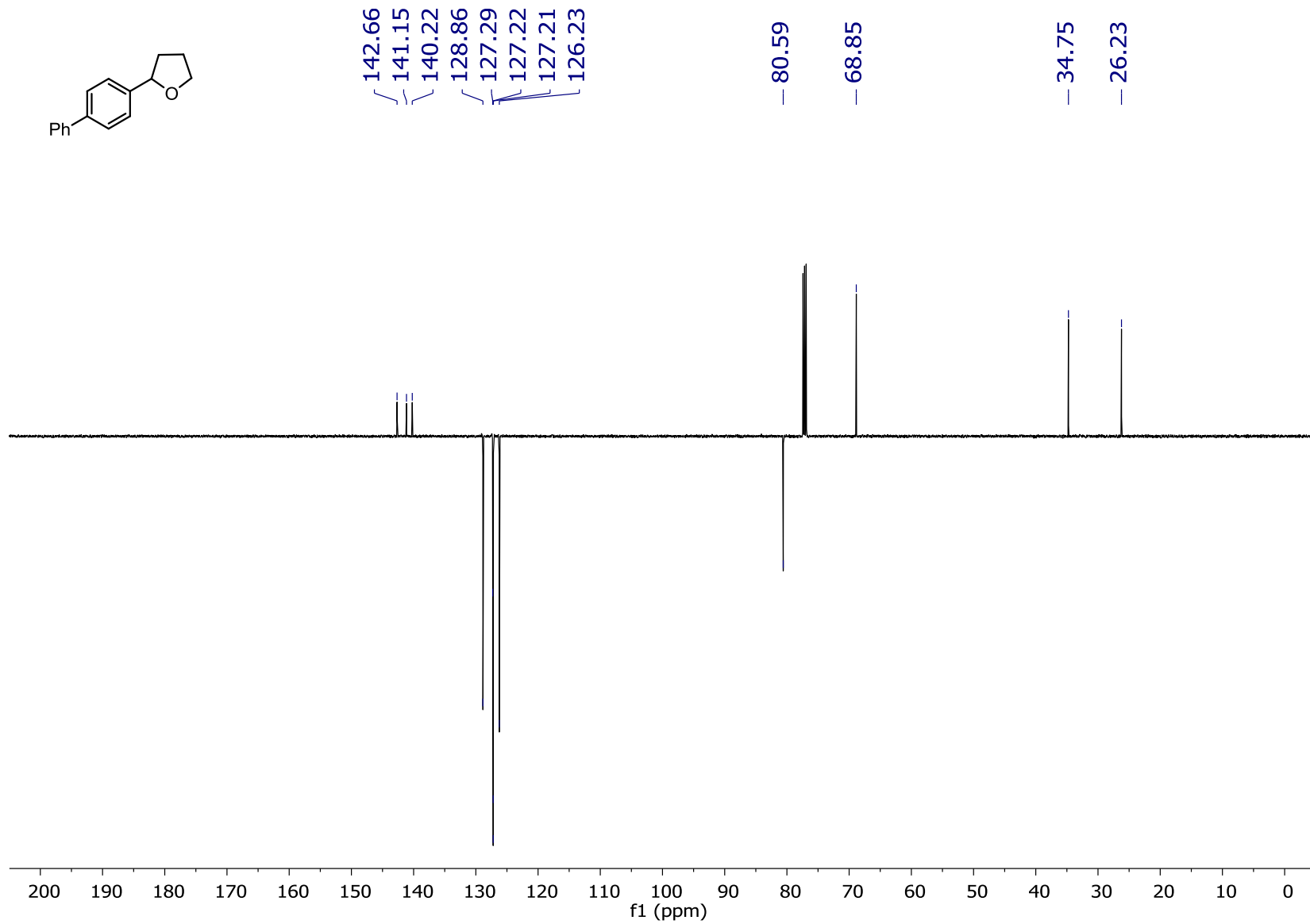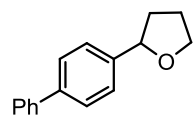
^{1}H NMR (501 MHz, CDCl$_3$): 2-(4-phenoxyphenyl)tetrahydrofuran (14)

^{13}C NMR (126 MHz, CDCl$_3$): 2-(4-phenoxyphenyl)tetrahydrofuran (14)
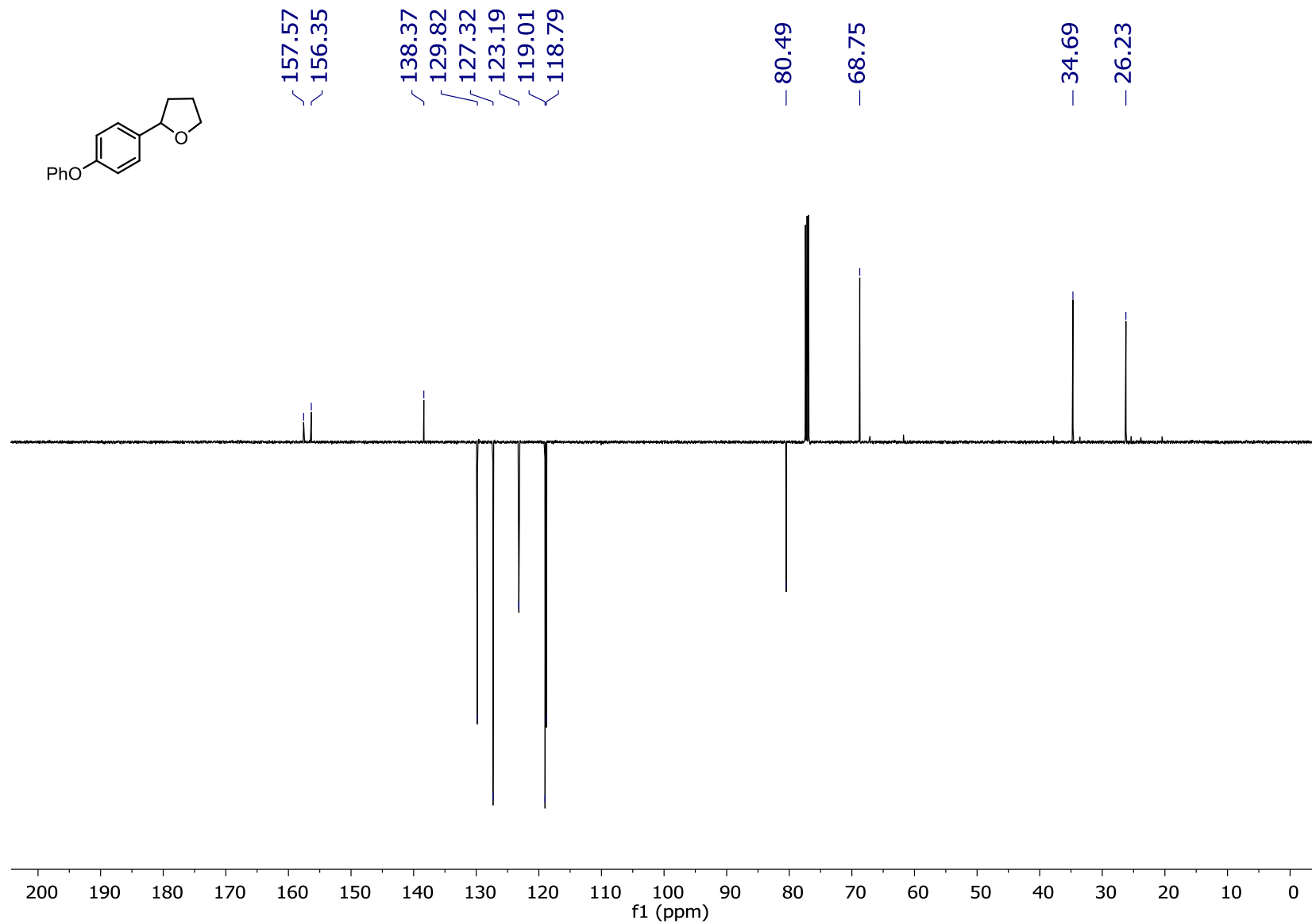
157.57
156.35
138.37
129.82
127.32
123.19
119.01
118.79
80.49
68.75
34.69
26.23

f1 (ppm)

^{1}H NMR (501 MHz, CDCl$_3$): 4-(tetrahydrofuran-2-yl)benzonitrile (15)

f1 (ppm)

1.97 1.99 1.00 1.05 1.03 1.03 2.12 1.04

¹³C NMR (126 MHz, CDCl₃): 4-(tetrahydrofuran-2-yl)benzonitrile (15)

The ^{13}C NMR (126 MHz, CDCl$_3$): 4-(tetrahydrofuran-2-yl)benzonitrile (15)

149.36
132.32
126.29
119.12
110.94
79.97
69.11
34.86
26.07

230 220 210 200 190 180 170 160 150 140 130 120 110 100 90 80 70 60 50 40 30 20 10 0 -10
f1 (ppm)
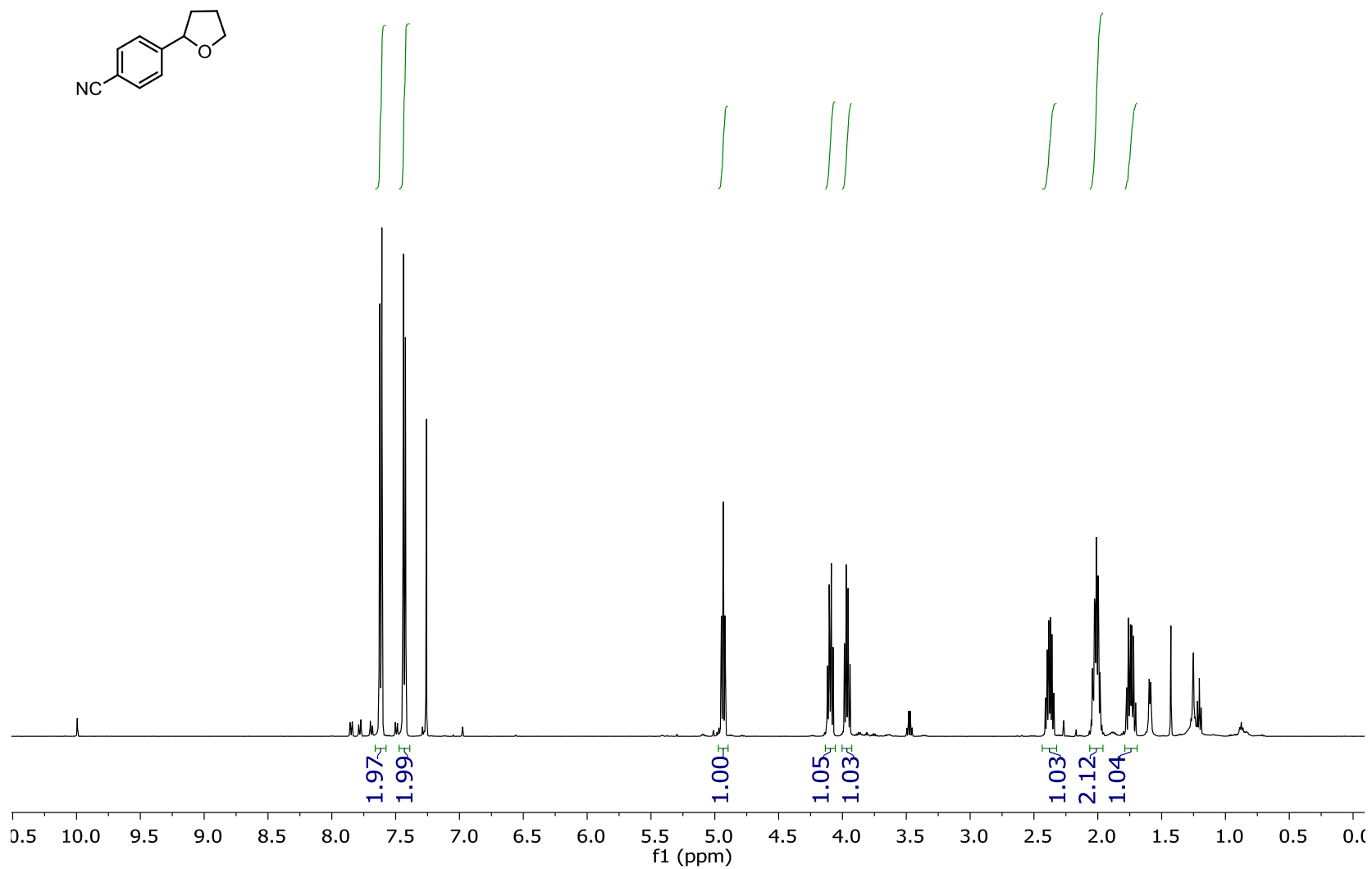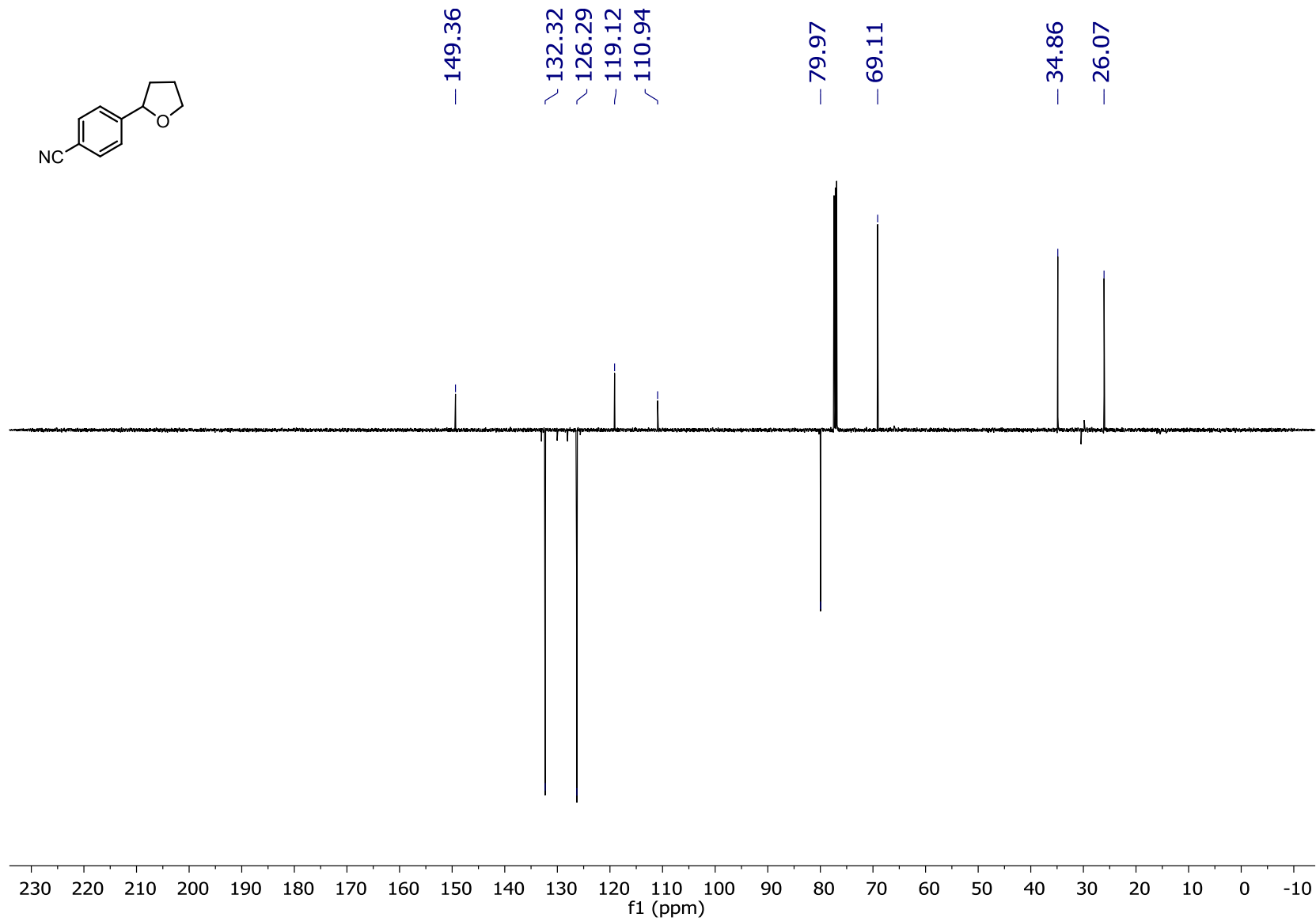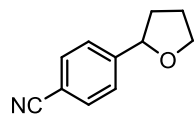
^{1}H NMR (501 MHz, CDCl$_3$): 1-(4-(tetrahydrofuran-2-yl)phenyl)ethan-1-one (16)

^{13}C NMR (126 MHz, CDCl$_3$): 1-(4-(tetrahydrofuran-2-yl)phenyl)ethan-1-one (16)

197.98

149.33

136.17
128.60
125.72

80.27

69.02

34.85
26.78
26.10

210 200 190 180 170 160 150 140 130 120 110 100 90 80 70 60 50 40 30 20 10 0
f1 (ppm)
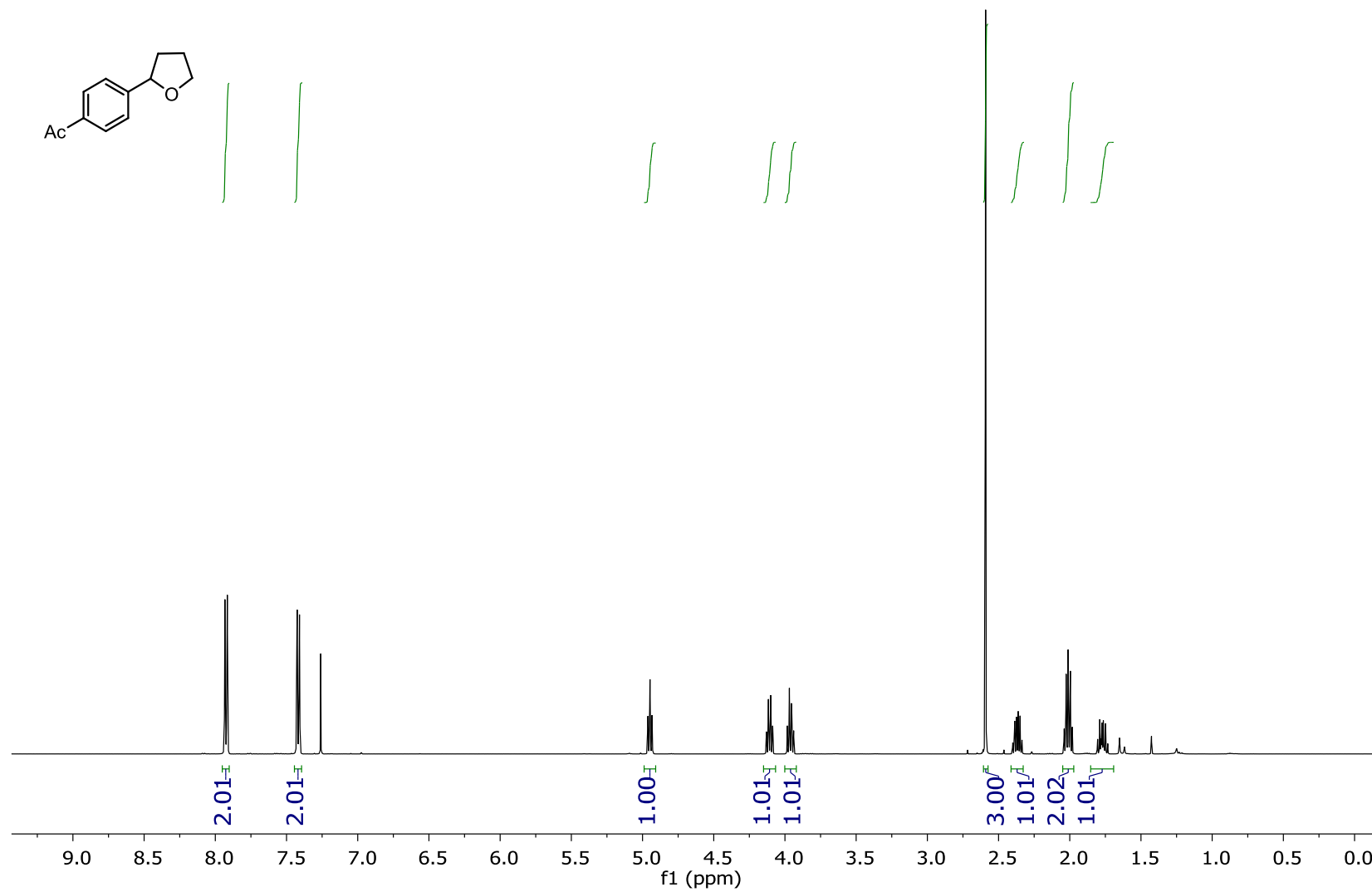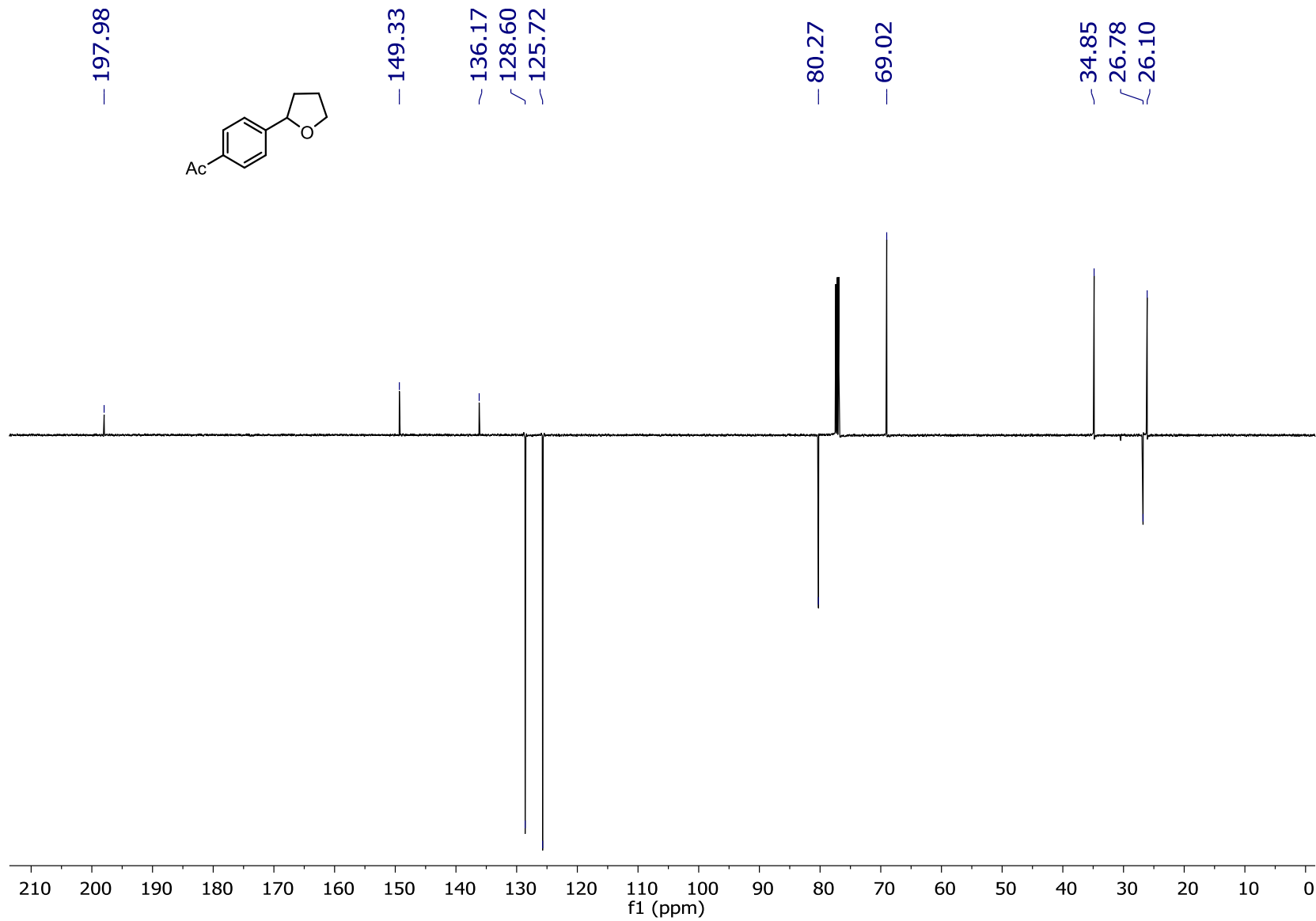
^{1}H NMR (501 MHz, CDCl$_3$): phenyl(4-(tetrahydrofuran-2-yl)phenyl)methanone (17)
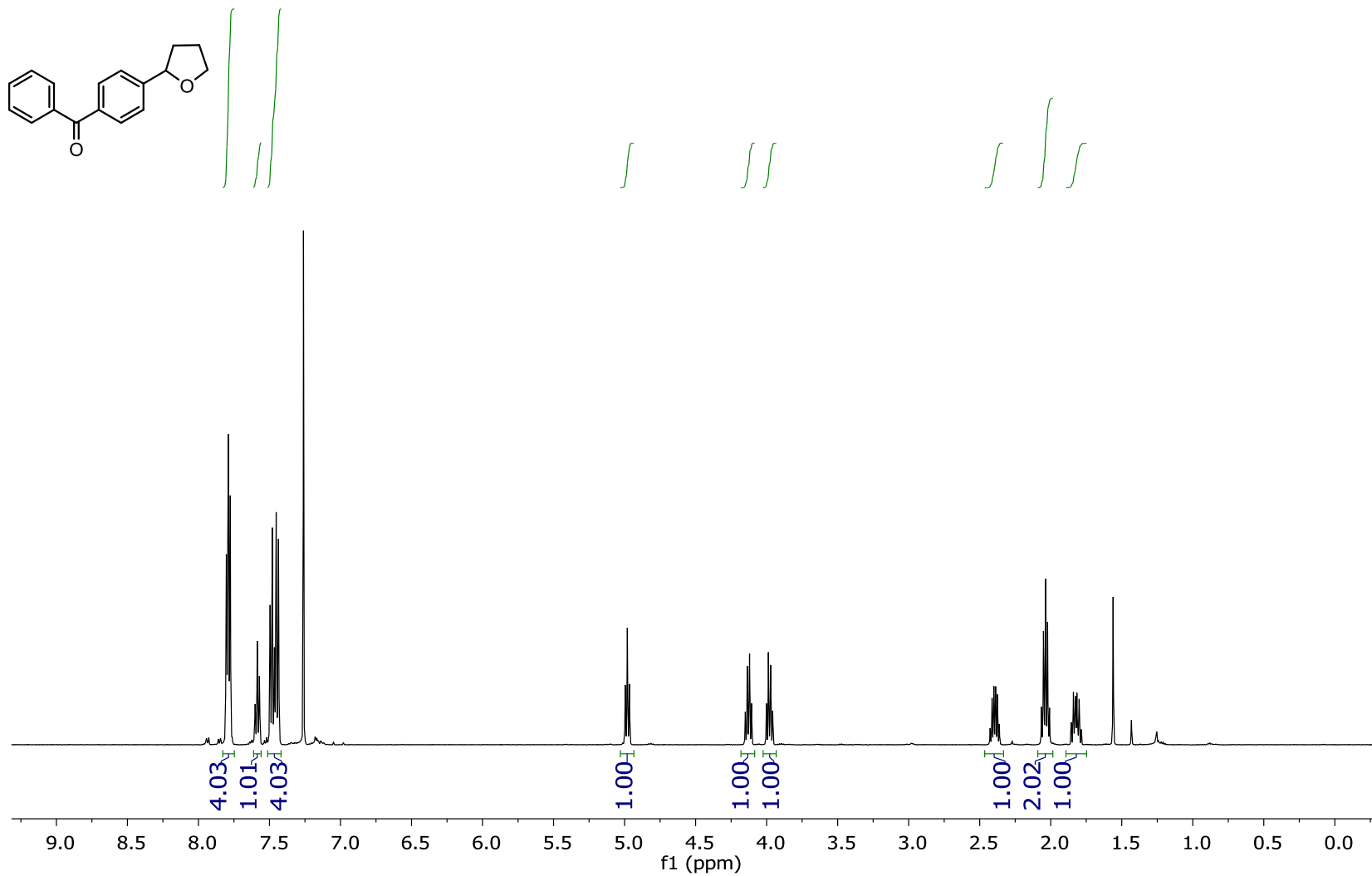
¹³C NMR (126 MHz, CDCl₃): phenyl(4-(tetrahydrofuran-2-yl)phenyl)methanone (17)

210 200 190 180 170 160 150 140 130 120 110 100 90 80 70 60 50 40 30 20 10 0
f1 (ppm)

¹H NMR (501 MHz, CDCl₃): 2-(naphthalene-1-yl)tetrahydrofuran (18)
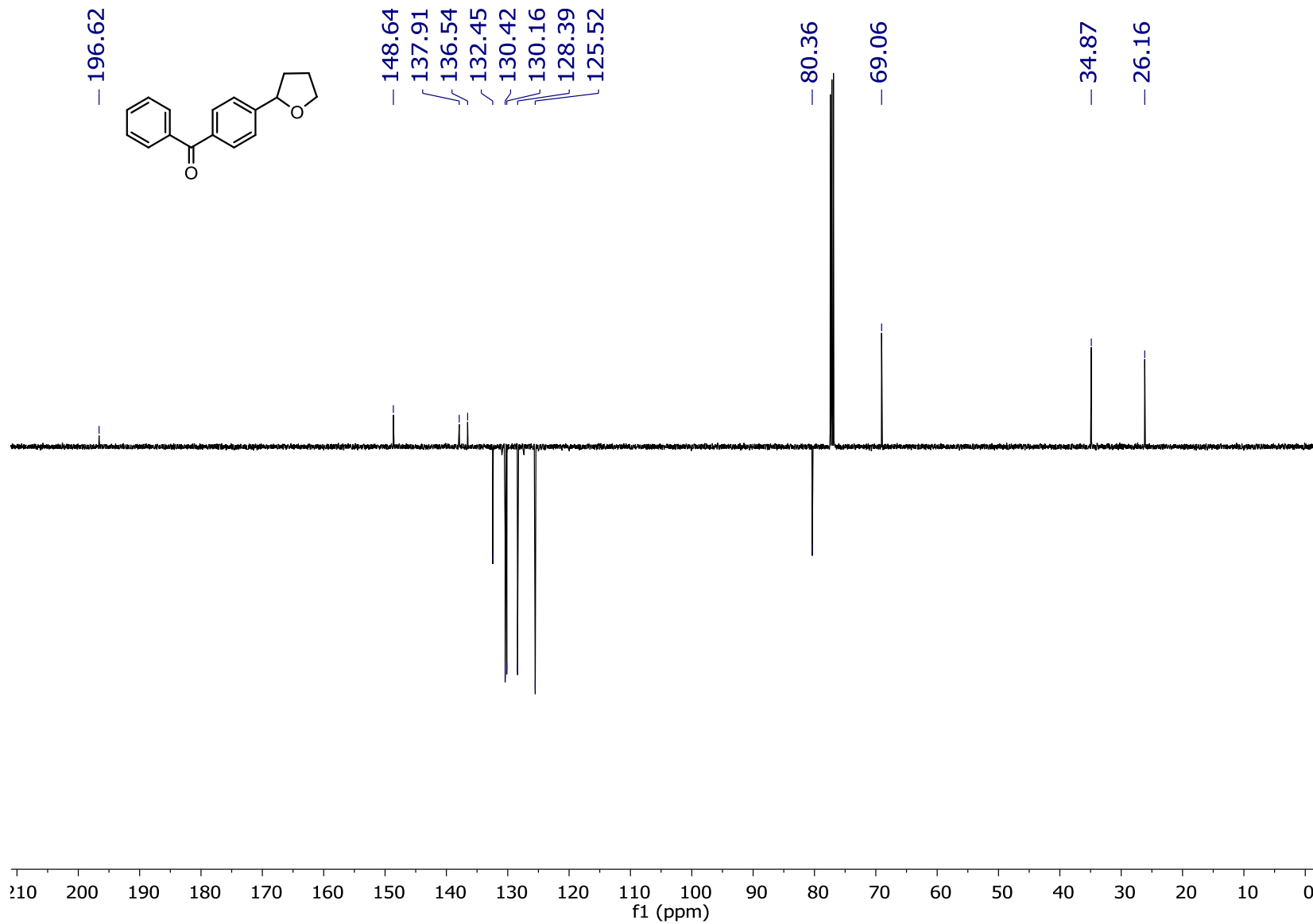
^{1}H NMR (501 MHz, CDCl₃): 2-(naphthalene-1-yl)tetrahydrofuran (18)
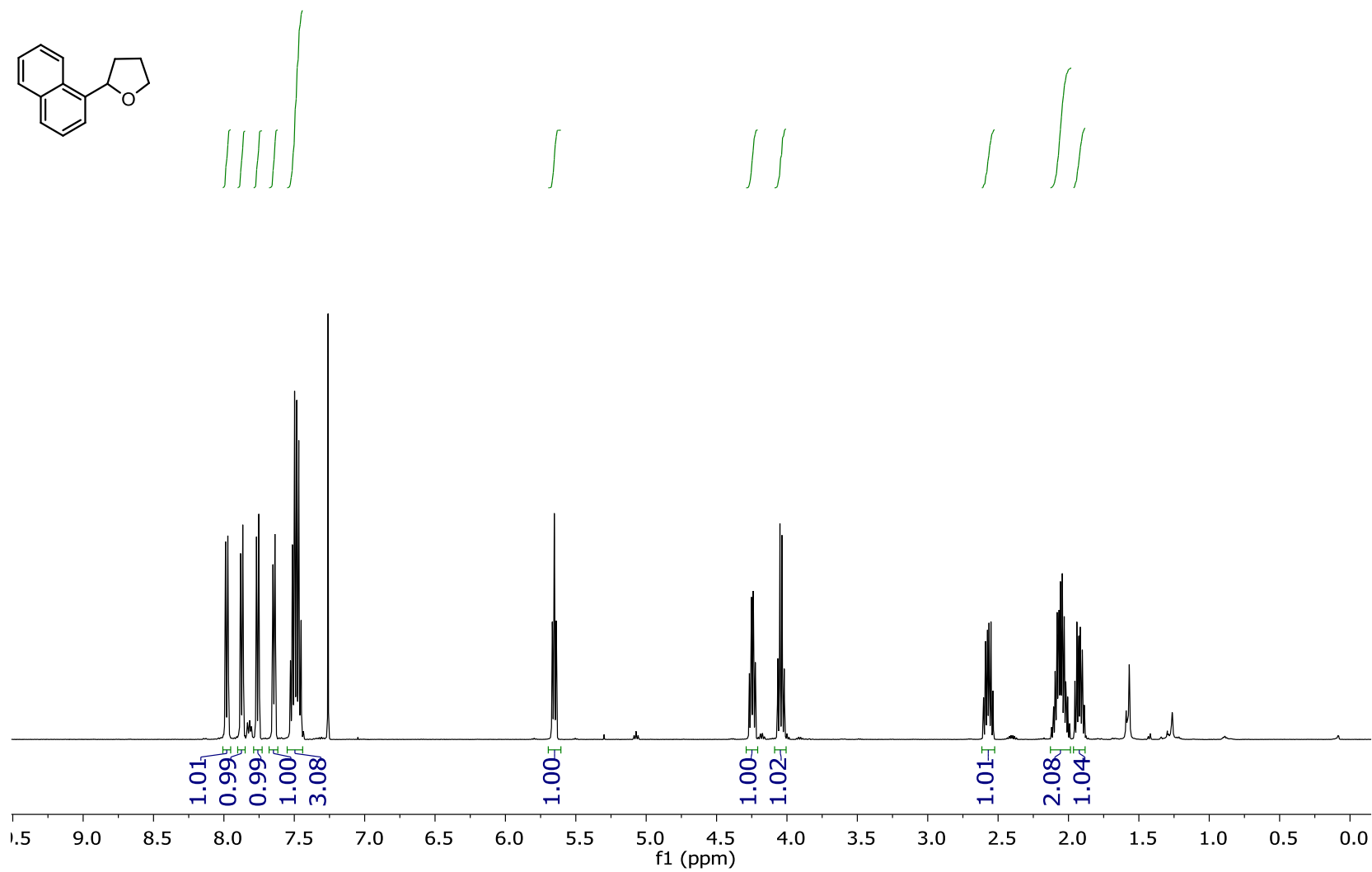
^{13}C NMR (126 MHz, CDCl$_3$): 2-(naphthalene-1-yl)tetrahydrofuran (18)

139.46
133.85
130.46
128.92
127.55
125.89
125.63
125.50
123.55
121.94

78.06

68.89

33.93

26.09

f1 (ppm)
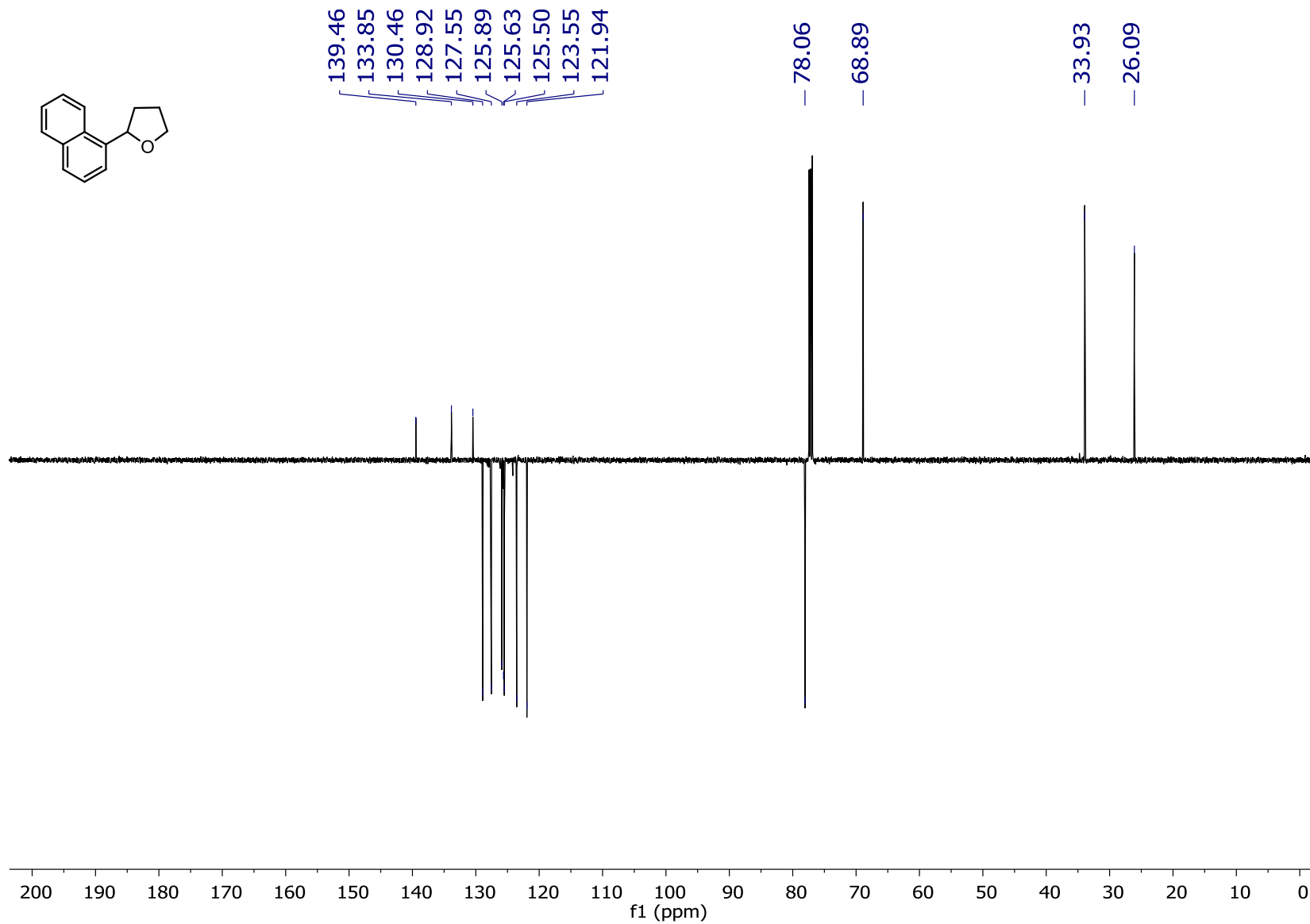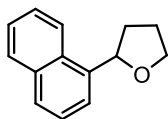
^{1}H NMR (501 MHz, CDCl$_3$): 5-(2-(tetrahydrofuran-2-yl)phenyl)furan-2-carbaldehyde (19).
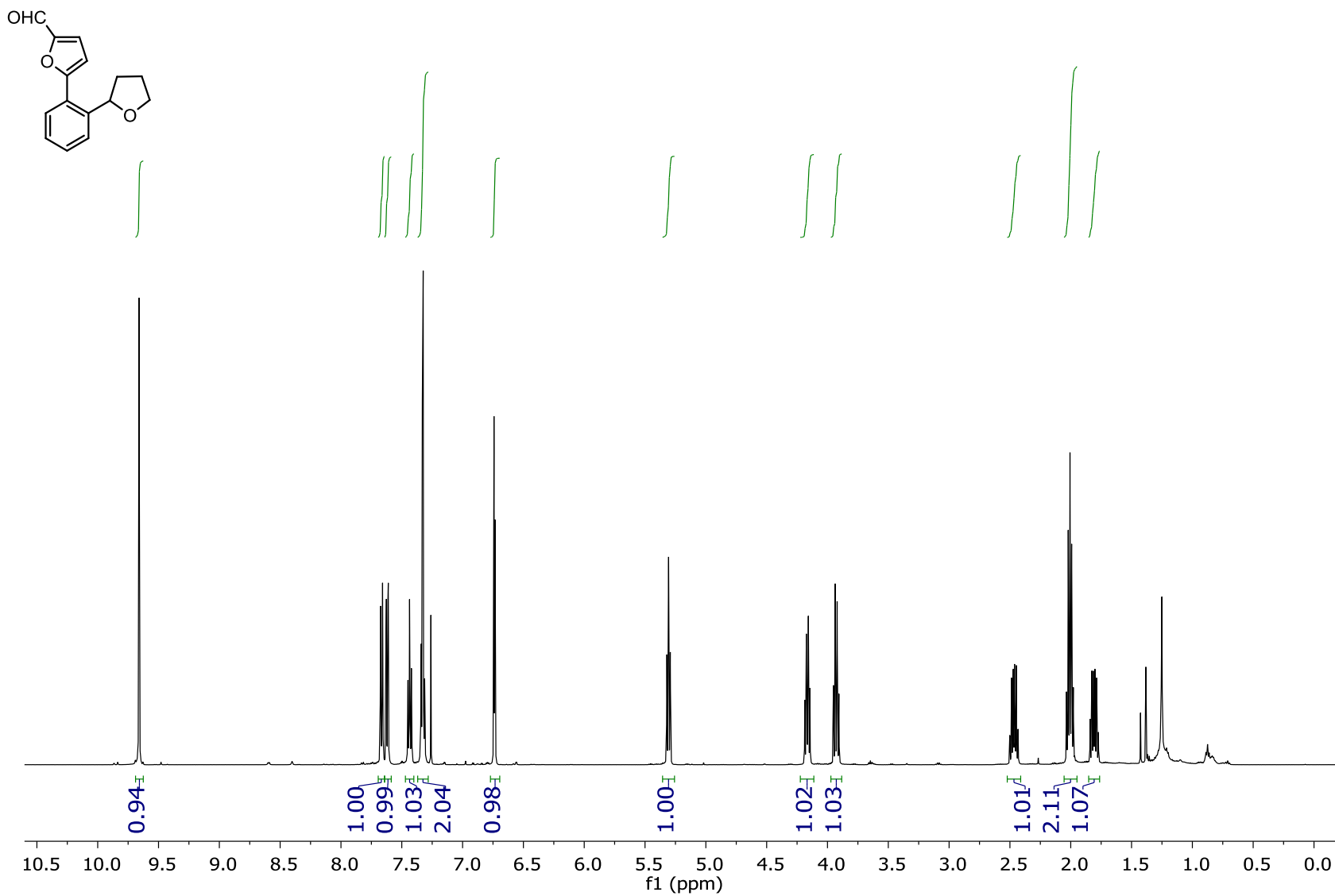
¹³C NMR (126 MHz, CDCl₃): 5-(2-(tetrahydrofuran-2-yl)phenyl)furan-2-carbaldehyde (19).
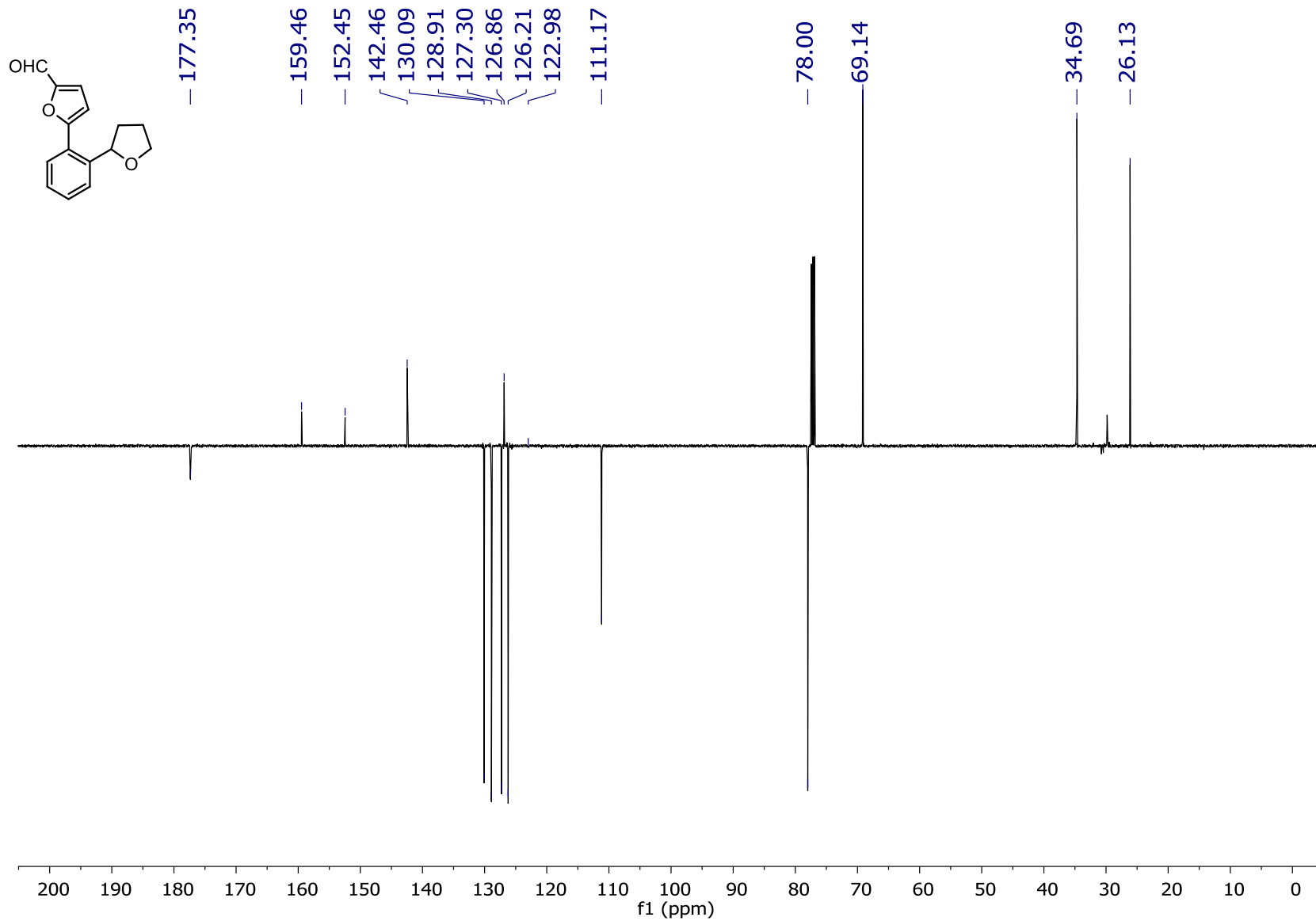
HSQC: 5-(2-(tetrahydrofuran-2-yl)phenyl)furan-2-carbaldehyde (19).
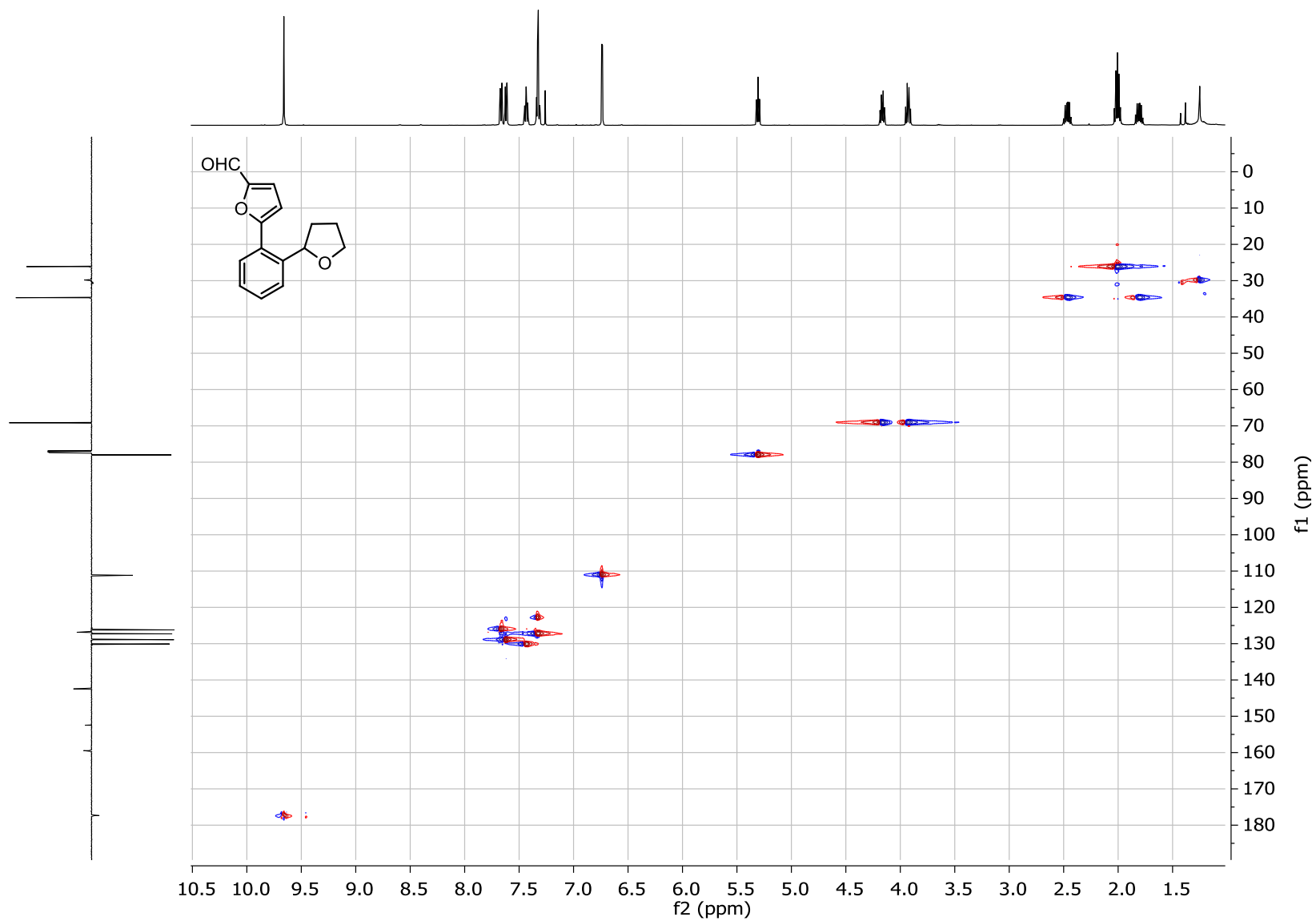
¹H NMR (501 MHz, CDCl₃): 2-methyl-6-(4-(tetrahydrofuran-2-yl)phenyl)pyridine (20)
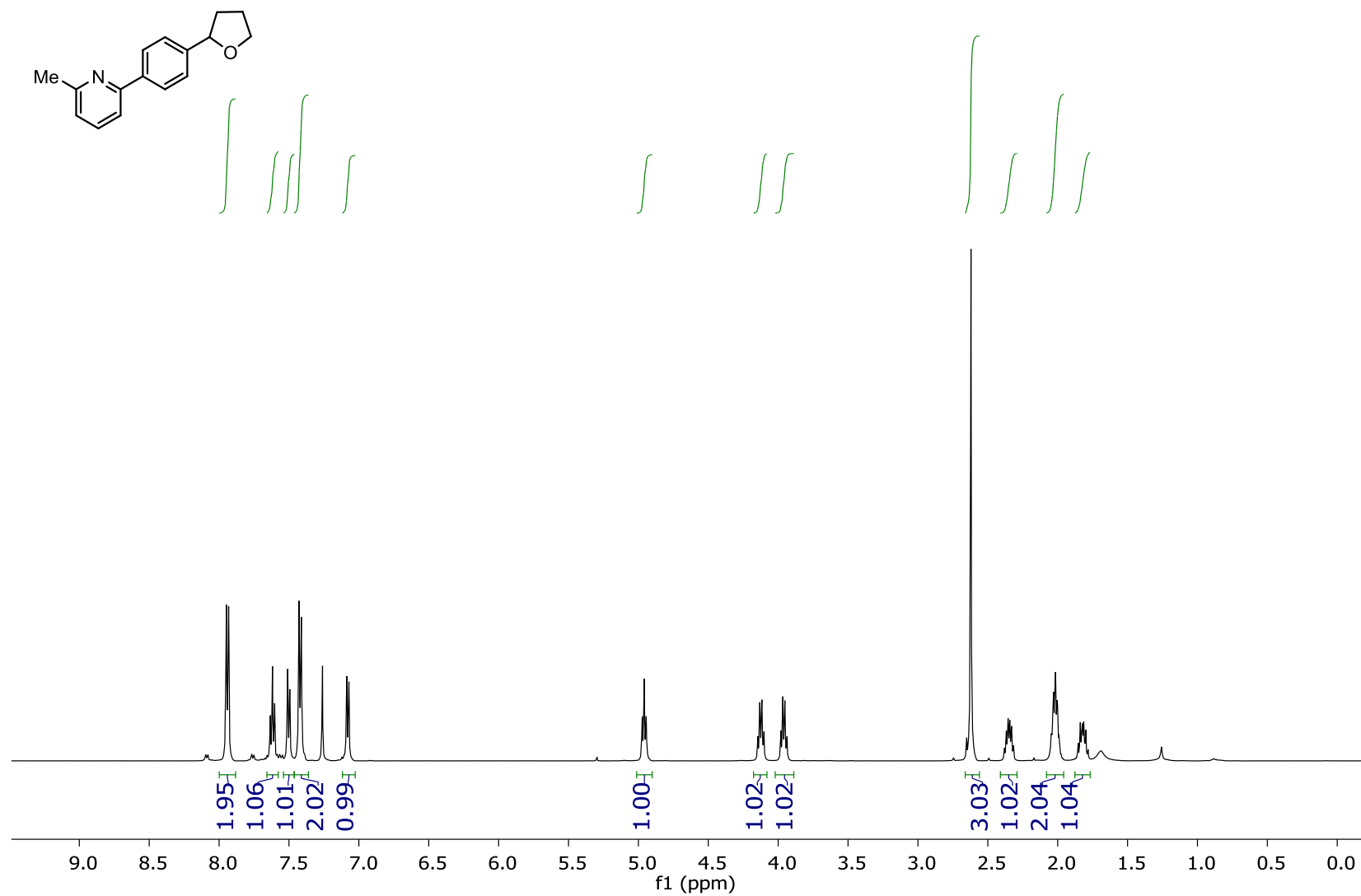
¹³C NMR (126 MHz, CDCl₃): 2-methyl-6-(4-(tetrahydrofuran-2-yl)phenyl)pyridine (20)
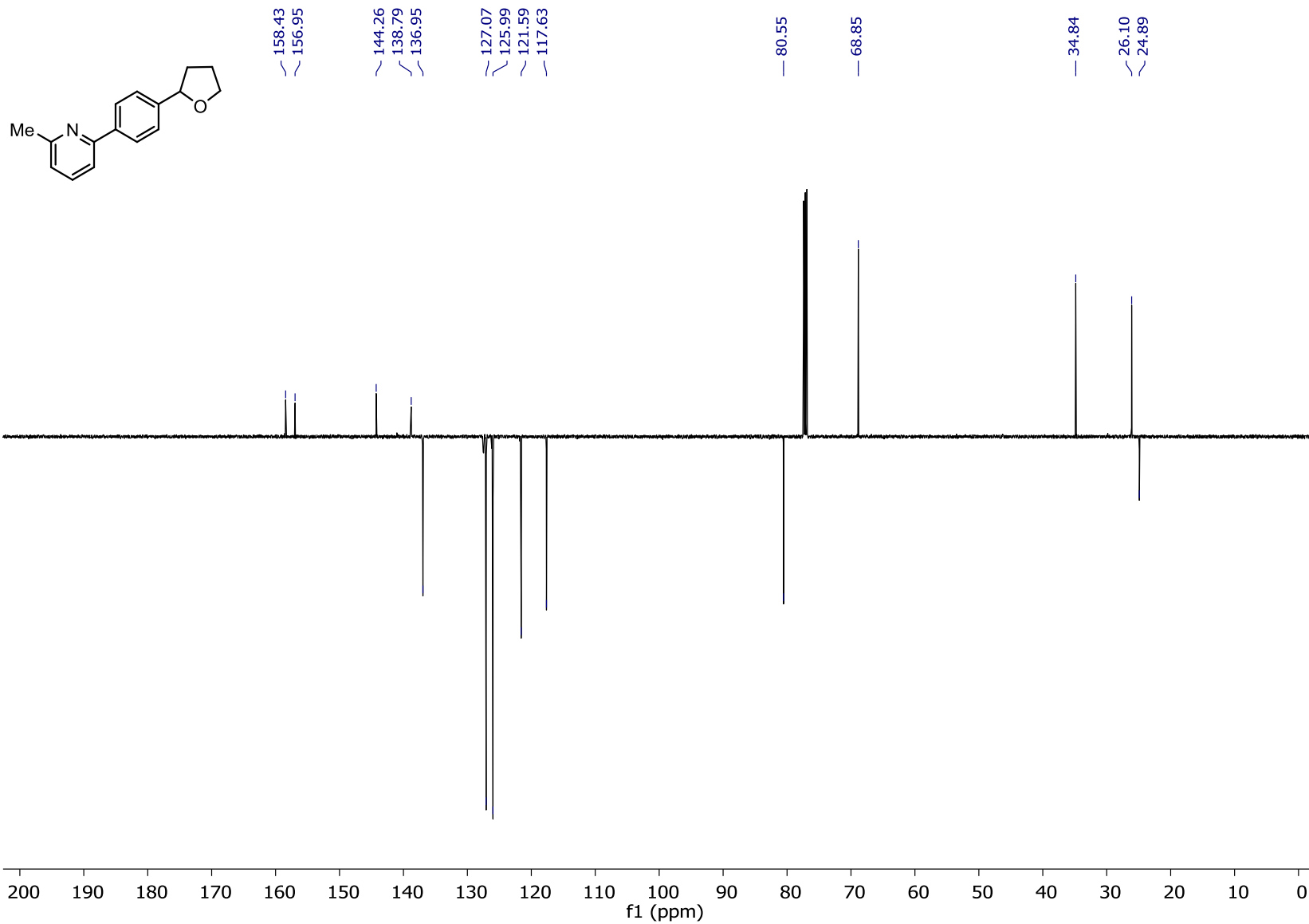
^{1}H NMR (501 MHz, CDCl$_3$): 4-(tetrahydrofuran-2-yl)-2-(trifluoromethyl)pyridine (21)
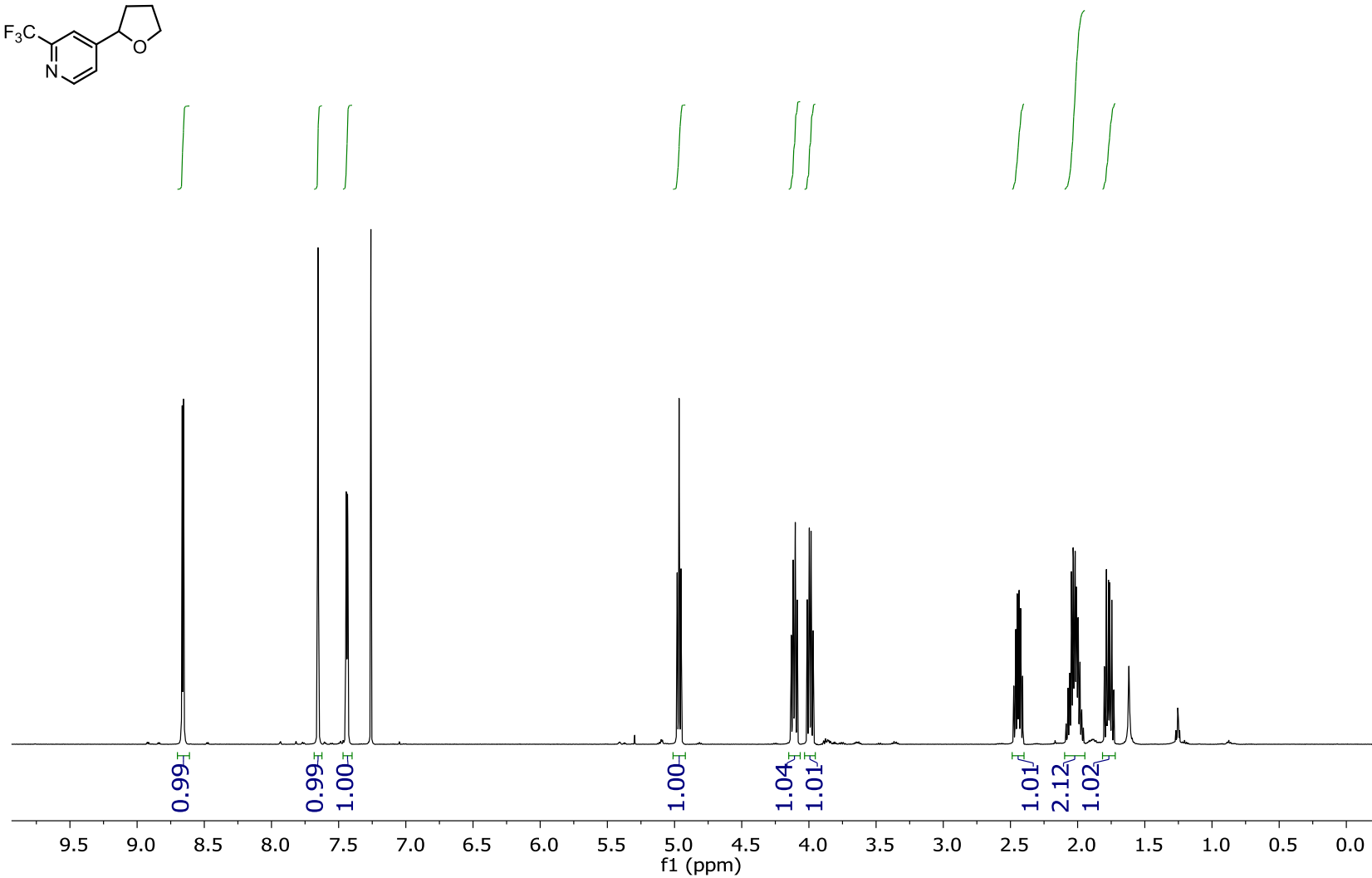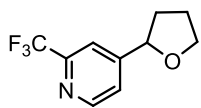
^{13}C NMR (126 MHz, CDCl$_3$): 4-(tetrahydrofuran-2-yl)-2-(trifluoromethyl)pyridine (21)

155.16
150.07
148.89
148.62
148.34
148.07
125.01
123.23
122.83
120.65
118.47
117.45
117.43
117.40
117.38
78.87
69.26
34.53
25.98

200 190 180 170 160 150 140 130 120 110 100 90 80 70 60 50 40 30 20 10 0
f1 (ppm)
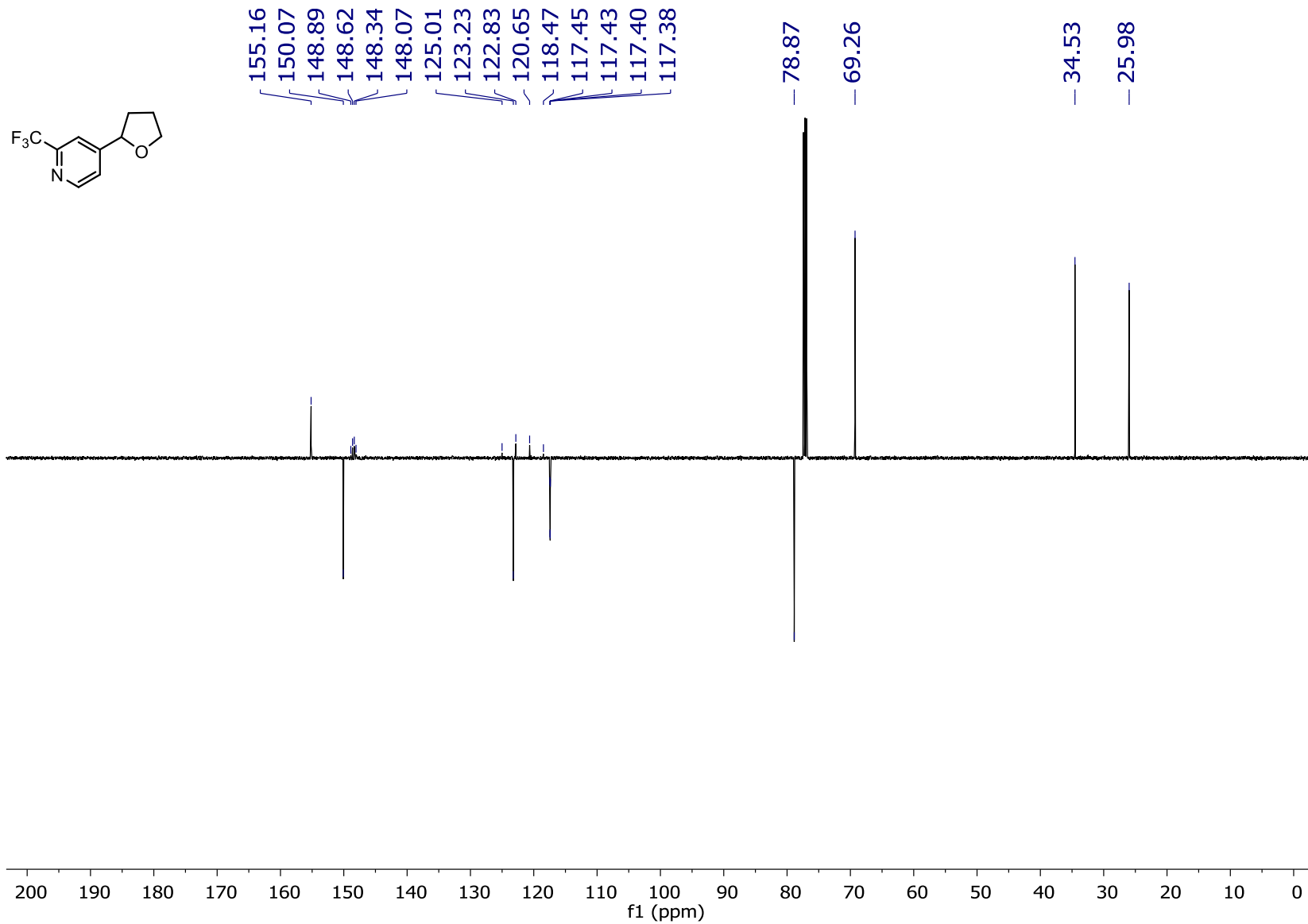
19F NMR (282 MHz, CDCl₃): 4-(tetrahydrofuran-2-yl)-2-(trifluoromethyl)pyridine (21)

-67.98

f1 (ppm)
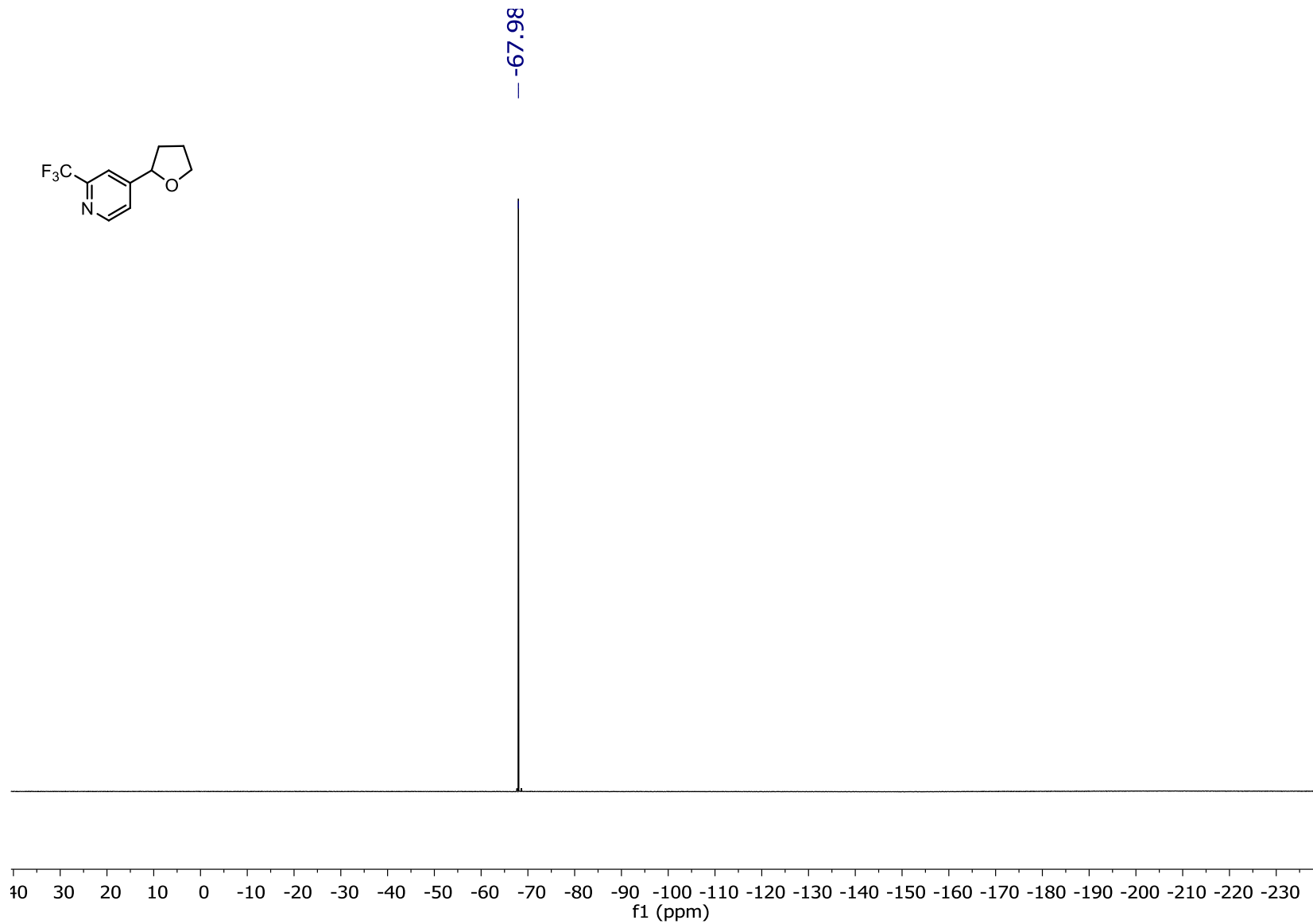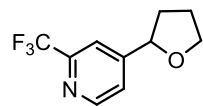
¹H NMR (501 MHz, CDCl₃): *tert*-butyl 5-(tetrahydrofuran-2-yl)-1H-indole-1-carboxylate (22)
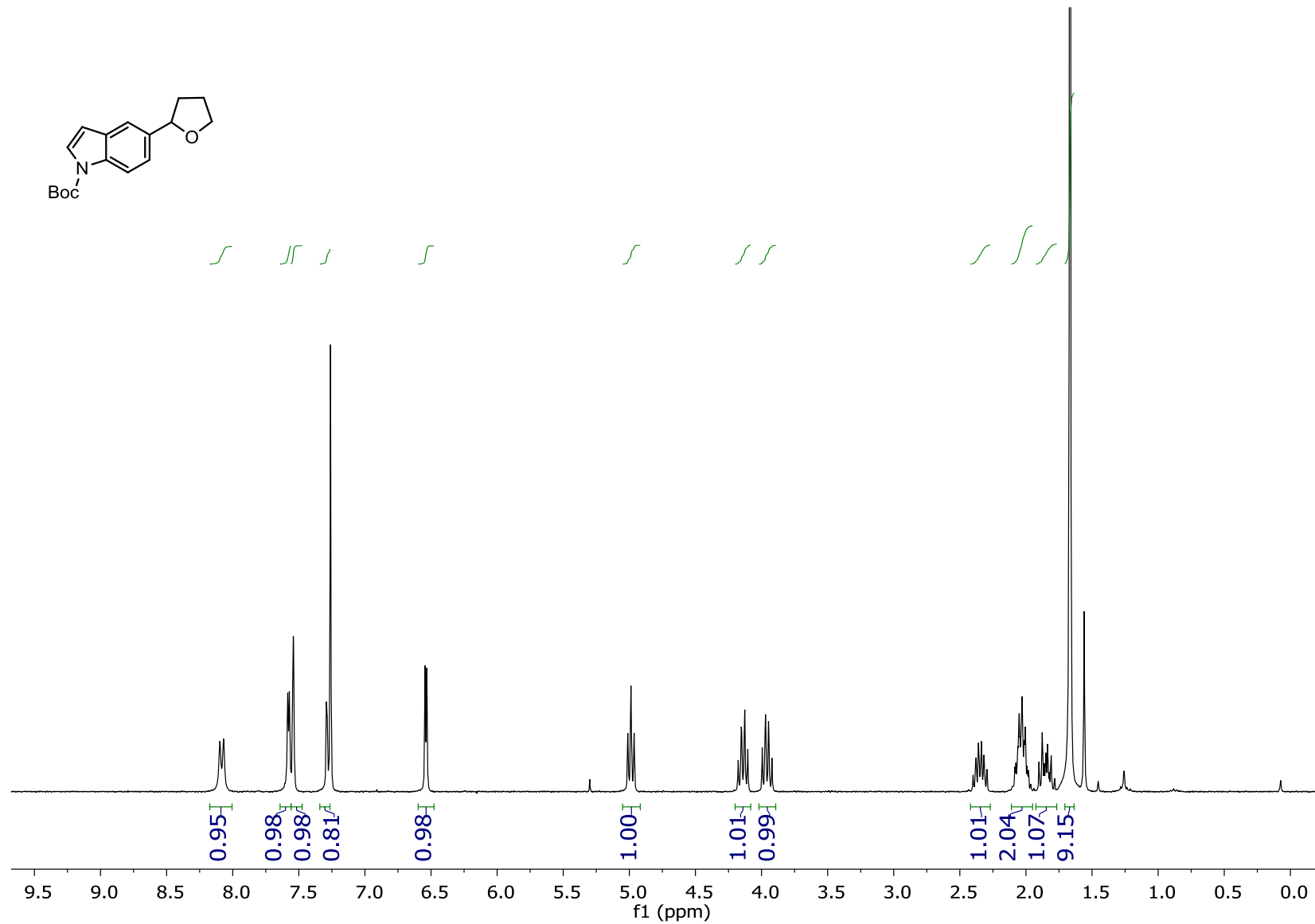
¹³C NMR (126 MHz, CDCl₃): *tert*-butyl 5-(tetrahydrofuran-2-yl)-1H-indole-1-carboxylate (22)

S99
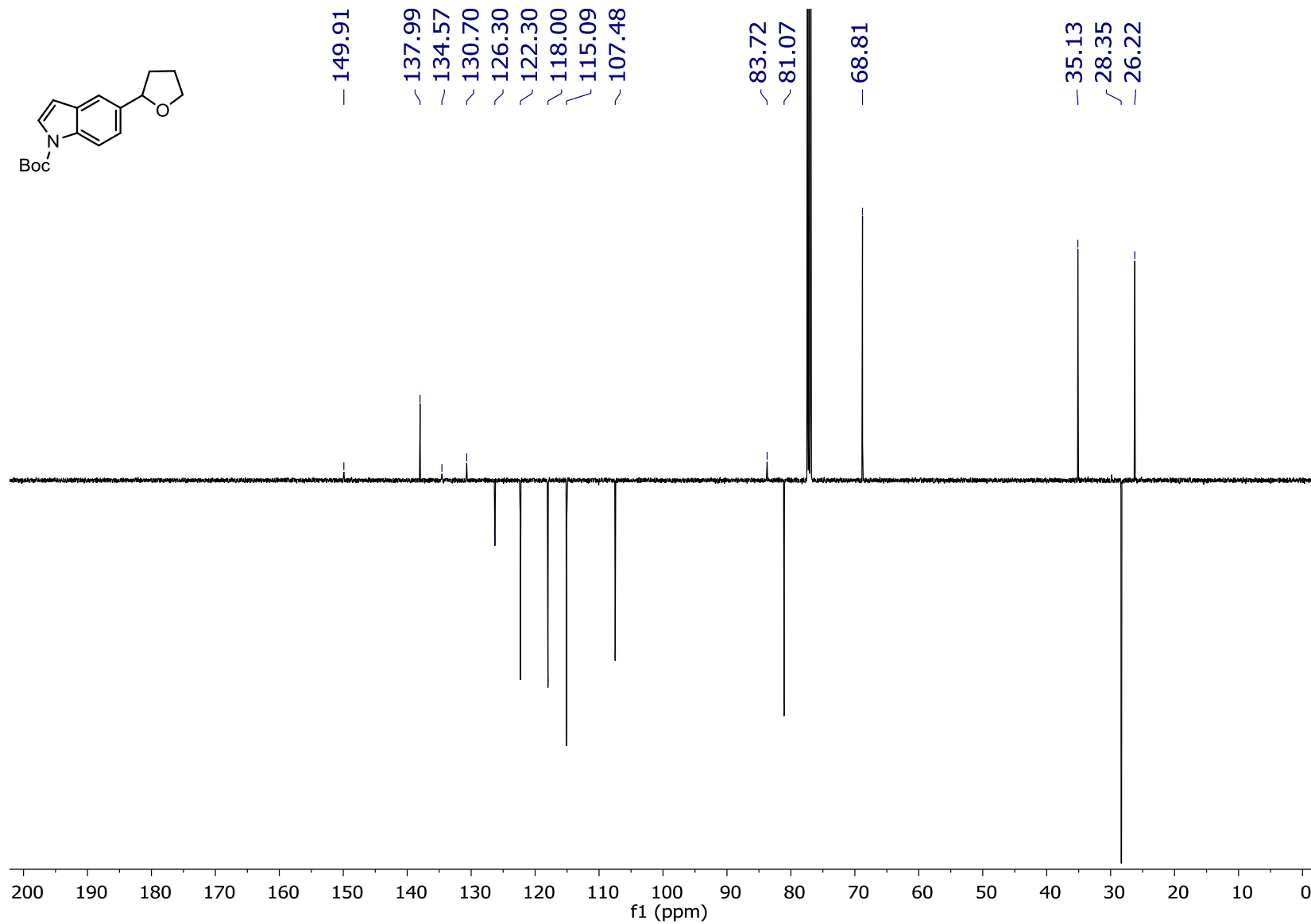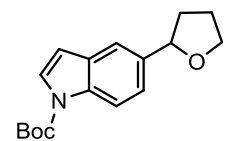
^{1}H NMR (501 MHz, CDCl$_3$): 6-(tetrahydrofuran-2-yl)quinoline (23)

0.94 0.98 0.95 0.97 0.96 0.96 1.00 0.99 1.02 0.97 2.08 1.05

f1 (ppm)
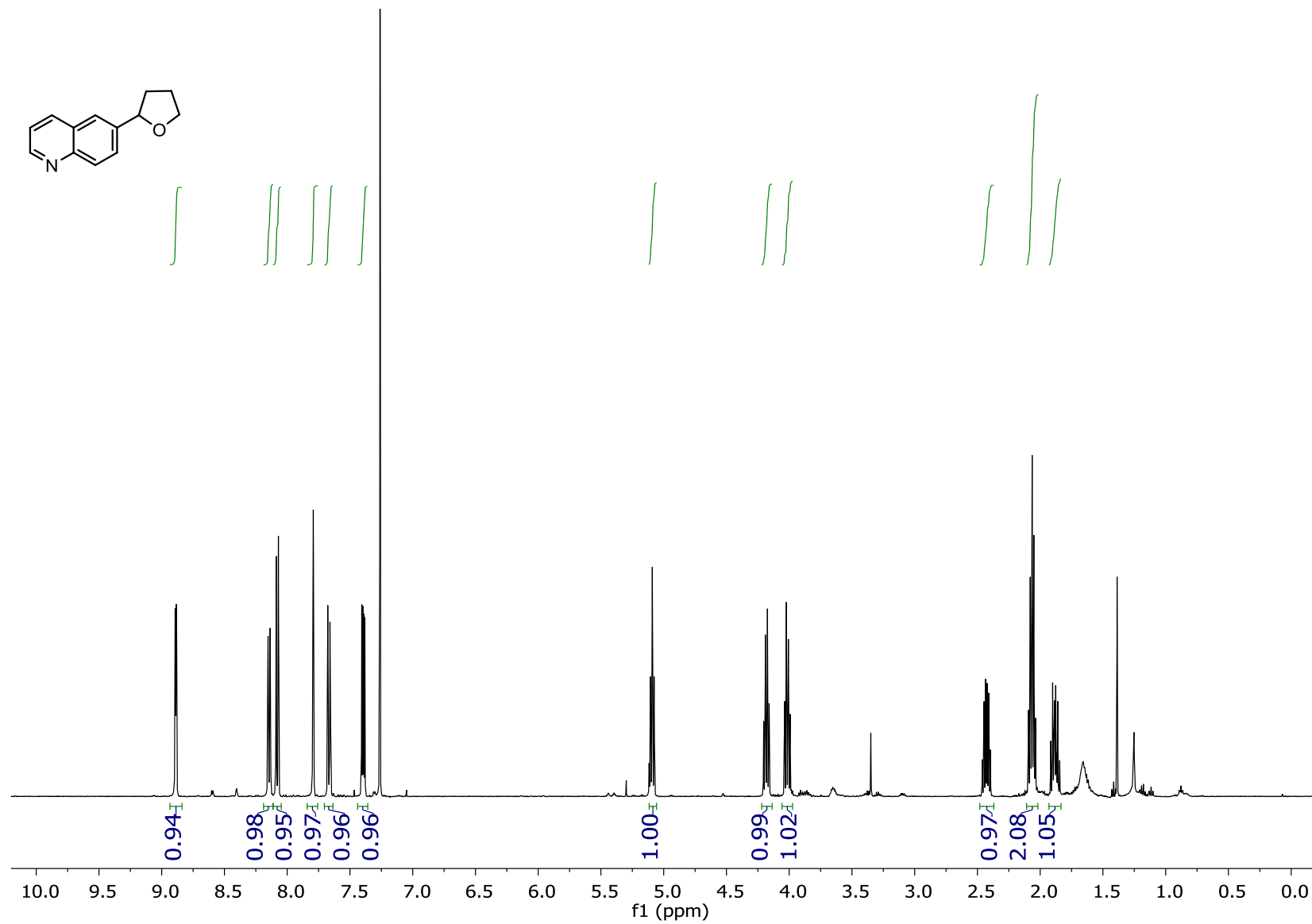
¹³C NMR (126 MHz, CDCl₃): 6-(tetrahydrofuran-2-yl)quinoline (23)
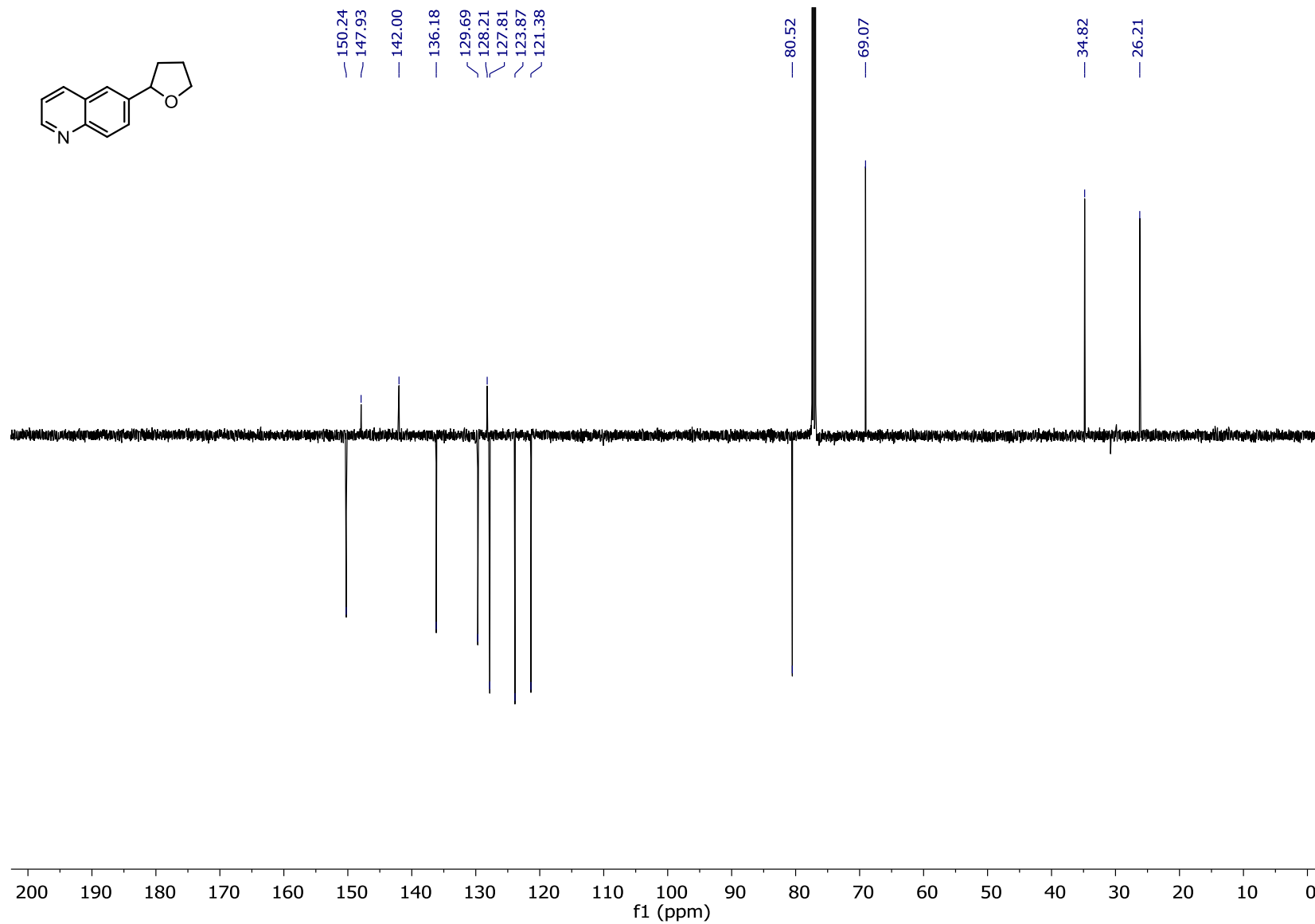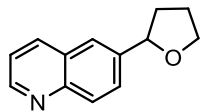
150.24
147.93
142.00
136.18
129.69
128.21
127.81
123.87
121.38
80.52
69.07
34.82
26.21
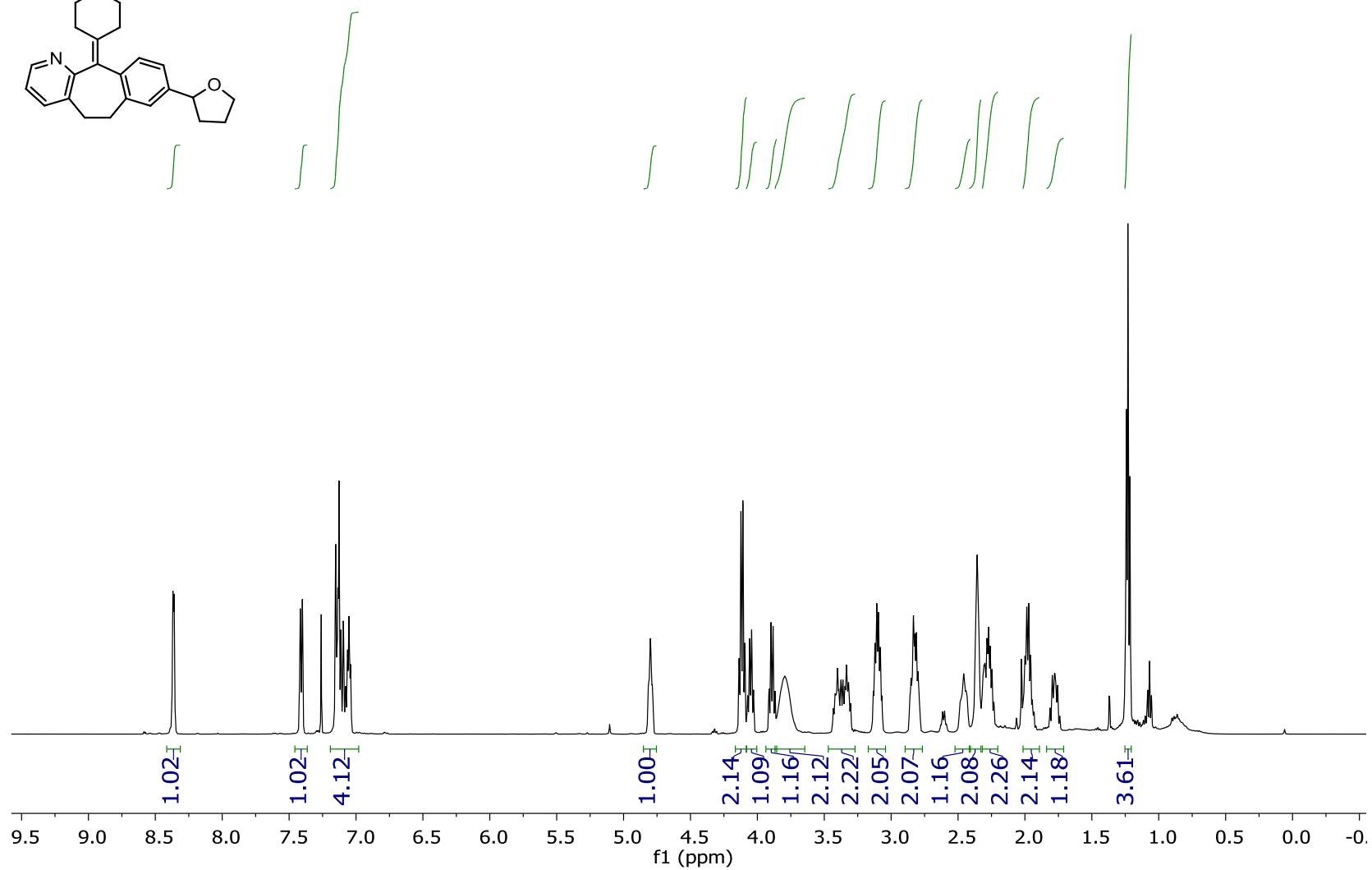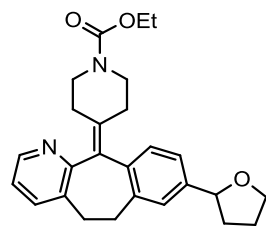
200 190 180 170 160 150 140 130 120 110 100 90 80 70 60 50 40 30 20 10 0
f1 (ppm)

S101

^{1}H NMR (501 MHz, CDCl$_3$): 24

¹³C NMR (126 MHz, CDCl₃): 24

^{13}C NMR (126 MHz, CDCl$_3$): 24

157.72
155.58
146.56
142.48
142.45
137.56
137.44
137.42
136.70
135.24
133.78
129.41
129.28
126.62
126.33
123.75
123.41
122.14

80.58
80.55

68.70

61.35

44.97
44.92
34.38
34.37
32.04
31.82
31.77
30.80
30.61
26.18
14.77

f1 (ppm)

200 190 180 170 160 150 140 130 120 110 100 90 80 70 60 50 40 30 20 10 0

HSQC: 24

S104

HMBC:24

S105
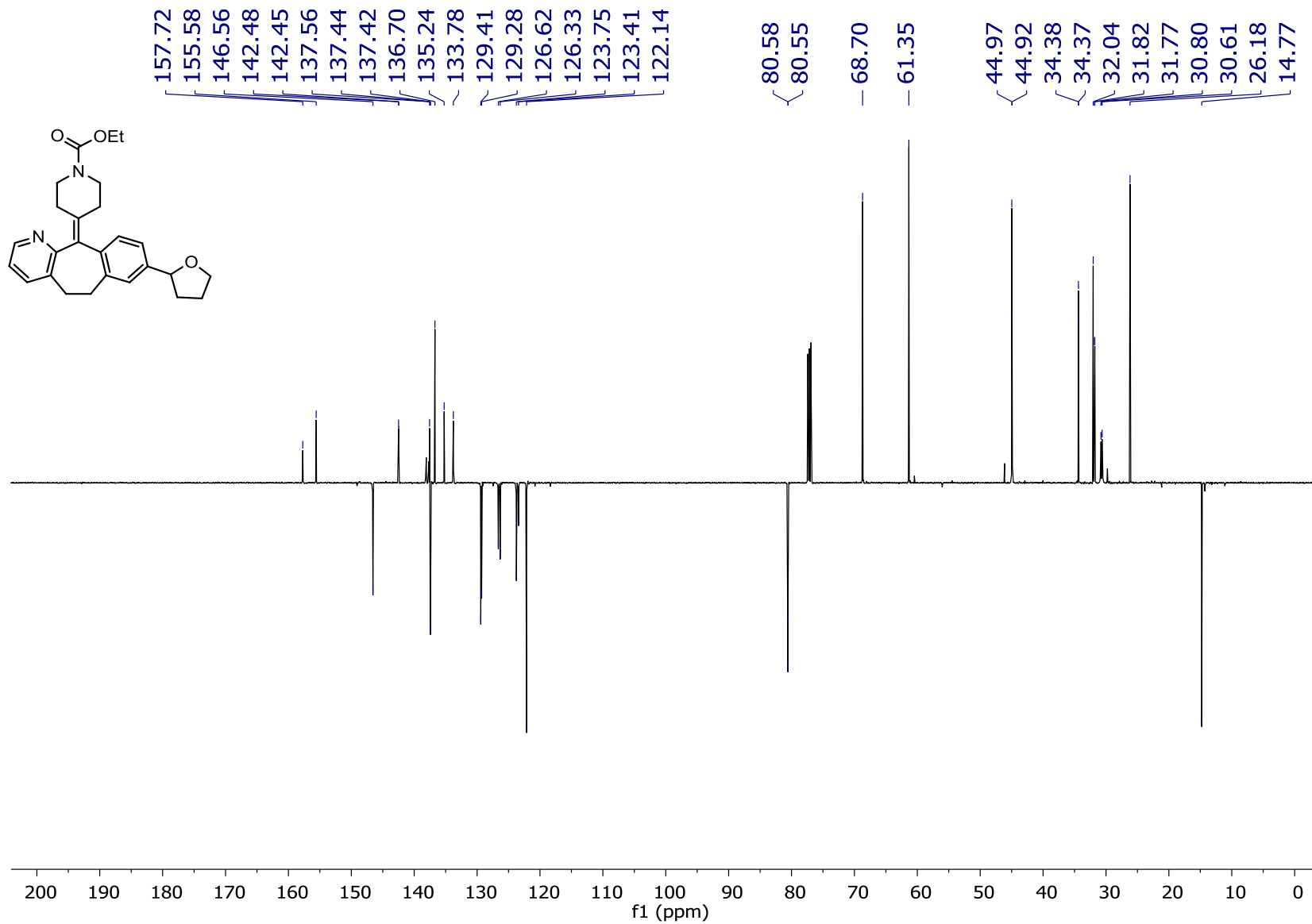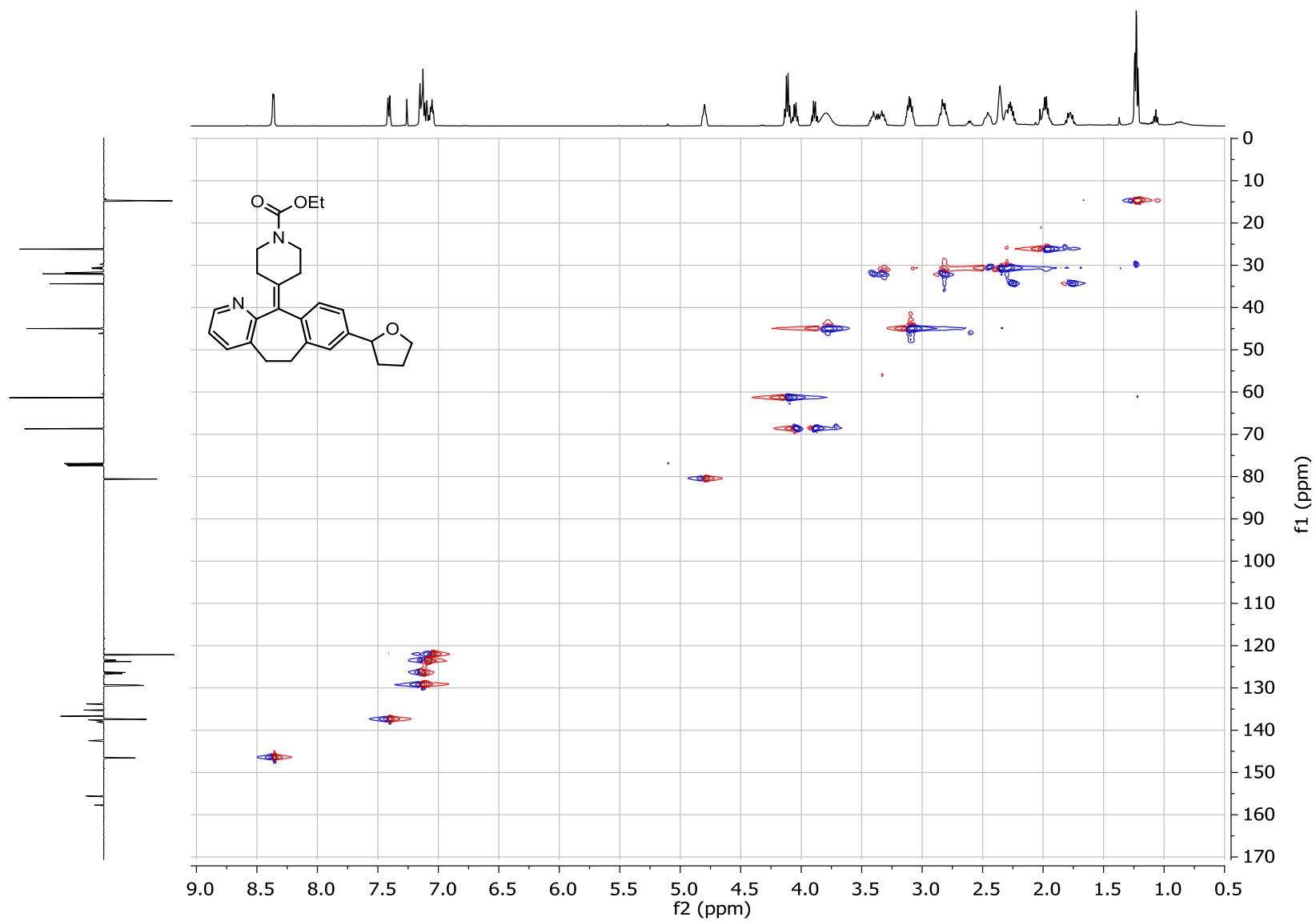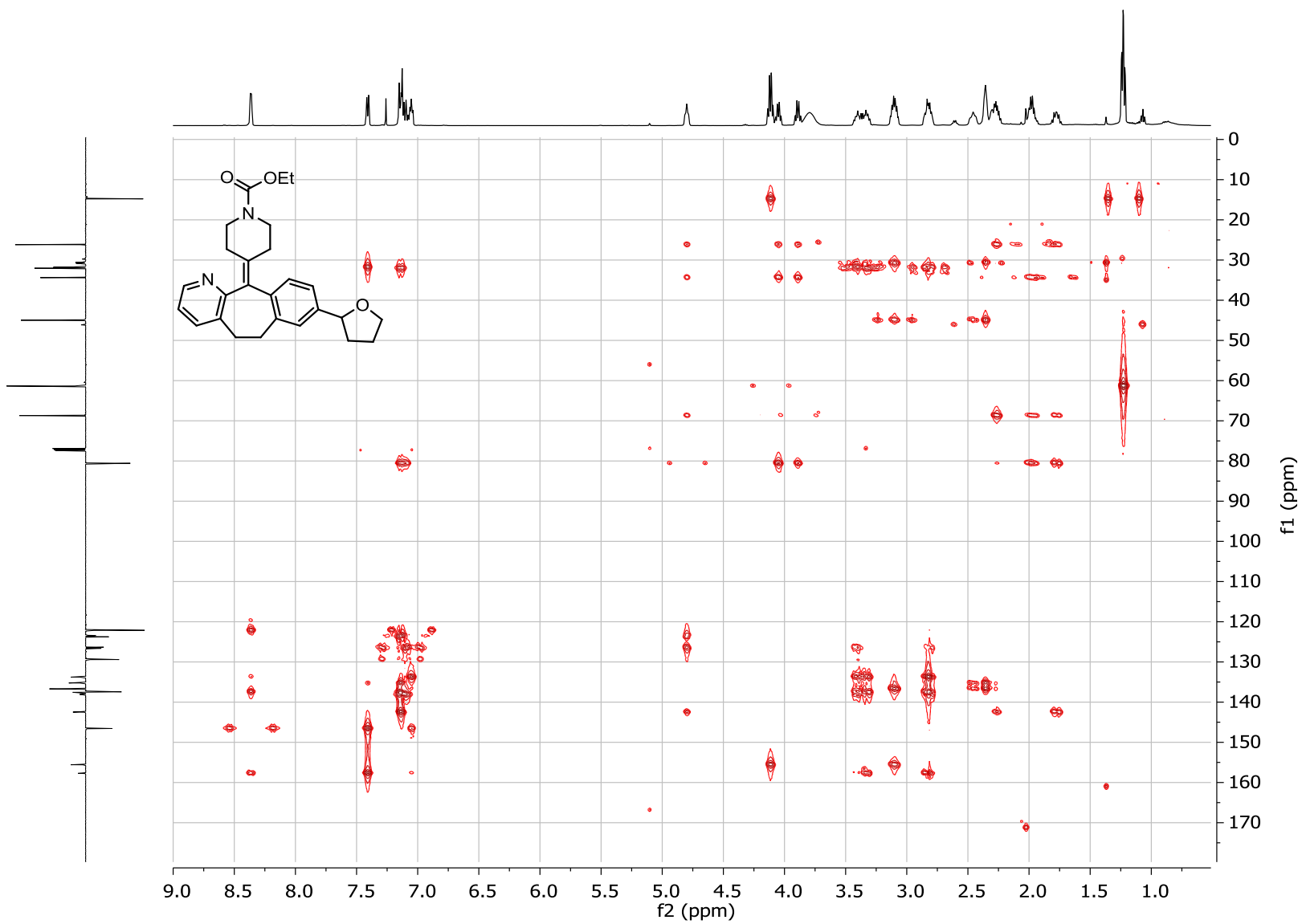
¹H NMR (501 MHz, CDCl₃): 1-(4-(tetrahydro-2H-pyran-2-yl)phenyl)ethan-1-one (25)

^{13}C NMR (126 MHz, CDCl$_3$): 1-(4-(tetrahydro-2H-pyran-2-yl)phenyl)ethan-1-one (25)

198.05
148.90
136.24
128.59
125.95
79.64
69.08
34.29
26.80
25.90
24.05

f1 (ppm)
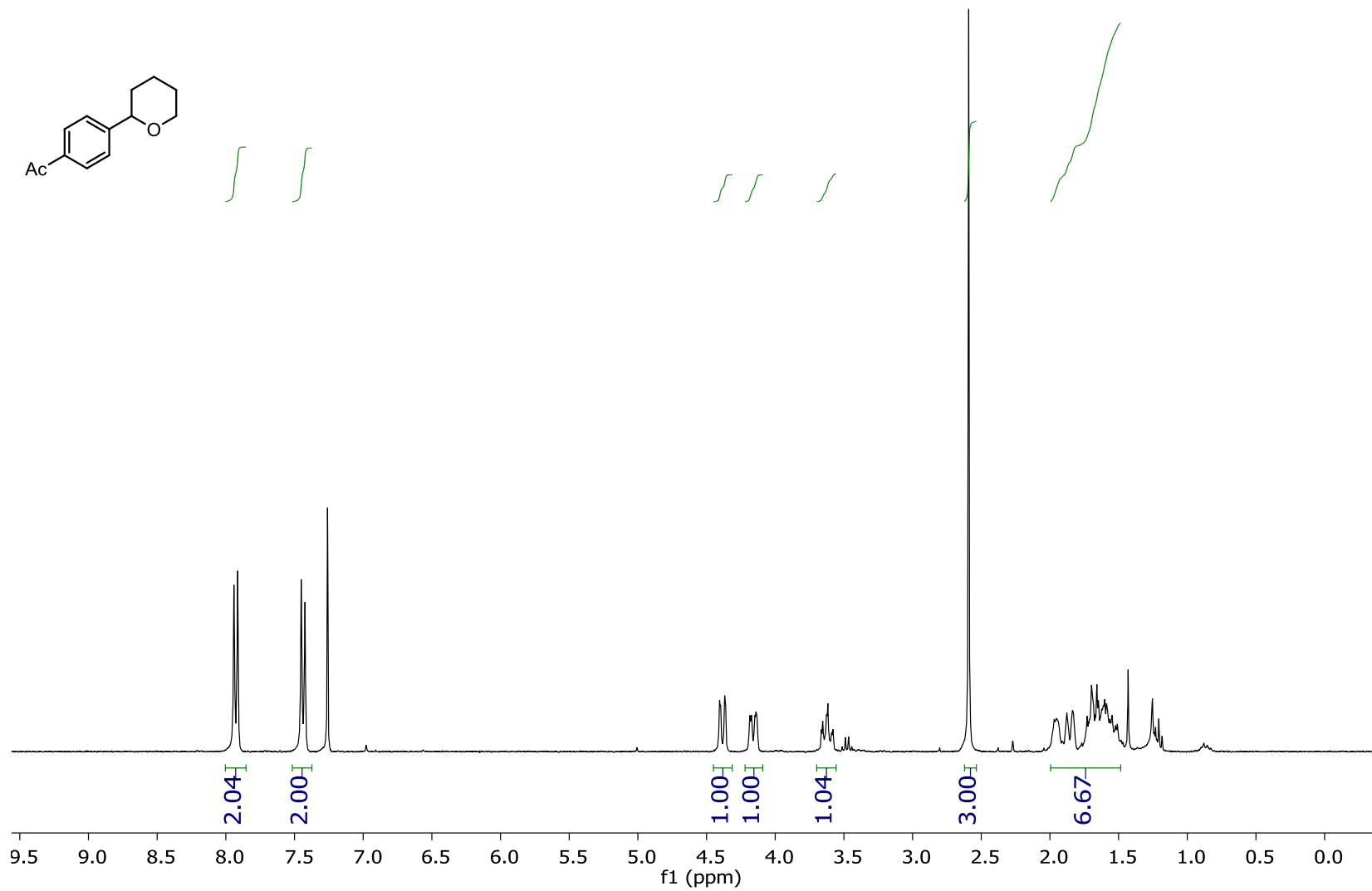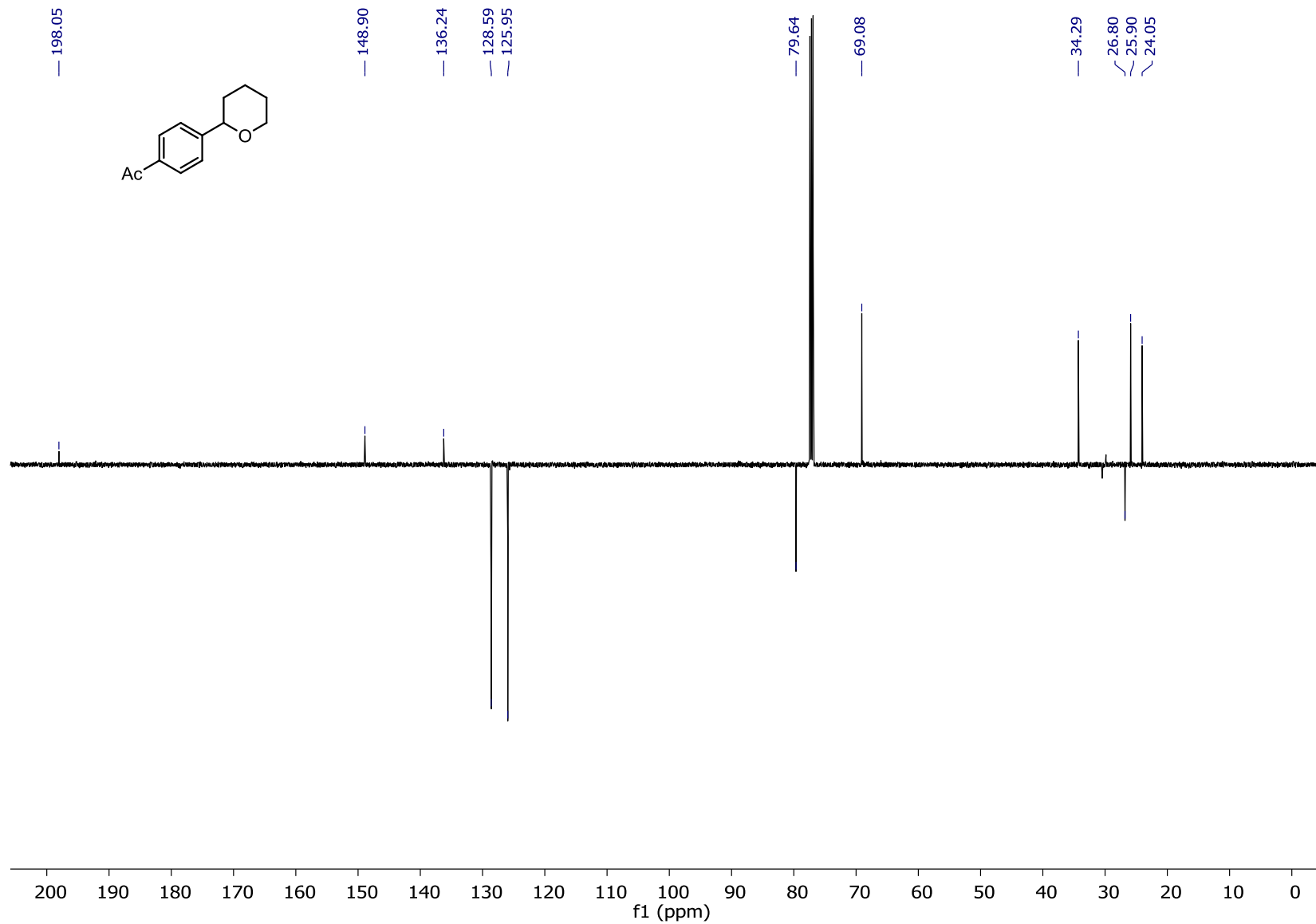
^{1}H NMR (501 MHz, CDCl$_3$): 1-(4-(1,4-dioxan-2-yl)phenyl)ethan-1-one (26)
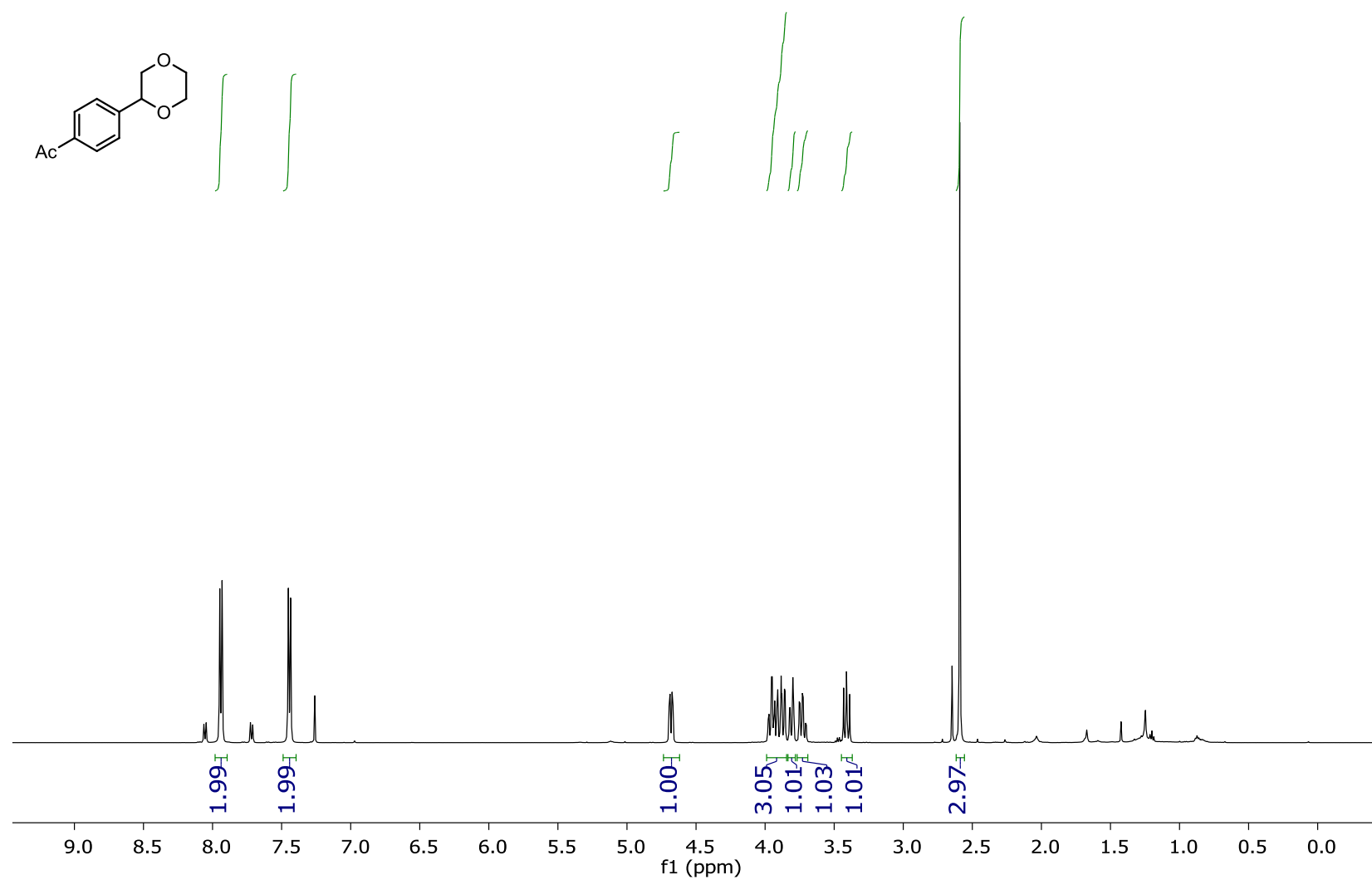
¹³C NMR (126 MHz, CDCl₃): 1-(4-(1,4-dioxan-2-yl)phenyl)ethan-1-one (26)
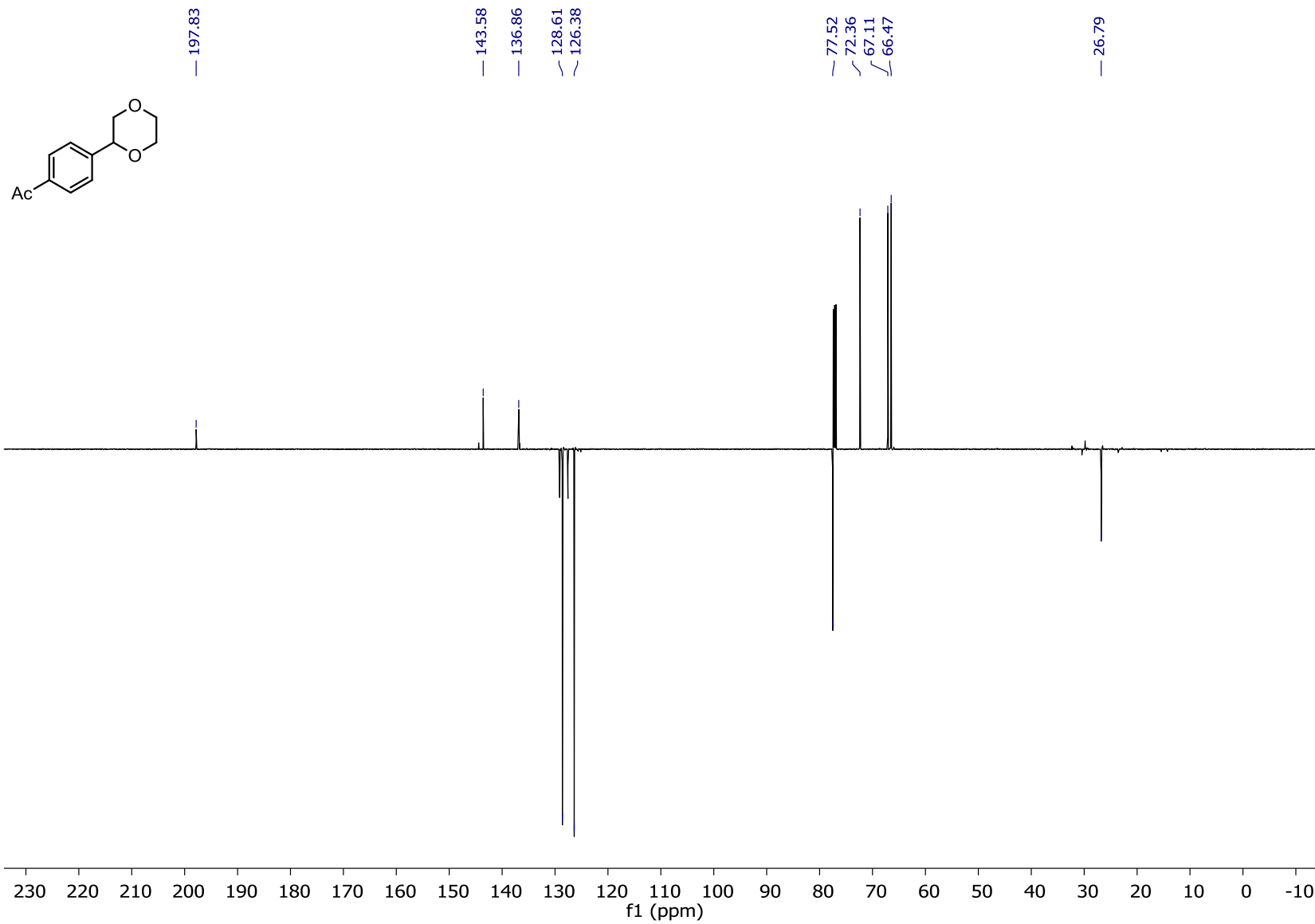
^{1}H NMR (501 MHz, CDCl$_3$): 1-(4-(1,2-dimethoxyethyl)phenyl)ethan-1-one (27a)

^{13}C NMR (126 MHz, CDCl$_3$): 1-(4-(1,2-dimethoxyethyl)phenyl)ethan-1-one (27a)

197.90
144.58
137.04
128.72
127.30
82.72
76.91
59.50
57.43
26.84

f1 (ppm)
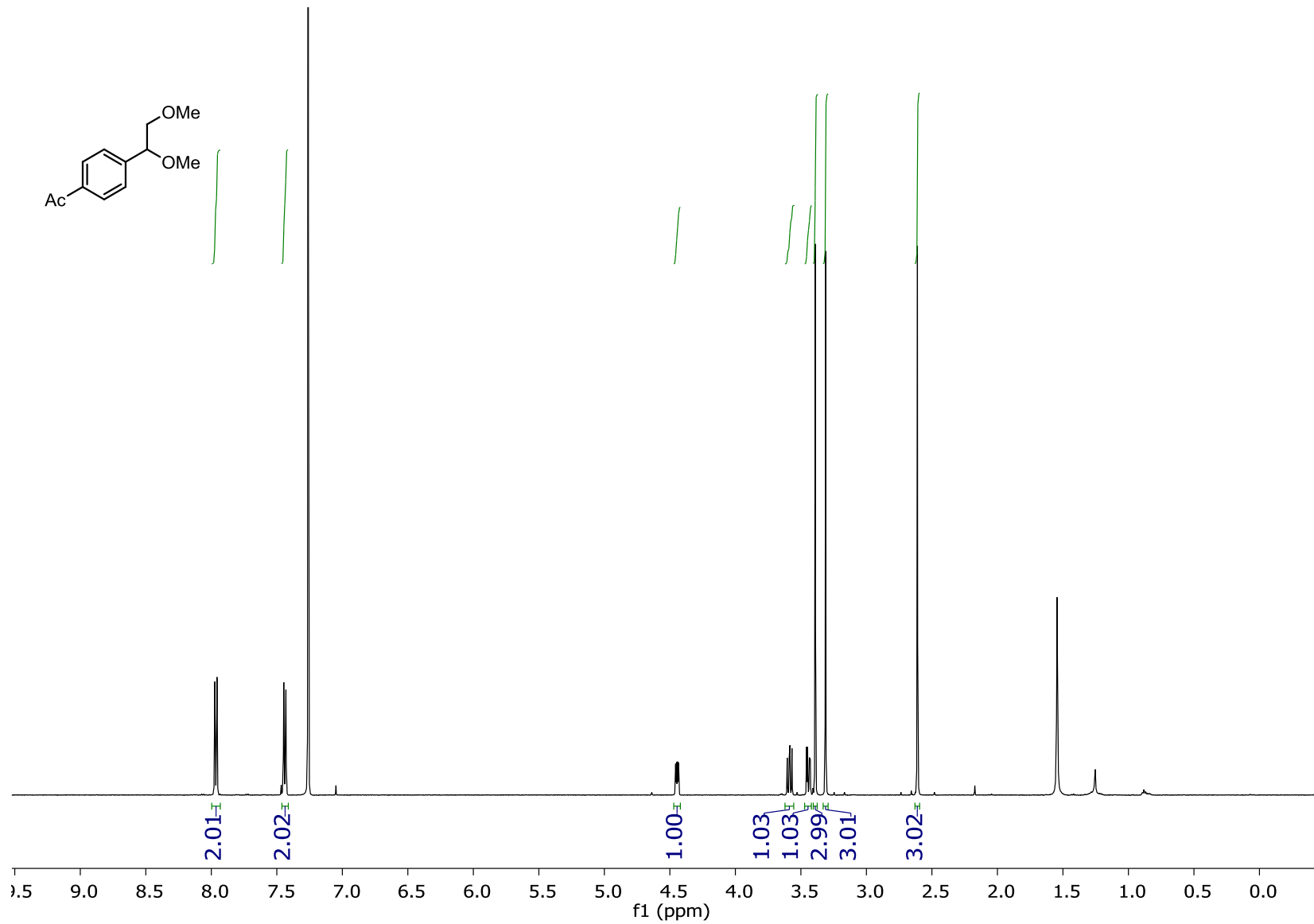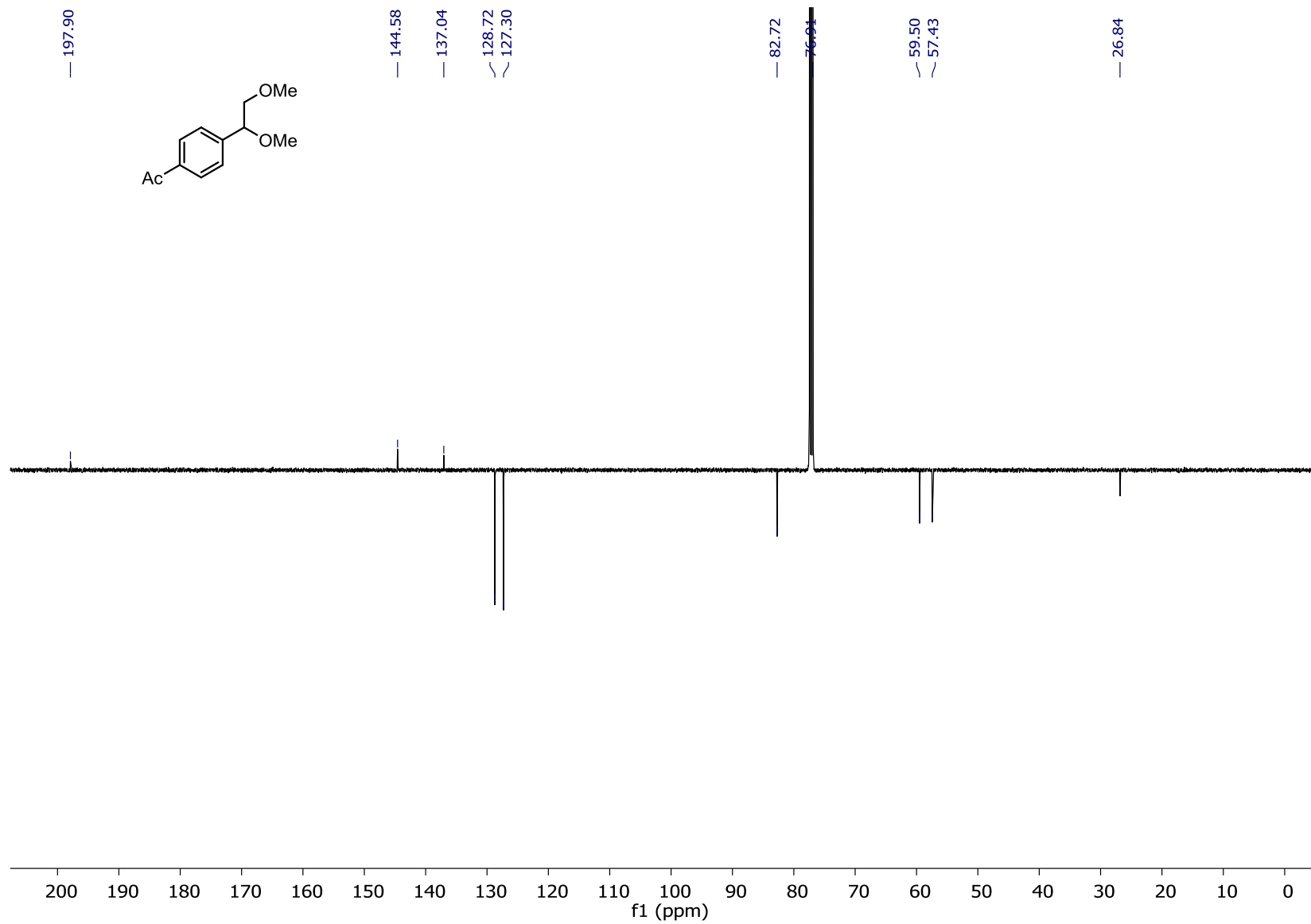
^{1}H NMR (501 MHz, CDCl$_3$): 1-(4-((2-methoxyethoxy)methyl)phenyl)ethan-1-one (27b)

^{13}C NMR (126 MHz, CDCl$_3$): 1-(4-((2-methoxyethoxy)methyl)phenyl)ethan-1-one (27b)

198.00

143.93
136.55
128.64
127.57

72.79
72.10
69.91

59.30

26.83

f1 (ppm)

200 190 180 170 160 150 140 130 120 110 100 90 80 70 60 50 40 30 20 10 0
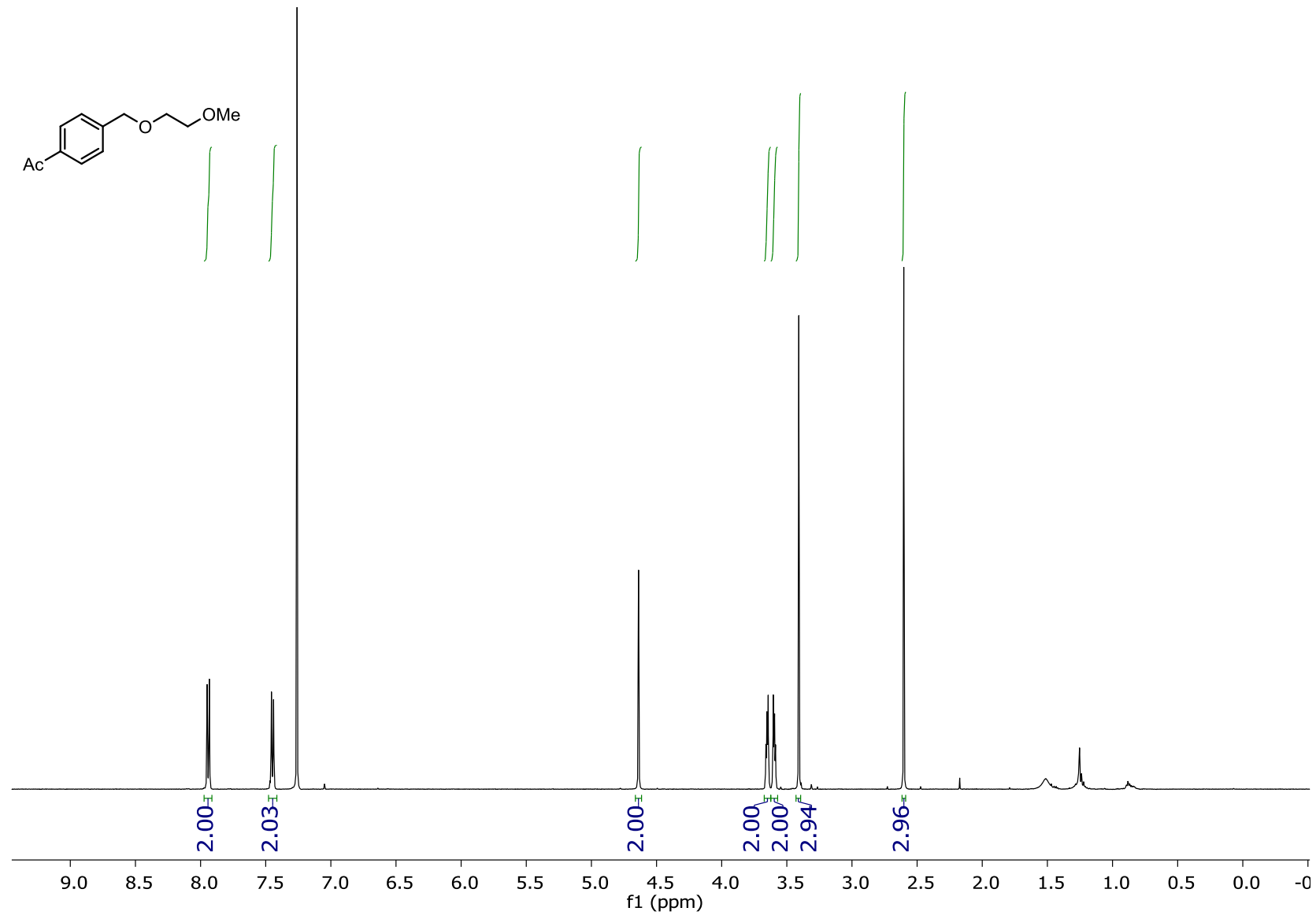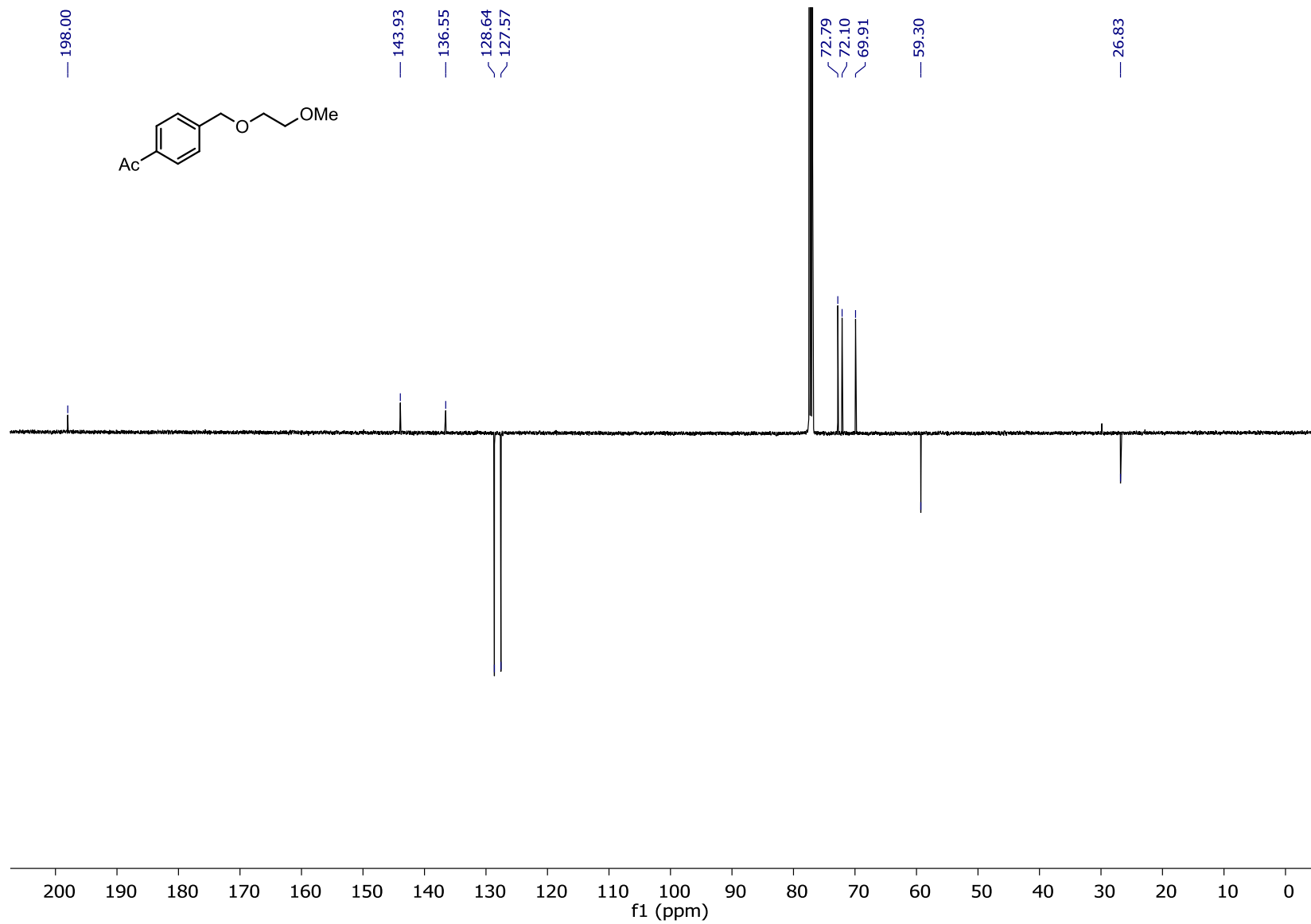
¹H NMR (501 MHz, CDCl₃): mixture of 27a and 27b
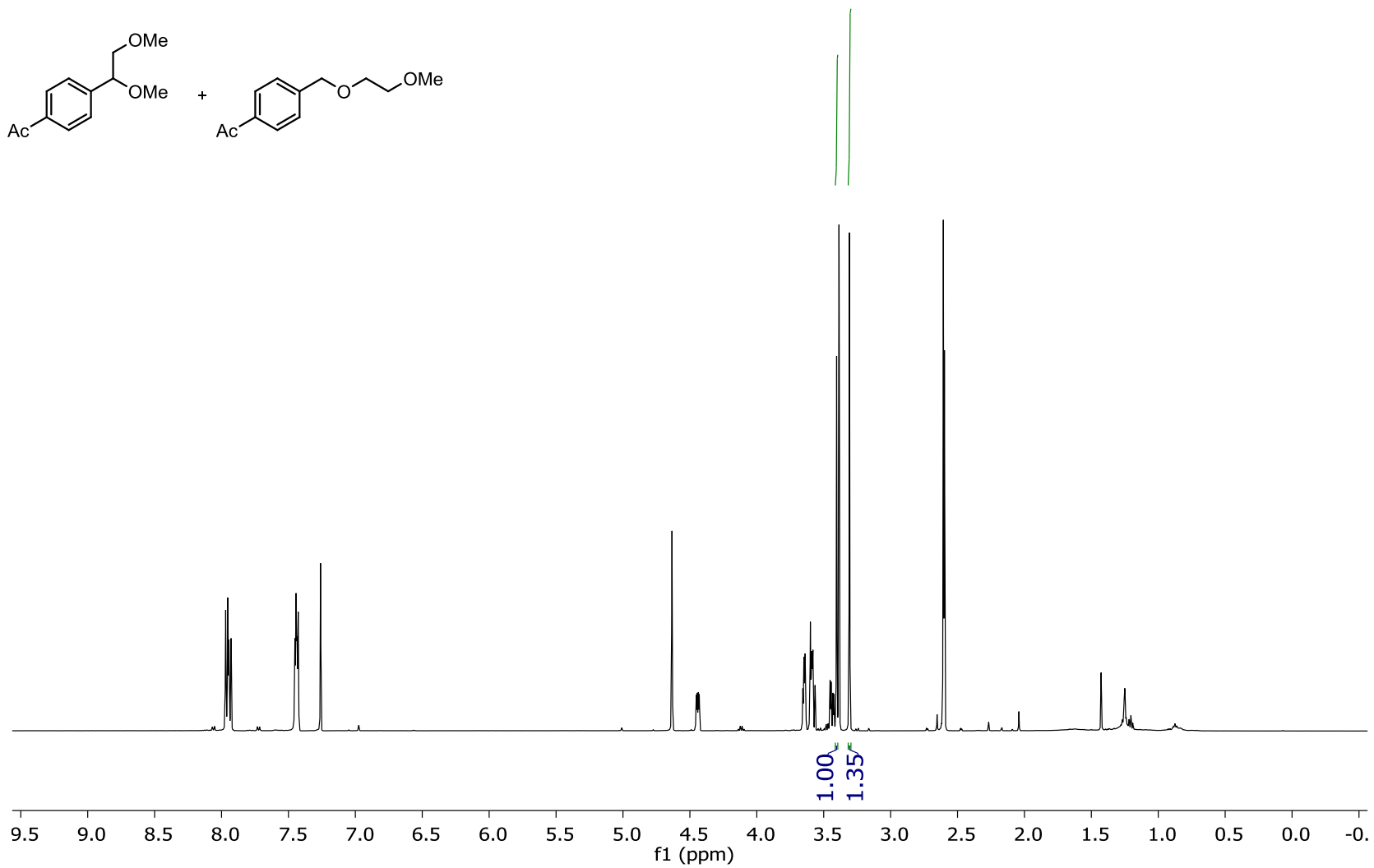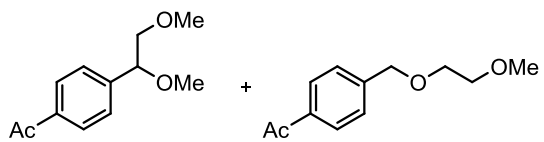
¹H NMR (501 MHz, CDCl₃): 1-(4-(phenoxymethyl)phenyl)ethan-1-one (28)
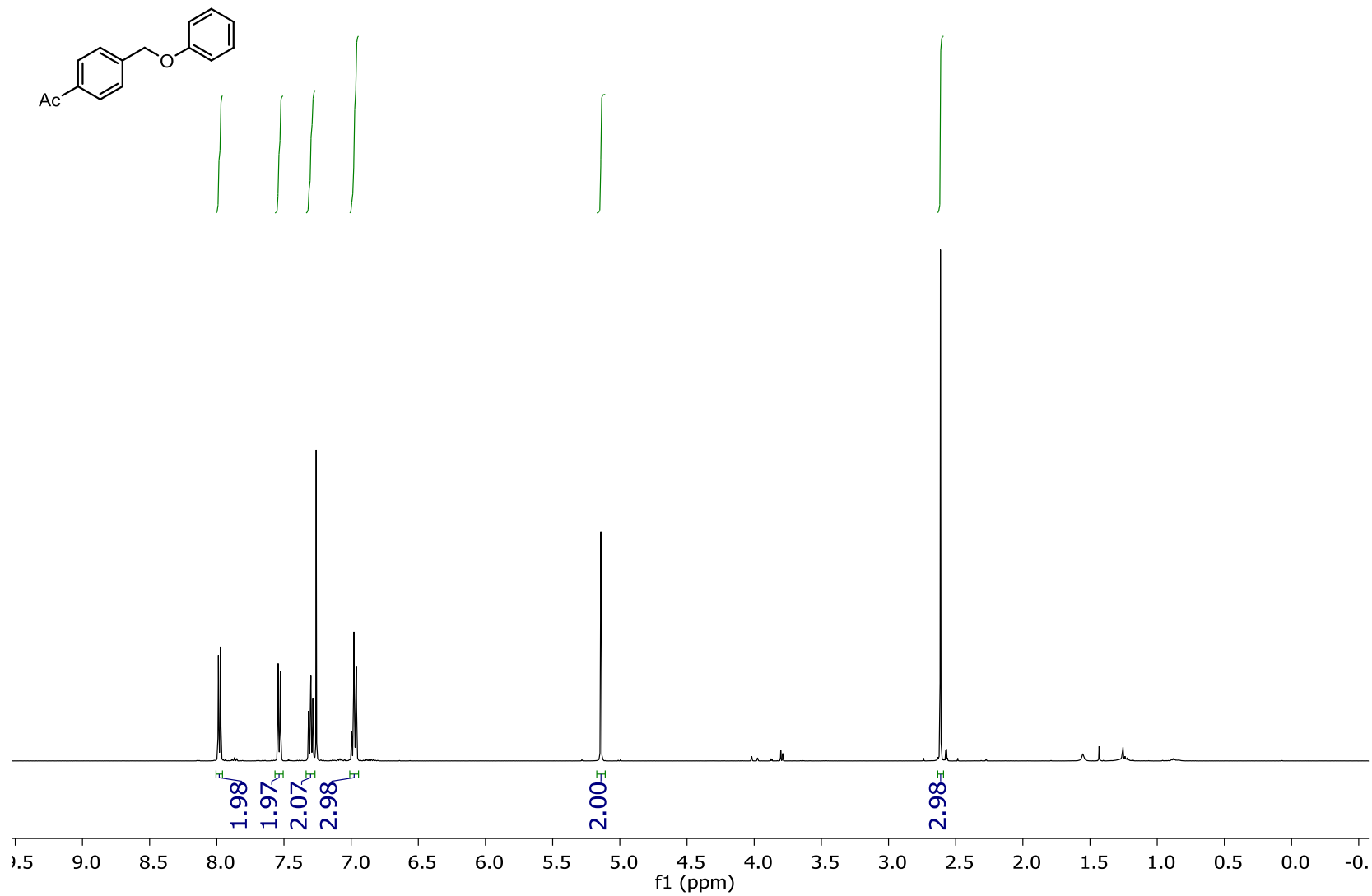
¹³C NMR (126 MHz, CDCl₃): 1-(4-(phenoxymethyl)phenyl)ethan-1-one (28)

— 197.87
— 158.54
— 142.66
— 136.77
— 129.71
— 128.80
— 127.28
— 121.39
— 114.95
— 69.31
— 26.83

200   190   180   170   160   150   140   130   120   110   100   90   80   70   60   50   40   30   20   10   0
f1 (ppm)

¹H NMR (501 MHz, CDCl₃): 2-methyl-6-(4-(tetrahydrofuran-2-yl-d7)phenyl)pyridine (32)
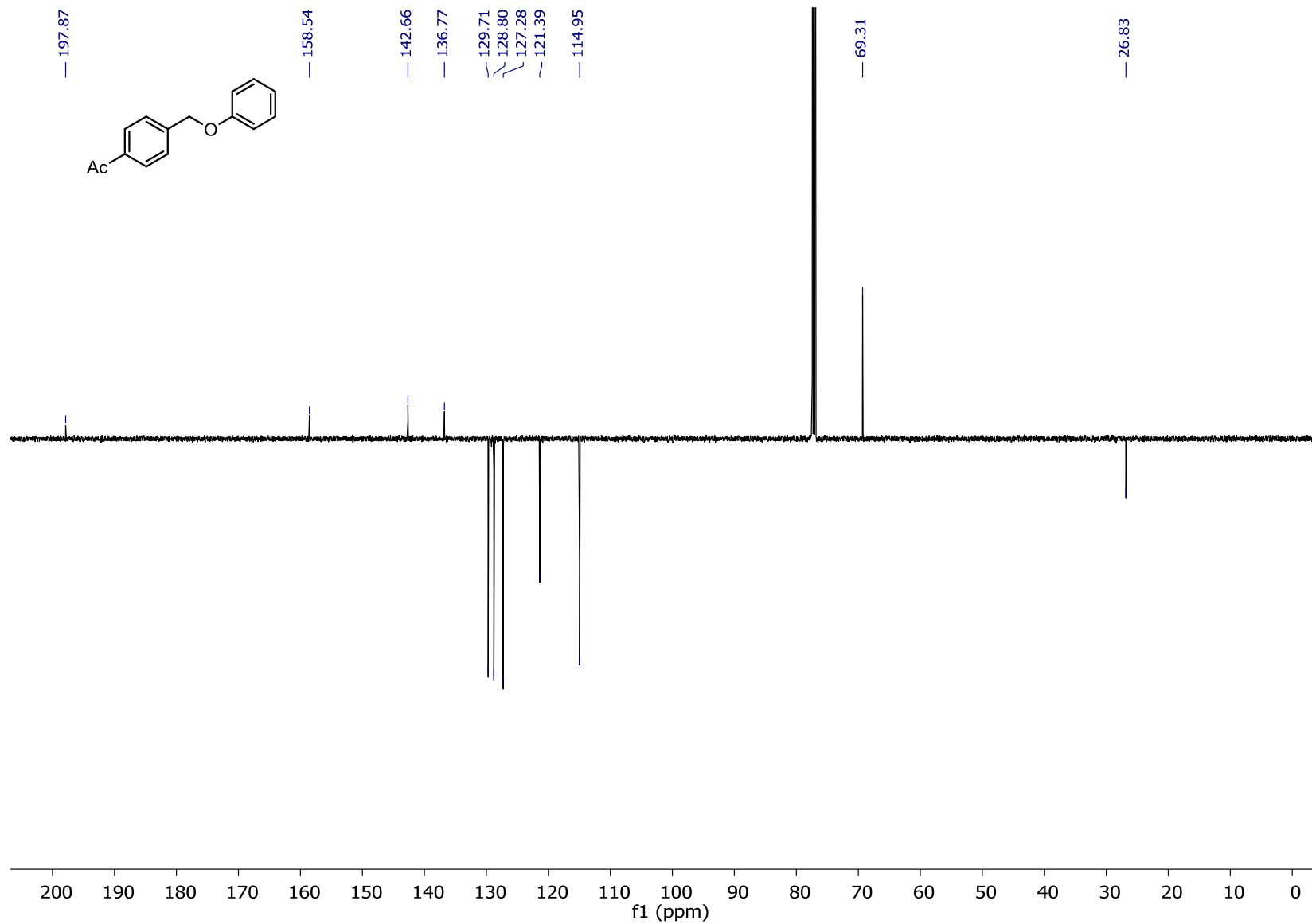
¹H NMR (501 MHz, CDCl₃): 2-methyl-6-(4-(tetrahydrofuran-2-yl-d7)phenyl)pyridine (32)
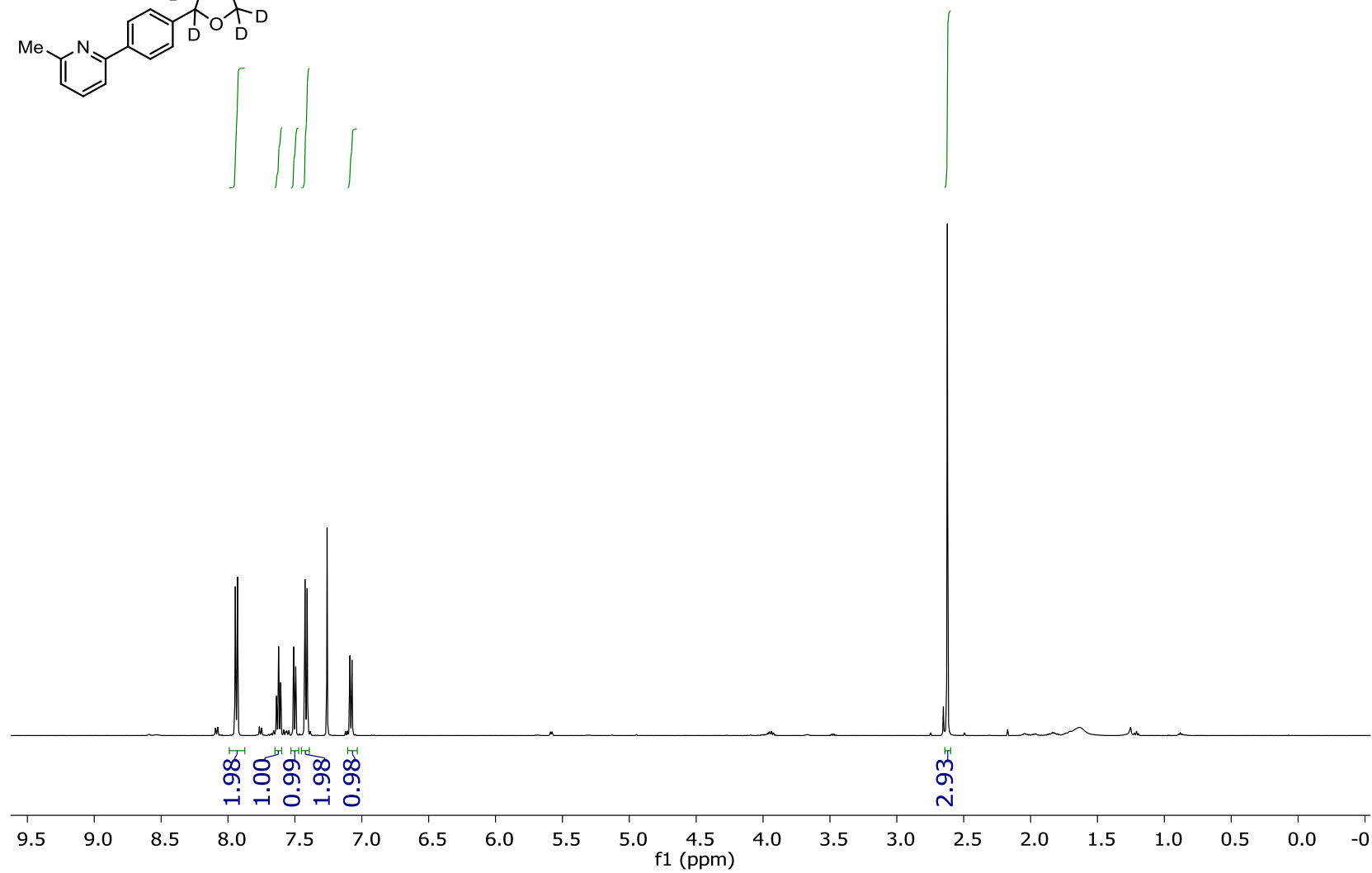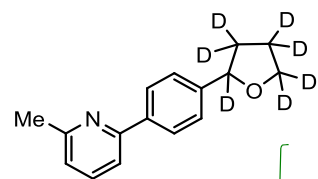
²H NMR (77 MHz, THF-h₈): 2-methyl-6-(4-(tetrahydrofuran-2-yl-d7)phenyl)pyridine (32)
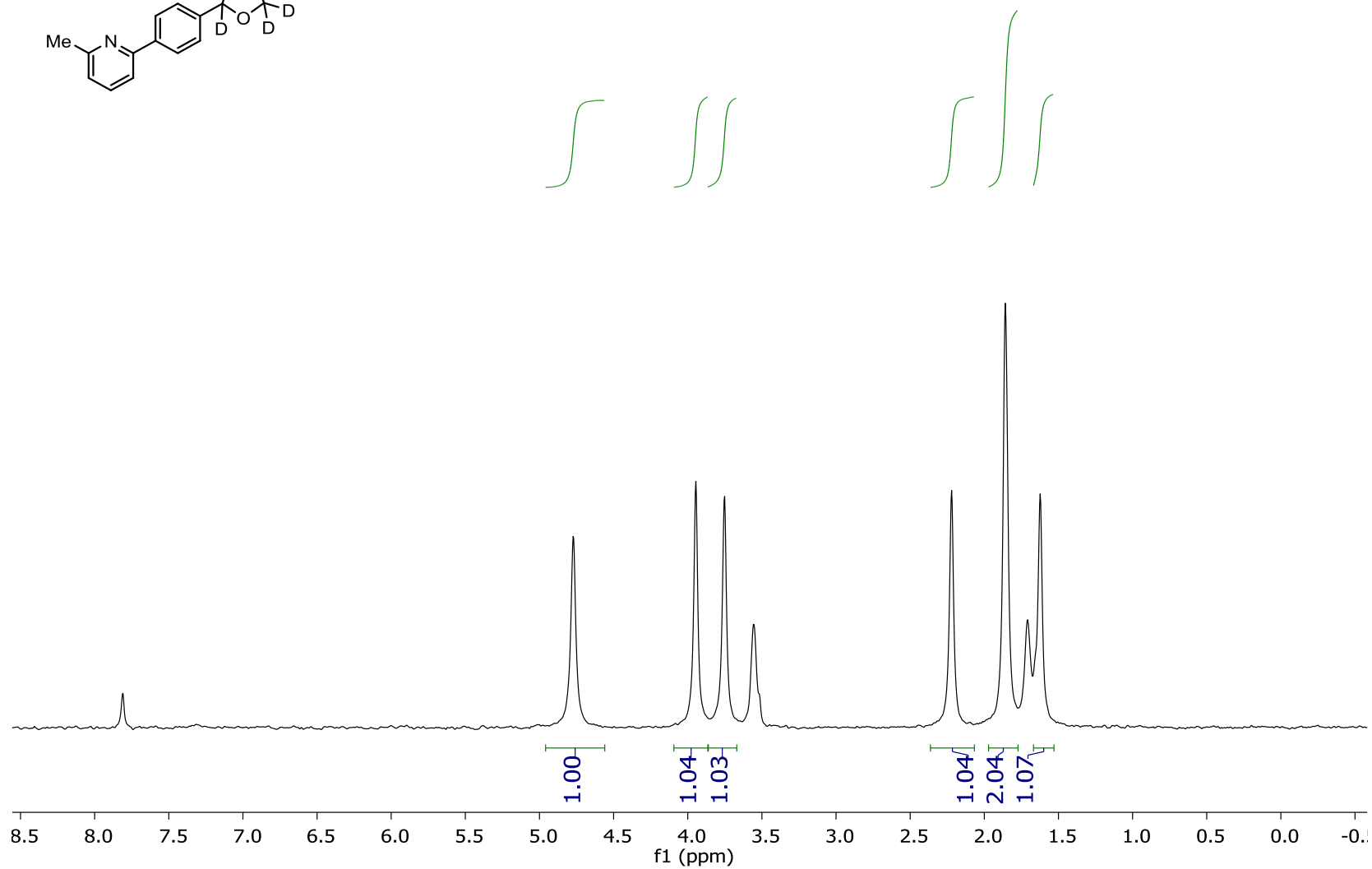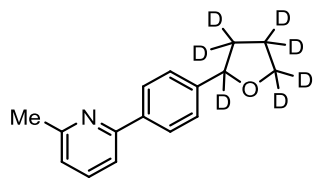
¹³C NMR (126 MHz, CDCl₃): 2-methyl-6-(4-(tetrahydrofuran-2-yl-d7)phenyl)pyridine (32)

^{1}H NMR (501 MHz, CDCl₃): 2-(4-chlorophenyl)-6-methylpyridine (30-Cl)
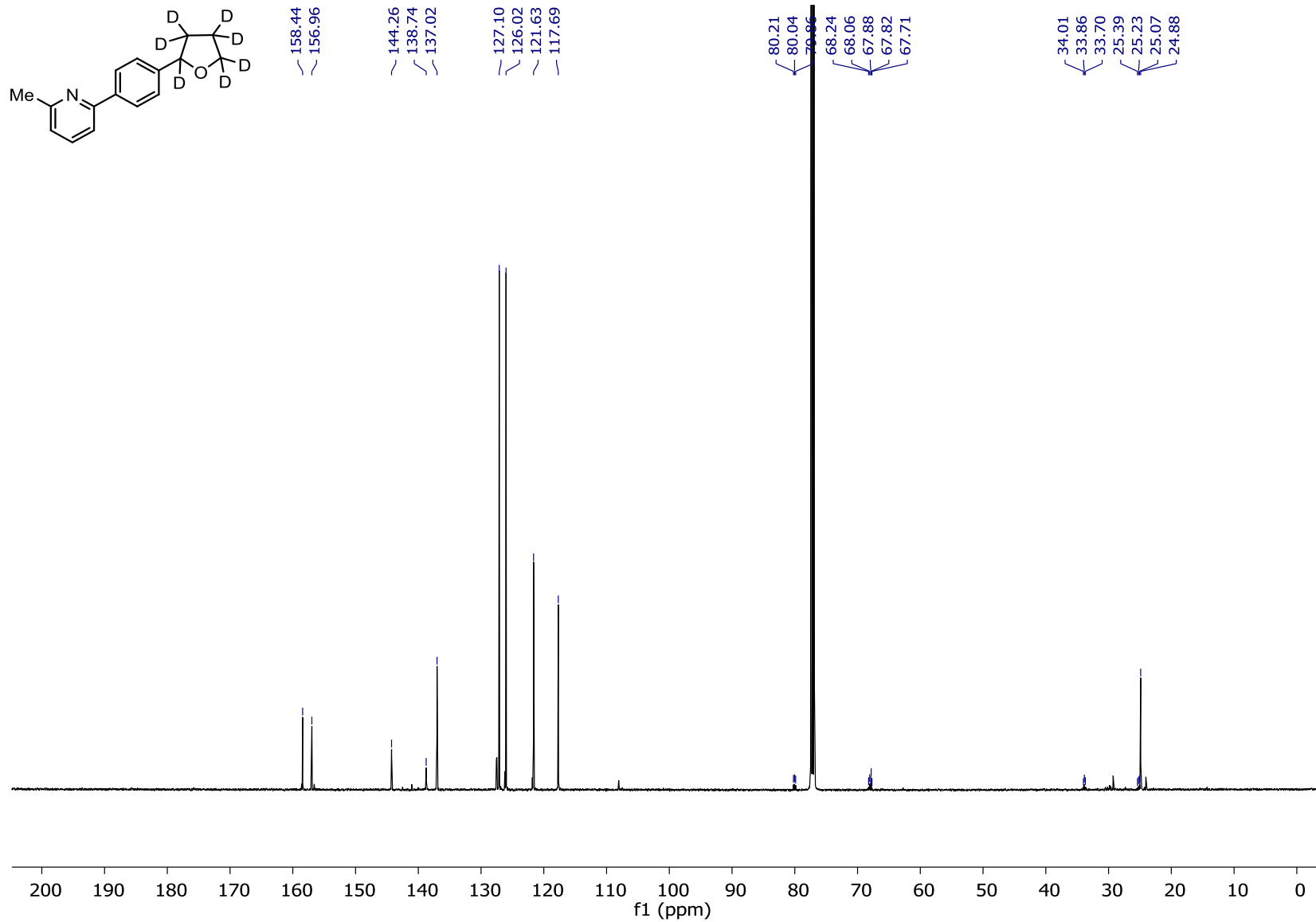
^{1}H NMR (501 MHz, CDCl$_3$): 2-(4-chlorophenyl)-6-methylpyridine (30-Cl)
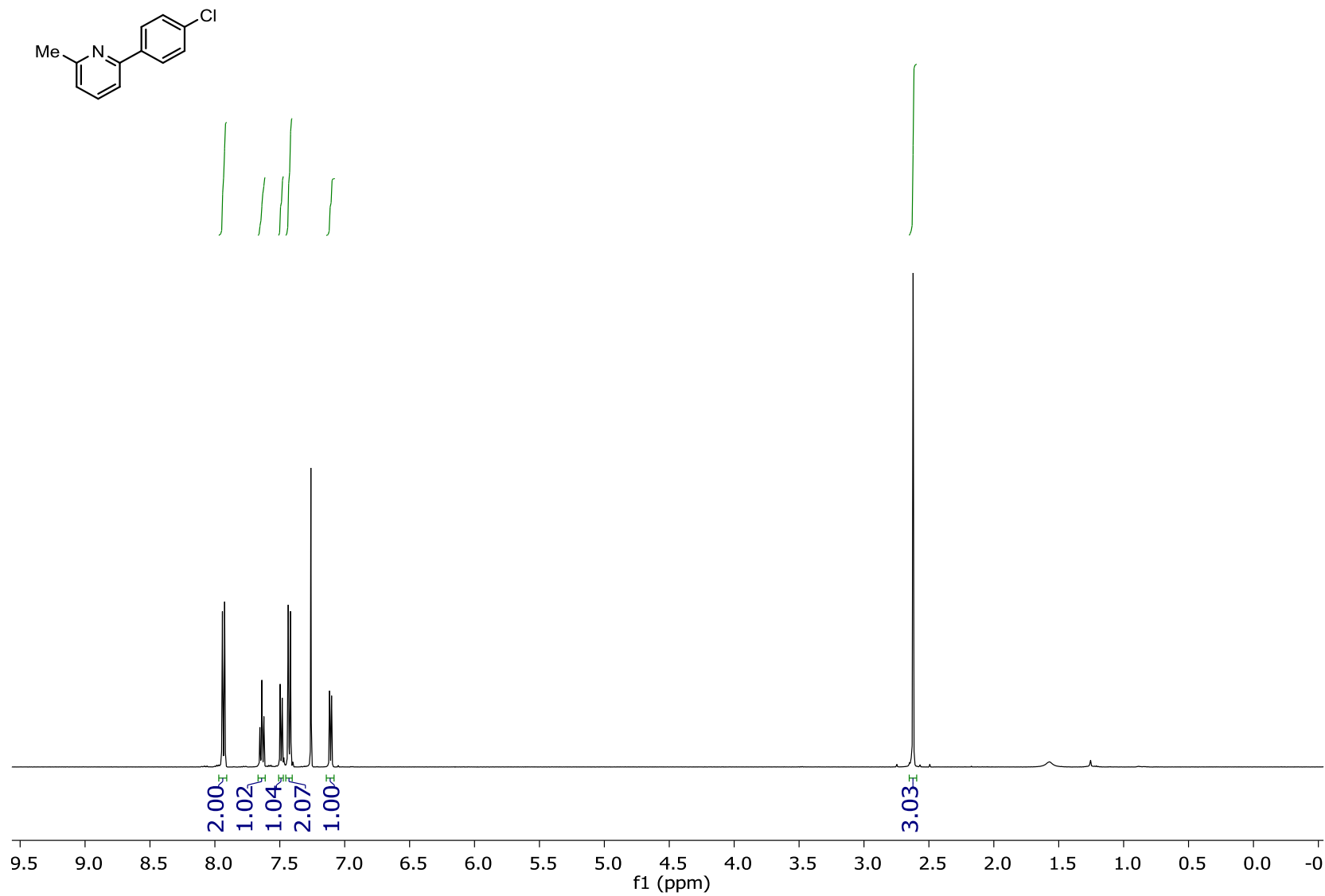
¹³C NMR (126 MHz, CDCl₃): 2-(4-chlorophenyl)-6-methylpyridine (30-Cl)

158.65
155.78
138.28
137.18
134.97
128.98
128.40
122.05
117.53
24.87

f1 (ppm)
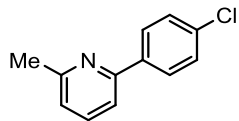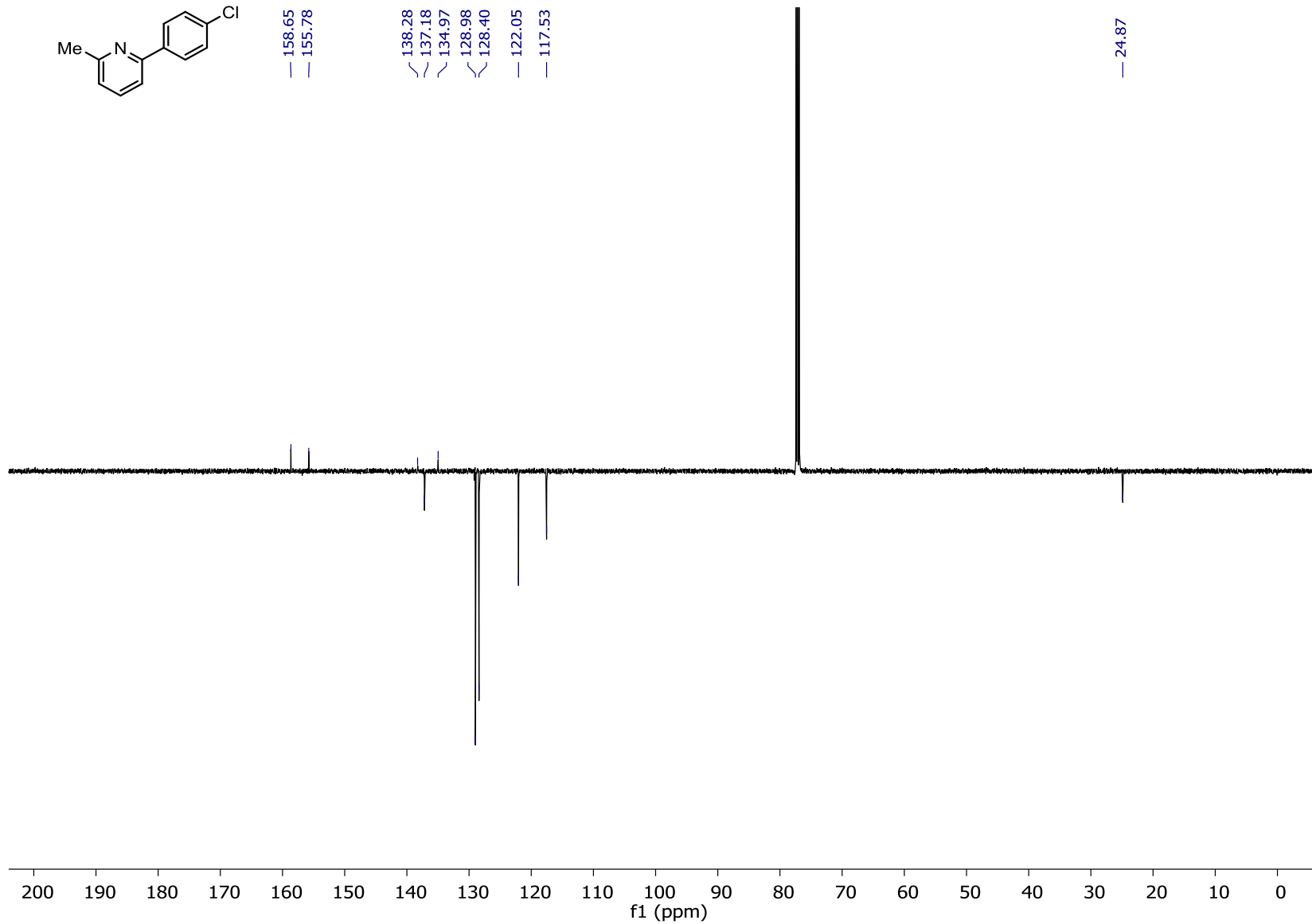
^{1}H NMR (501 MHz, CDCl$_3$): 2-(4-bromophenyl)-6-methylpyridine (30-Br)
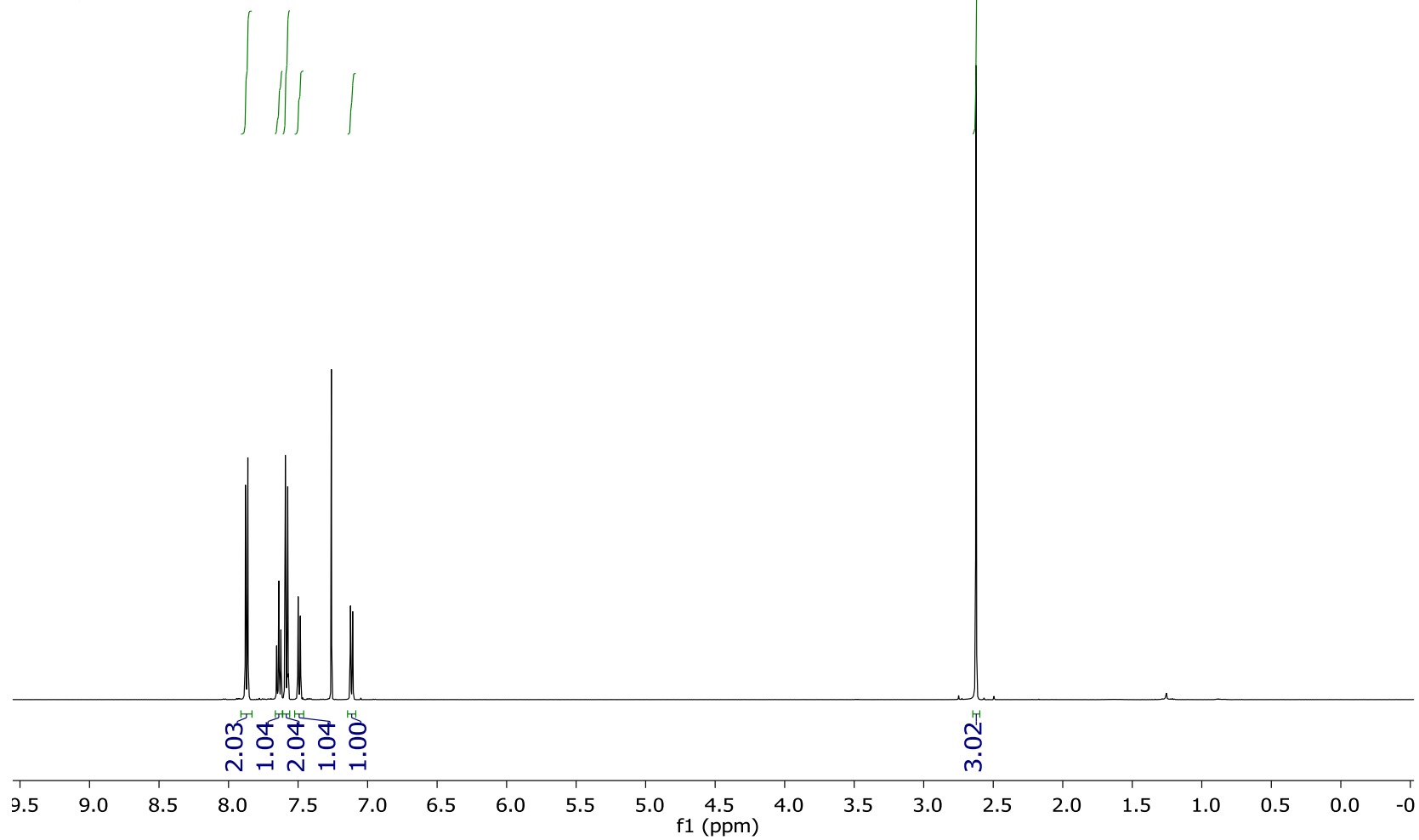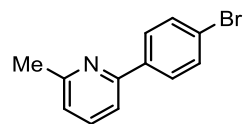
¹³C NMR (126 MHz, CDCl₃): 2-(4-bromophenyl)-6-methylpyridine (30-Br)

f1 (ppm)

¹**H NMR (501 MHz, CDCl₃): 2-(4-iodophenyl)-6-methylpyridine (30-I)**
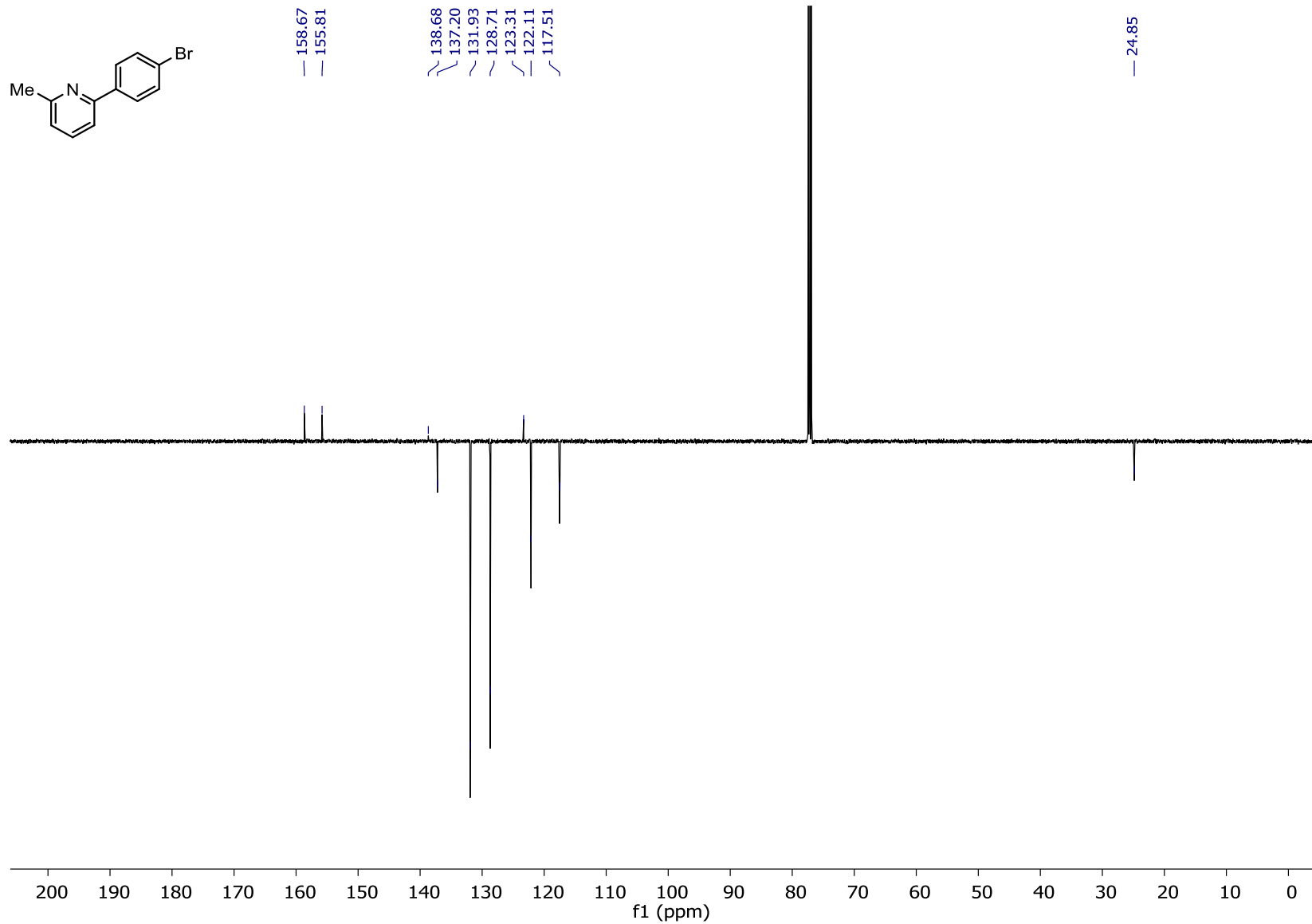
¹H NMR (501 MHz, CDCl₃): 2-(4-iodophenyl)-6-methylpyridine (30-I)
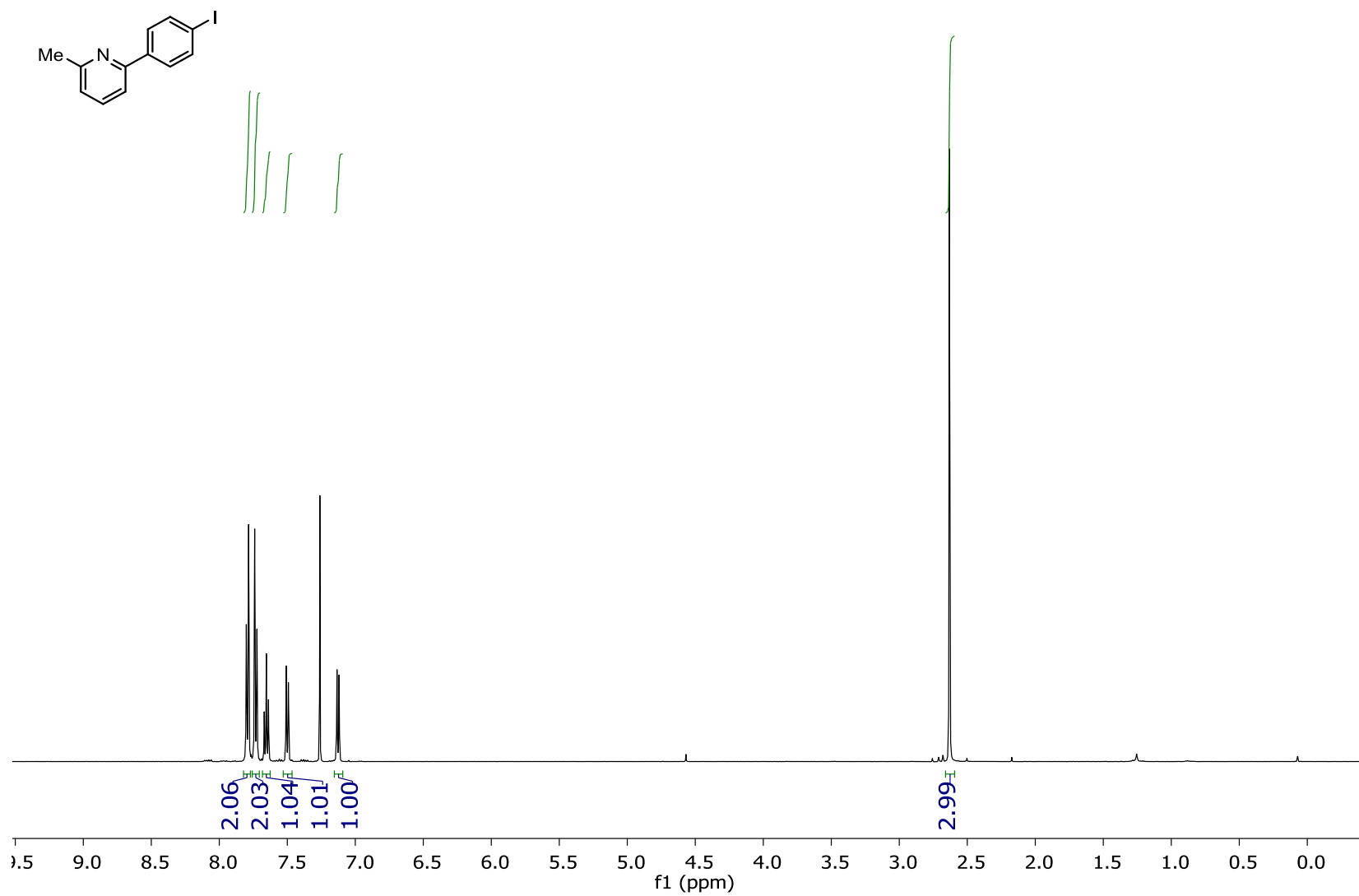
^{13}C NMR (126 MHz, CDCl₃): 2-(4-iodophenyl)-6-methylpyridine (30-I)
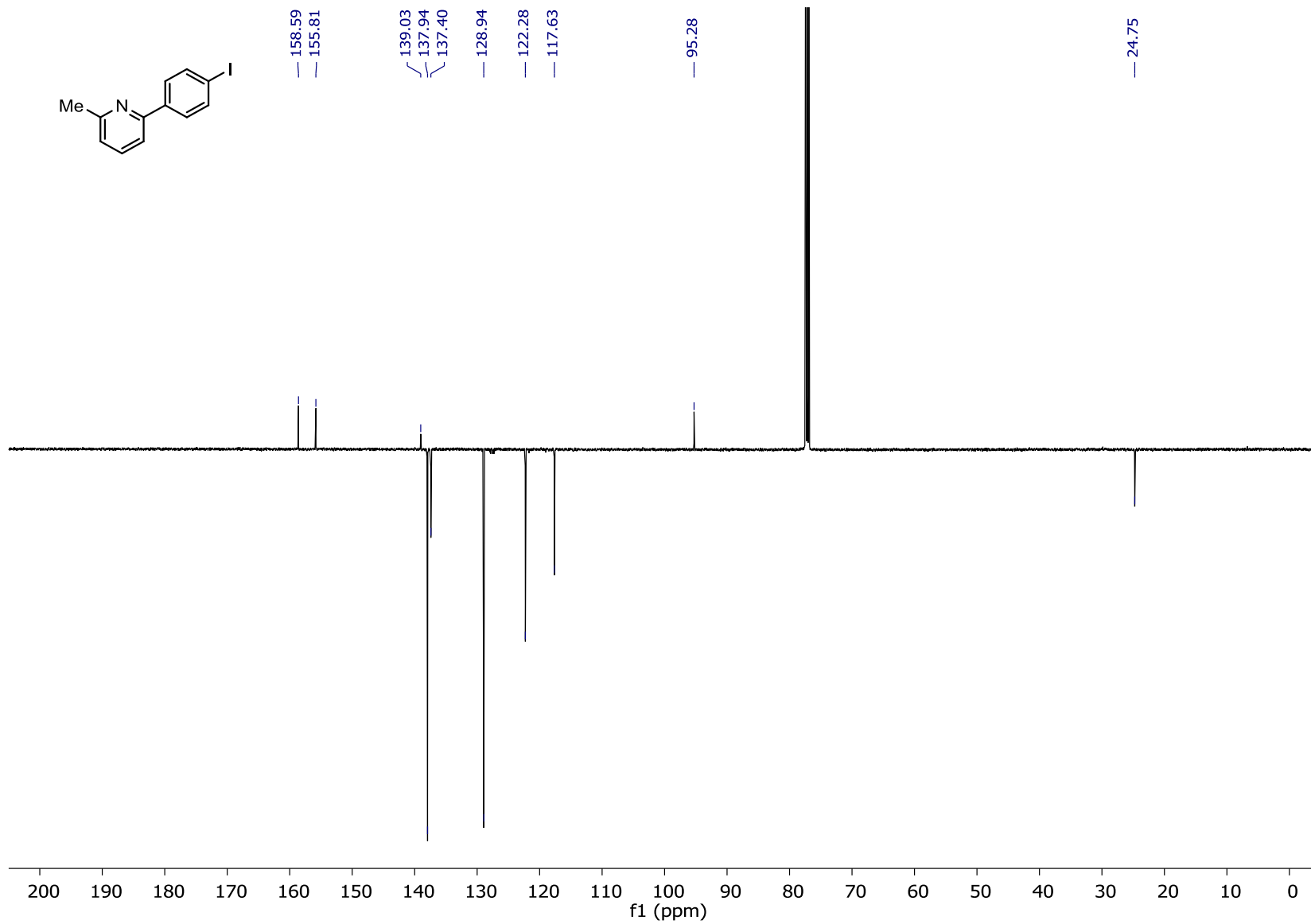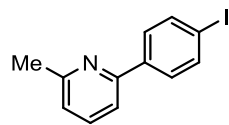
¹H NMR (501 MHz, CDCl₃): 2-methyl-6-phenylpyridine

^{13}C NMR (126 MHz, CDCl$_3$): 2-methyl-6-phenylpyridine

158.48
157.10
139.90
137.01
128.82
128.81
127.13
121.73
117.76
24.91

f1 (ppm)
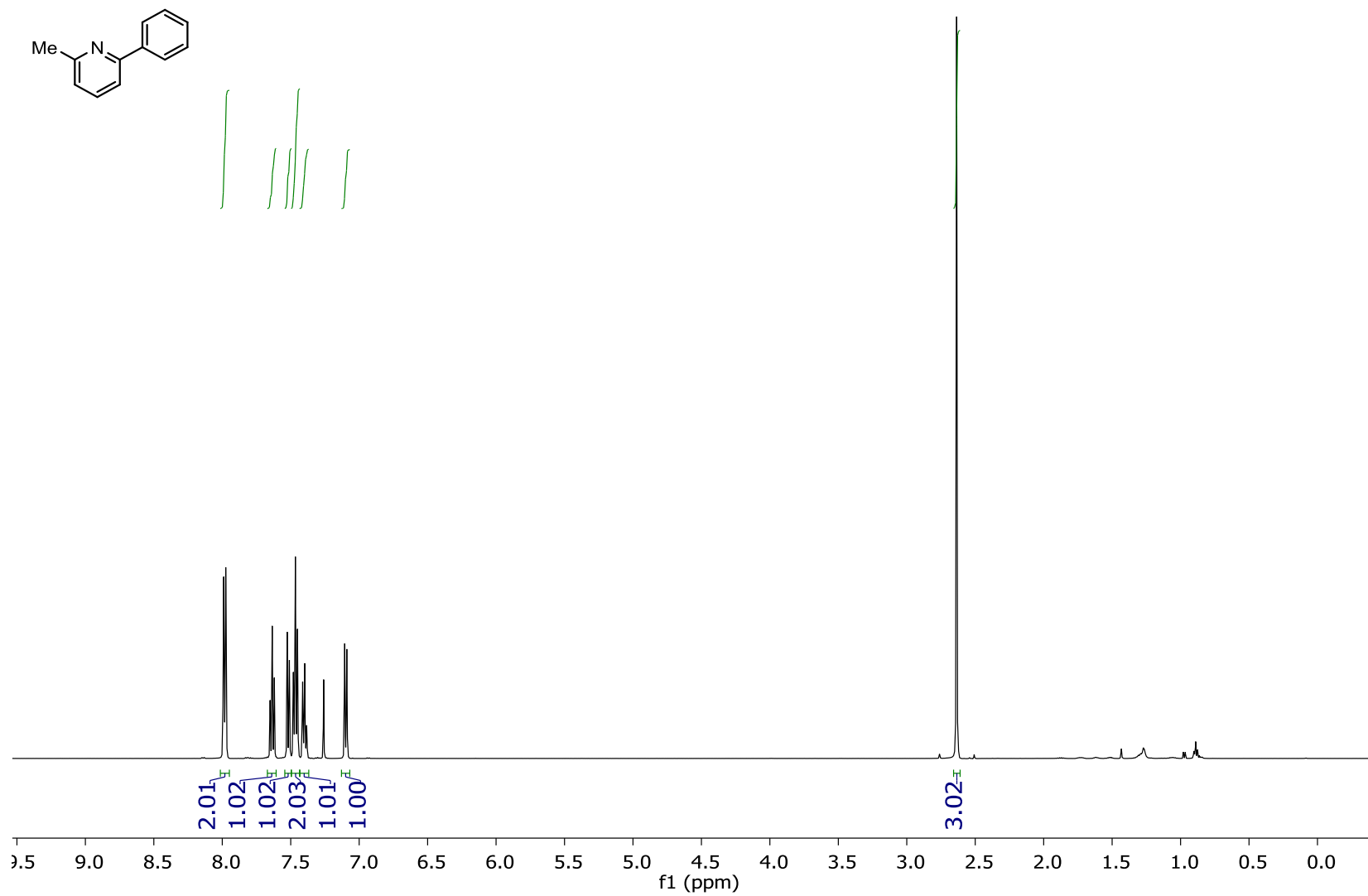
¹H NMR (501 MHz, CDCl₃): 2-methyl-6-(phenyl-4-d)pyridine (31)

^{1}H NMR (501 MHz, CDCl$_3$): 2-methyl-6-(phenyl-4-d)pyridine (31)

1.97 1.06 1.01 2.01 1.00 2.98

f1 (ppm)

^{2}H NMR (77 MHz, THF-h$_8$): 2-methyl-6-(phenyl-4-d)pyridine (31)

— 7.34

f1 (ppm)

^{13}C NMR (126 MHz, CDCl$_3$): 2-methyl-6-(phenyl-4-d)pyridine (31)

158.50
157.13
139.94
137.01
128.71
128.53
128.34
127.13
121.72
117.77
24.93

f1 (ppm)

^{1}H NMR (501 MHz, CDCl$_3$): 2-(4-fluorophenyl)tetrahydrofuran

^{1}H NMR (501 MHz, DCM-d$_{2}$): [(dtbbpy)Ni(*o*-tolyl)Cl] (33)

¹³C NMR (126 MHz, DCM-d₂): [(dtbbpy)Ni(*o*-tolyl)Cl] (33)

^{1}H NMR (501 MHz, DCM-d$_2$): [(dtbbpy)Ni(p-tolyl)Cl] (34)

^{13}C NMR (126 MHz, DCM-d$_2$): [(dtbbpy)Ni(*p*-tolyl)Cl] (34)

163.54
162.57
155.87
152.58
151.88
149.08
144.50
135.87
131.38
126.81
123.28
123.14
117.35
116.65
35.35
35.29
30.05
29.84
20.32

f1 (ppm)

¹H NMR (501 MHz, THF-d₈): [Ni(dtbbpy)(cod)]

¹³C NMR (126 MHz, THF-d₈): [Ni(dtbbpy)(cod)]

¹³C NMR (126 MHz, THF-d₈): [Ni(dtbbpy)(cod)]